Equilibrium of gas hydrates in presence of a hydrocarbon gas hhase

Duyen Le Quang

Ecole Nationale Supérieure des Mines
SAINT-ETIENNE

NNT : **2013 EMSE 0726**

THÈSE

présentée par

Duyen LE QUANG

pour obtenir le grade de
Docteur de l'École Nationale Supérieure des Mines de Saint-Étienne

Spécialité : Génie des Procédés

ÉQUILIBRE DES HYDRATES DE GAZ EN PRESENCE D'UN MELANGE D'HYDROCARBURES GAZEUX

Soutenue à Saint Etienne, le 18 décembre 2013

Membres du jury

Président :	Didier DALMAZZONE	Professeur, ENSTA, Paris
Rapporteurs :	Nicolas VON SOLMS	Associate Professor, CERE- Technical University of Denmark
	Christophe COQUELET	Professeur, Directeur CTP, Paris tech
Directeur de thèse :	Jean-Michel HERRI	Professeur, ENSM, Saint-Etienne
	Baptiste BOUILLOT	Maitre de conférence, ENSM, Saint-Etienne
Invités éventuels:	Pierre DUCHET-SUCHAUX	TOTAL, Paris
	Philippe GLENAT	TOTAL, Pau

Spécialités doctorales :	Responsables :
SCIENCES ET GENIE DES MATERIAUX	K. Wolski Directeur de recherche
MECANIQUE ET INGENIERIE	S. Drapier, professeur
GENIE DES PROCEDES	F. Gruy, Maître de recherche
SCIENCES DE LA TERRE	B. Guy, Directeur de recherche
SCIENCES ET GENIE DE L'ENVIRONNEMENT	D. Graillot, Directeur de recherche
MATHEMATIQUES APPLIQUEES	O. Roustant, Maître-assistant
INFORMATIQUE	O. Boissier, Professeur
IMAGE, VISION, SIGNAL	JC. Pinoli, Professeur
GENIE INDUSTRIEL	A. Dolgui, Professeur
MICROELECTRONIQUE	

EMSE : Enseignants-chercheurs et chercheurs autorisés à diriger des thèses de doctorat (titulaires d'un doctorat d'État ou d'une HDR)

AVRIL	Stéphane	PR2	Mécanique et ingénierie	CIS
BATTON-HUBERT	Mireille	PR2	Sciences et génie de l'environnement	FAYOL
BENABEN	Patrick	PR1	Sciences et génie des matériaux	CMP
BERNACHE-ASSOLLANT	Didier	PR0	Génie des Procédés	CIS
BIGOT	Jean Pierre	MR(DR2)	Génie des Procédés	SPIN
BILAL	Essaid	DR	Sciences de la Terre	SPIN
BOISSIER	Olivier	PR1	Informatique	FAYOL
BORBELY	Andras	MR(DR2)	Sciences et génie de l'environnement	SMS
BOUCHER	Xavier	PR2	Génie Industriel	FAYOL
BRODHAG	Christian	DR	Sciences et génie de l'environnement	FAYOL
BURLAT	Patrick	PR2	Génie Industriel	FAYOL
COURNIL	Michel	PR0	Génie des Procédés	DIR
DARRIEULAT	Michel	IGM	Sciences et génie des matériaux	SMS
DAUZERE-PERES	Stéphane	PR1	Génie Industriel	CMP
DEBAYLE	Johan	CR	Image Vision Signal	CIS
DELAFOSSE	David	PR1	Sciences et génie des matériaux	SMS
DESRAYAUD	Christophe	PR2	Mécanique et ingénierie	SMS
DOLGUI	Alexandre	PR0	Génie Industriel	FAYOL
DRAPIER	Sylvain	PR1	Mécanique et ingénierie	SMS
FEILLET	Dominique	PR2	Génie Industriel	CMP
FOREST	Bernard	PR1	Sciences et génie des matériaux	CIS
FORMISYN	Pascal	PR0	Sciences et génie de l'environnement	DIR
FRACZKIEWICZ	Anna	DR	Sciences et génie des matériaux	SMS
GARCIA	Daniel	MR(DR2)	Génie des Procédés	SPIN
GERINGER	Jean	MA(MDC)	Sciences et génie des matériaux	CIS
GIRARDOT	Jean-jacques	MR(DR2)	Informatique	FAYOL
GOEURIOT	Dominique	DR	Sciences et génie des matériaux	SMS
GRAILLOT	Didier	DR	Sciences et génie de l'environnement	SPIN
GROSSEAU	Philippe	DR	Génie des Procédés	SPIN
GRUY	Frédéric	PR1	Génie des Procédés	SPIN
GUY	Bernard	DR	Sciences de la Terre	SPIN
GUYONNET	René	DR	Génie des Procédés	SPIN
HAN	Woo-Suck	CR	Mécanique et ingénierie	SMS
HERRI	Jean Michel	PR1	Génie des Procédés	SPIN
INAL	Karim	PR2	Microélectronique	CMP
KERMOUCHE	Guillaume	PR2	Mécanique et Ingénierie	SMS
KLOCKER	Helmut	DR	Sciences et génie des matériaux	SMS
LAFOREST	Valérie	MR(DR2)	Sciences et génie de l'environnement	FAYOL
LERICHE	Rodolphe	CR	Mécanique et ingénierie	FAYOL
LI	Jean Michel		Microélectronique	CMP
MALLIARAS	Georges	PR1	Microélectronique	CMP
MOLIMARD	Jérôme	PR2	Mécanique et ingénierie	CIS
MONTHEILLET	Franck	DR	Sciences et génie des matériaux	SMS
PERIER-CAMBY	Laurent	PR2	Génie des Procédés	DFG
PIJOLAT	Christophe	PR0	Génie des Procédés	SPIN
PIJOLAT	Michèle	PR1	Génie des Procédés	SPIN
PINOLI	Jean Charles	PR0	Image Vision Signal	CIS
POURCHEZ	Jérémy	CR	Génie des Procédés	CIS
ROUSTANT	Olivier	MA(MDC)		FAYOL
STOLARZ	Jacques	CR	Sciences et génie des matériaux	SMS
SZAFNICKI	Konrad	MR(DR2)	Sciences et génie de l'environnement	CMP
TRIA	Assia		Microélectronique	CMP
VALDIVIESO	François	MA(MDC)	Sciences et génie des matériaux	SMS
VIRICELLE	Jean Paul	MR(DR2)	Génie des Procédés	SPIN
WOLSKI	Krzystof	DR	Sciences et génie des matériaux	SMS
XIE	Xiaolan	PR0	Génie industriel	CIS

ENISE : Enseignants-chercheurs et chercheurs autorisés à diriger des thèses de doctorat (titulaires d'un doctorat d'État ou d'une HDR)

BERGHEAU	Jean-Michel	PU	Mécanique et Ingénierie	ENISE
BERTRAND	Philippe	MCF	Génie des procédés	ENISE
DUBUJET	Philippe	PU	Mécanique et Ingénierie	ENISE
FORTUNIER	Roland	PR	Sciences et Génie des matériaux	ENISE
GUSSAROV	Andrey	Enseignant contractuel	Génie des procédés	ENISE
HAMDI	Hédi	MCF	Mécanique et Ingénierie	ENISE
LYONNET	Patrick	PU	Mécanique et Ingénierie	ENISE
RECH	Joël	MCF	Mécanique et Ingénierie	ENISE
SMUROV	Igor	PU	Mécanique et Ingénierie	ENISE
TOSCANO	Rosario	MCF	Mécanique et Ingénierie	ENISE
ZAHOUANI	Hassan	PU	Mécanique et Ingénierie	ENISE

Mise à jour : 07/04/2013

PR 0	Professeur classe exceptionnelle
PR 1	Professeur 1ère classe
PR 2	Professeur 2ème classe
PU	Professeur des Universités
MA (MDC)	Maître assistant
DR	Directeur de recherche

Ing.	Ingénieur
MCF	Maître de conférences
MR (DR2)	Maître de recherche
CR	Chargé de recherche
EC	Enseignant-chercheur
IGM	Ingénieur général des mines

SMS	Sciences des Matériaux et des Structures
SPIN	Sciences des Processus Industriels et Naturels
FAYOL	Institut Henri Fayol
CMP	Centre de Microélectronique de Provence
CIS	Centre Ingénierie et Santé

Remerciements

Je tiens à remercier Monsieur Jean-Michel HERRI, Professeurs de l'École des Mines de Saint-Etienne, d'avoir accepté de diriger cette recherche et de m'avoir accompagné toujours avec un mot d'encouragement positif. Non seulement, Il est mon professeur qui m'apporté son soutien scientifique, mais aussi Il est également mon grand frère avec qui j'ai appris beaucoup de choses pour bien adapter en France, Faire une convention de collaboration entre École National supérieure des Mines de Saint Etienne et mon école des mines de Hanoi, au Vietnam.

Je remercie vivement Monsieur. Baptiste BOUILLOT au poste de Co- encadrant et Madame. Ana CAMEIRAO, et Madame Yamina OUABBAS qui m'ont apporté le soutien nécessaire pour mener à bien ce travail.

J'adresse mes remerciements aux, Fabien CHAUVY, Albert BOYER, Alain LALLEMAND et Jean- Pierre POYET Technicien de laboratoire pour leur aide technique pendant ma thèse. Je n'oublie pas de remercier tous les membres de l'équipe hydrate qui m'aiderait depuis je suis venu en France.

Merci aux mes parents qui ont toujours confiance en moi, et surtout sont supporter dans tout la vie, et un très grand merci à ma femme et aux mes enfants, LE QUANG Minh et LE QUANG Duy Khanh (Etienne) toujours m'apporté ses soutien dans la vie quotidienne Merci pour tes amours et tes présences dans les moments importants de ma vie. Merci la famille de LE QUANG Du mon petit frère pour ses partages des moments difficiles. Je remercie le Ministère de l'Éducation et de la Formation qui m'a accepte de faire cette thèse en m'accordant toujours un poste enseignant chercheur a école des mines de Hanoi.

Mes remerciements vont également aux toutes les personnes de l'ENSM-SE, doctorants, enseignants chercheurs, personnel et stagiaires qui m'apporté leur soutiens leur amial, ses conseilles.

Je tiens à vous remercier très chaleureusement !!!

List of Figure

List of Table

1. INTRODUCTION

This work is a contribution to the global understanding of the coupling between kinetic and thermodynamic to explain the clathrate hydrate composition during their crystallization to form a solid phase from a water liquid phase and an hydrocarbon gas phase.

In the laboratory, we faced new experimental facts that opened questioning after comparing the classical modeling of clathrate hydrates following the approach of van der Waals and Platteeuw (1959), with our experimental data following a new procedure that we published, allowing to determine the hydrate composition during crystallization and at equilibrium (Herri et al, 2011).

Our first tentative was to program a java code implementing the van der Waals and Platteeuw (1959) that is a combination of classical thermodynamic and statistical thermodynamic to calculate for example the pressure and composition of clathrate hydrate at Gas/Liquid Water/Hydrate equilibrium given a temperature and a gas phase composition. The procedure to program such a routine is particularly well documented, especially from the books of Sloan and coworkers (1998, 2008) which provide the community with all the internal parameters. In this document, the parameters are called reference parameters if they correspond to the parameters implemented in the classical thermodynamic side, or Kihara parameters if they correspond to the statistical thermodynamic side.

A first questioning that concerned our laboratory was to retain the best set of reference parameters. In fact, Sloan and coworkers (1998, 2008) are working with a set of reference parameters from their laboratory (Dharmawandhana, 1980) but they don't explain the reason to choice this set of parameters from others values that can found in the literature. From new experimental data inherited from three research program devoted to gas separation in the domain of CO_2 capture, the laboratory has evaluated the best set of reference parameters to model their equilibrium data (Herri et al, 2011) to retain the ones from Handa and Tse (1986). At this occasion, we discovered that the literature data are not coherent together, and we began to suspect the crystallization to form non equilibrium hydrates.

Herri and Kwaterski (2012) have proposed a theoretical approach to explain the fact that gas hydrates can not form at equilibrium. In fact, Gas Hydrates are crystalline water based solids composed of a three dimensional network of water molecules. They form a network of cavities in which molecules of light gases can be encapsulated depending on their size and

affinity. Gas hydrates can by their nature not be classified as chemical compounds since they do not possess a definite stoechiometry. In contrast they have to be regarded as solid solution phases, the stoechiometry of which is not fixed but depends on the composition of the surrounding liquid. We agree that, at equilibrium, the composition dependence of the hydrate phase can be described by means of the classical van der Waals and Platteeuw model (1959) In the framework of the model, Langmuir constants, are used for expressing the relative ability of light components to get enclathrated within the cavities. In the model, the enclathratation is described by means of a Langmuir absorption where the composition if fixed from kinetic consideration based on the balance between the absorption rate and desorption rate. At equilibrium, these rates are equal, but Herri and Kwaterski (2012) have showed that, under crystallization, there rates could be not equal. And in this case, both the growth rate and the hydrate composition become dependent on the competition between the different molecules to get enclathrated in the structure under formation. In addition, they turn out to become dependent on the gas diffusion around the hydrate crystals, and so, the geometry of the system needs to be taken into account, especially the mass transfer at the Gas/liquid interface. The procedure results in the definition of a non-equilibrium hydrate composition with a new analytical expression of the composition.

My contribution to this global understanding has been to evaluate the hydrate composition for a new type of gases, based on hydrocarbon molecules only, corresponding to oil industry. In our case, Nitrogen is a minor gas whereas it has been the dominant gas in the previous program devoted to CO_2 capture.

My contribution has been first to re-evaluate properly the Kihara parameters from experimental data from literature. This step implies to compile and implement all the literature data in the data base of our modeling program, called GasHyDyn. Then, from these experimental data, the program can optimize Kihara parameters from a procedure that can be trivial in some cases where literature data are rich enough to optimize directly the parameters, but the procedure is complex as the literature data are rare or not coherent together. This optimization has been very time consuming.

My second contribution has been to propose new experimental data, from hydrocarbon gas mixtures, and to test our model against. The experimental approach has been also very time consuming, and the value of one equilibrium point could be weeks, during which we praise technical problems to forget us. Electricity shutdown, sudden pressure leaks, or other problems have been our every day life.

2. DEFINITION AND STRUCTURE OF GAS HYDRATES

2.1. DEFINITION

Clathrates gas hydrates, often called gas hydrates, are crystalline phases in which gas molecules are inserted as guests in a solid structure composed of water molecules. The water molecules interact themselves by hydrogen bonds, to form a cavities networks, partially filled by the gas molecules.

2.2. STRUCTURE

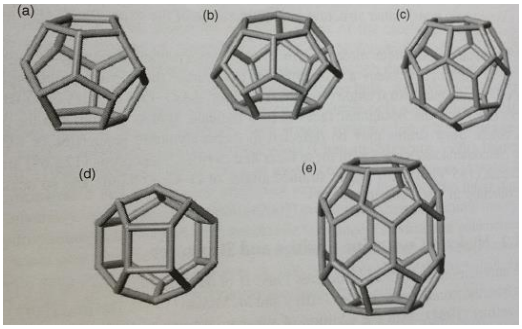

Figure 1 Geometries of the 5 type cavities in gas clathrate hydrates (Sloan and Koh, 2007)

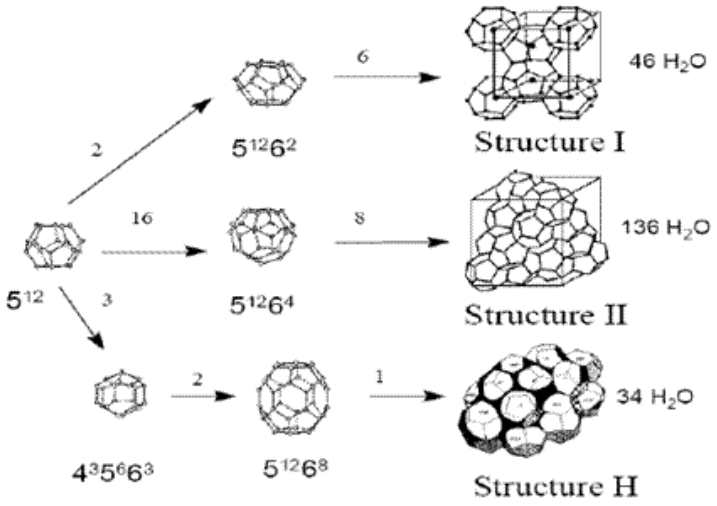

Figure 2 : Geometry of structures sI, sII, sH clathrates (Sloan, 1990)

The clathrates are ice-like compounds in the sense that they correspond to a re-organisation of the water molecules to form a solid. The crystallographic structure is based on H-bonds. The clathrates of water are also designated improperly as “porous ice” because the water molecules build a solid network of cavities in which gases, volatile liquids or other small molecules could be captured.

The clathrates of gases, called gas hydrates, have been studied intensively due to their occurrence in deep sea pipelines where they cause serious problems of flow assurance.

Each structure is a combination of different types of polyhedra sharing faces between them. Jeffrey (1984) suggested the nomenclature e^f to describe each polyhedra: e is the number of edges of the face, and f is the number of faces with e edges. Five types of cavities (Figure 1) have been reported (Sloan and Koh, 2007) : 1) the pentagonal dodecahedron 5^{12}; 2) the 14-hedron, $5^{12}6^2$, consisting of twelve pentagonal and two hexagonal faces; 3) the 16-hedron, $5^{12}6^4$, consisting of twelve pentagonal and four hexagonal faces; 4) the dodecahedron cavity ,$4^35^66^3$, has three square faces and six pentagonal faces and three hexagonal faces; 5) the largest icosahedrons cavity, $5^{12}6^8$, has 12 pentagonal faces and 6 hexagonal faces.

From the combination of the five types of cavities, three different structures have been established precisely, called I, II and H (Sloan, 1998, Sloan and Koh, 2007), graphically reported on Figure 2 and which properties are detailed on Table 1.

Table 1 Structure of gas hydrates

	SI		**SII**		**SH**		
	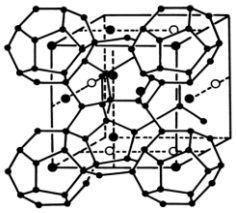		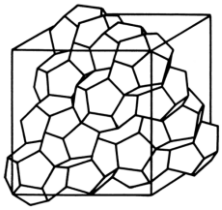		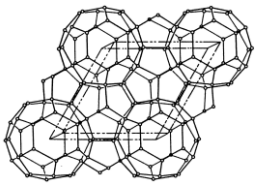		
Cavity	5^{12}	$5^{12}6^2$	5^{12}	$5^{12}6^4$	5^{12}	$4^35^66^3$	$5^{12}6^8$
Type of cavity (j: indexing number)	1	2	1	3	1	5	4
Number of cavities (m_j)	2	6	16	8	3	2	1
Average cavity radius (nm)(1)	0.395	0.433	0.391	0.473	0.391	0.406	0.571
Variation in radius, % (2)	3.4	14.4	5.5	1.73			
Coordination number	20	24	20	28	20	20	36
Number of water	42		136		134		

molecules			
Cell parameters (nm)	a_0 = 1.1956 (3)	a_0 =1.7315 (4)	a=1.2217, b=1.0053 (5)
Thermal expansivity $\alpha = \frac{1}{a}\left(\frac{\partial a}{\partial T}\right)$(6)	$\alpha = a_1 + a_2\left(T - T_0\right) + a_3\left(T - T_0\right)^2$ $\frac{a - a_0}{a_0} + 1 = \exp\left[a_1\left(T - T_0\right) + \frac{a_2}{2}\left(T - T_0\right)^2 + \frac{a_3}{3}\left(T - T_0\right)^3\right]$		
	$a_1 = 1.1280\,10^{-4}$ $a_2/2 = 1.8003\,10^{-7}$ $a_3/3 = -1.5898\,10^{-11}$	$a_1 = 6.7659\,10^{-5}$ $a_2/2 = 6.1706\,10^{-8}$ $a_3/3 = -6.2649\,10^{-11}$	
Cell volume (nm^3)	1.709 (3)	5.192 (4)	1.22994 (5)

(1) Sloan (1998).

(2) Variation in distance of oxygen atoms from centre of cages (Sloan, 1998).

(3) For ethane hydrate, from (Udachin, 2002).

(4) For tetrahydrofuran hydrate, from Udachin (2002).

(5) For methylcyclohexane-methane hydrate, from Udachin (2002)

(6) Hester et al, 2007

More details about the cell parameters can be found in Hester et al (2007). They measured the hydrate lattice parameters for four Structure I (C_2H_6, CO_2, 47% C_2H_6 + 53% CO_2, and 85% CH_4 + 15% CO_2) and seven Structure II (C_3H_8, 60% CH_4 + 40% C_3H_8, 30% C_2H_6 + 70% C_3H_8, 18% CO_2 + 82% C_3H_8, 87.6% CH_4 + 12.4% i-C_4H_{10}, 95% CH_4 + 5% $C_5H_{10}O$, and a natural gas mixture).The measurements have been compared to literature data with Structure I (Figure 3) from EtO (Rondinone et al, 2002), CD_4 (Gutt et al, 2000), CO_2 (Ikeda et al, 1999), Xe (Ikeda et al, 2000), TMO-d6 (Rondinone et al, 2002) CH_4 (Shpakov et al, 1998; Ogienko et al, 2006) CH_4+CO_2 (Takeya et al, 2006), and Structure II (Figure 4) from THF (Tse, 1987), TMO-d6(Rondinone et al, 2002), C_3H_8 (Choumakos et al, 2003), C_3H_8(Jones et al, 2003), CH_4+C_2H_6(Rawn et al, 2002), Air (Takeya et al, 2000), THF-d8(Jones et al, 2003). Hester et al (2007) conclude that both sI and sII hydrates, with a few exceptions, had a common thermal expansivity, independent of hydrate guest, following the correlation given in Table 1

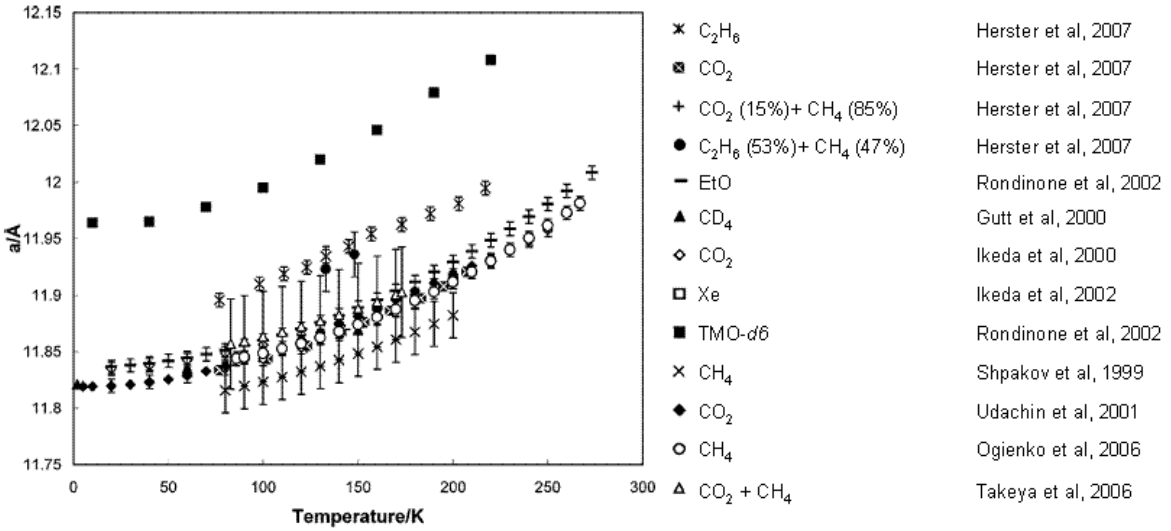

Figure 3: Lattice parameters versus temperature for varius sI Hydrates, modified from Hester et al (2007)

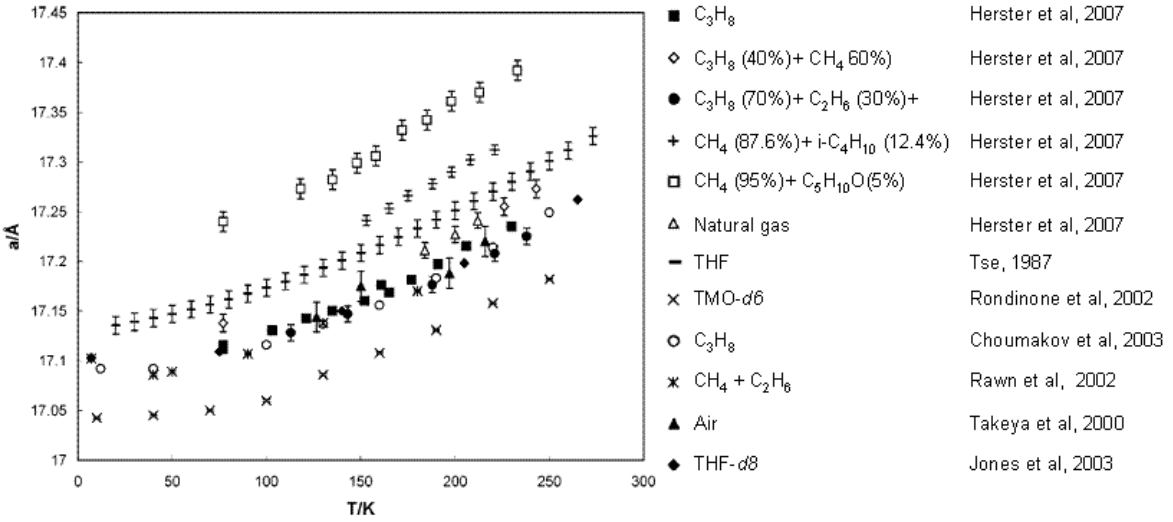

Figure 4 : Lattice parameters versus temperature for varius sII Hydrates, modified from Hester et al (2007)

2.3. OCCUPATION IN THE HYDRATE CAGES

One of the base hypothesis of the model of van der Waals and Platteeuw (1959) which describe the occupancy of cavities by gas molecules is to consider that only one molecule can enter inside, and depending on their side, their affinity varies from one type of cavity to another one. A comparison of guest molecule sizes and cavities sizes is showed on Figure 5 by Sloan and Koh (2007), modified from an original publication of Von Stackelber (1949).

The interest of this figure is to give an indication of the best cavity for each type of gas molecule.

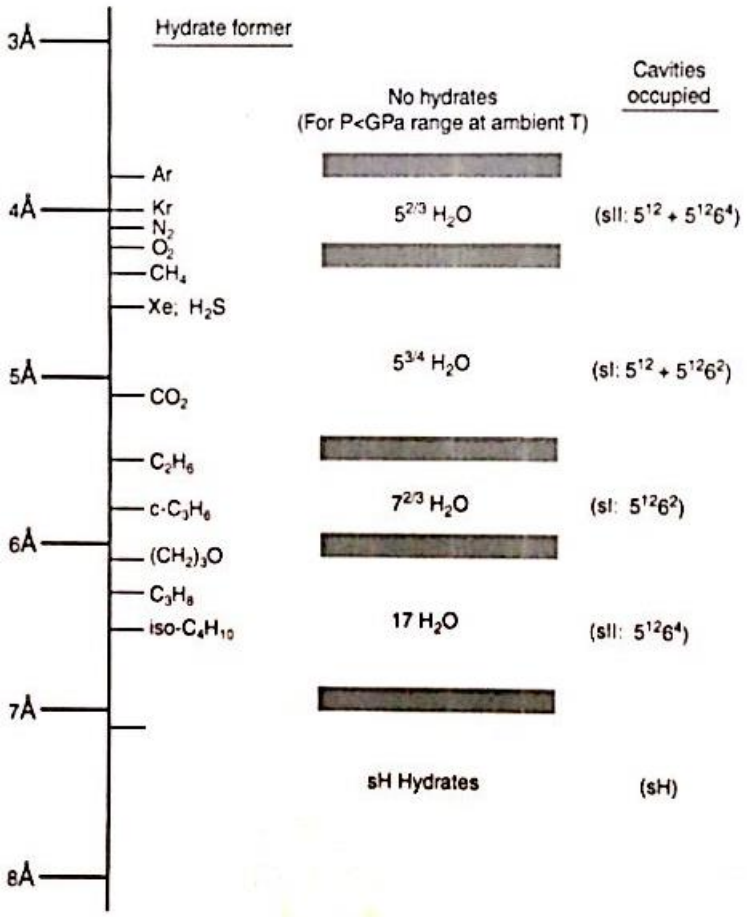

Figure 5 Comparison of guet molecule sizes and cavities occupied as simple hydrates (Sloan and Koh, 2007)

2.4. NUMBER OF HYDRATION

From a given structure, and assuming a full occupancy of cavities, it is possible to give the hydratation number of structure, the number of water molecules per number of gas molecule.

$$n\_hyd = \frac{Number\_molar\_water}{Number\_molar\_gas} \quad (1)$$

With 46 water molecules per unit cell, for a total number of 8 cavities, the number of hydration of structure SI is 46/8=5.75. The number of hydration of structure SII is 136/24 = 5.67. For Structure SH, the maximum number of hydration is 34/6 = 5.67

But, full occupancy of cavities is never the case, because sometimes big gas molecules can occupy only the largest cavities, and also because the cavities are not fully occupied. The Table 2 presents a set of experimental data.

Table 2 Hydration number for simple hydrates of natural Gas components from Handa (1986a,b)

Component	n	reference
Methane	6.0	Handa(1986a,b)
	5.99	Circone et al.(2006)
	5.77	Glew (1962)
	7.0	Roberts et al. (1941)
	7.18	Deaton and Frost (1946)
	6.0	Galloway et al. (1970)
	7.4	De Roo et al. (1983)
	6.3	De Roo et al. (1983)
Ethane	7.67	Handa(1986a,b)
	7.0	Roberts et al. (1941)
	8.25	Deaton and Frost (1946)
	8.24	Galloway et al. (1970)
Propane	17.0	Handa(1986a,b)
	5.7	Miller and Strong (1946)
	17.95	Deaton and Frost (1946)
	18.0	Knox et al. (1961)
	17.0	Cady (1983a)
isobutane	17.0	Handa(1986b)
	17.1	Uchida and Hayano (1964)
	17.5	Rouher and Barduhn (1969)

2.5. MOLAR VOLUME OF GAS HYDRATES

The molar volume of hydrates can be defined to the mole number of water molecules in the hydrate, or in relation to the mole number of gas molecules.

If it is defined to the mole number of water molecules, the molar volume is constant and depends only on the structure. For example, the molar volume of SI structure, composed of 46 water molecules with a lattice parameter of 12.03 Å is (Assane, 2008):

$$V_m^{H-water} = \frac{(12.03.10^3)N_a}{46} \quad (2)$$

Where N_a is the Avogadro number (N_a = 6.02x10^{23} molecules / molar)

In the other definition, the molar volume of the hydrate follow mole of gas is calculated as:

$$V_m^{H-gas} = V_m^{H-water}.n\_hyd \quad (3)$$

where *n_hyd* is the hydration number.

In the Table 3 we present different properties of hydrates CO_2 and CH_4 at temperature of 274^{o}K.

Table 3 Molar volume and density of hydrates CO_2 and CH_4 (Assane, 2008)

consists	CO_2	CH_4
Number of molecules in the unit cell	46	
Structure and Volume unit cell (Å ^{3})	SI,1741	
Density ideal (kg/m^3)	980	912.5
Real number hydratation real at 274 K and P_{eq}	6.24	6.05
Real density at 274 K and P_{eq} (kg/m^3)	1099.5	906.4
Molar volume per molecule water (m^3/mol)	2.28x10^{-5}	
Molar volume per molecule gas (m^3/mol)	1.31x10^{-4}	
Real molar volume at 273 K and P_{eq} (kg/m^3)	1.42x10^{-4}	1.38x10^{-4}

3. GAS PHASE

To calculate the equilibrium parameters, the fugacity coefficient ϕ components of the gas phase have to be determined. It can be calculated using thermodynamic relations at the pressure P (Danesh, 1998).

$$\ln\phi = \ln\frac{f}{P} = \int_0^P (Z-1)\frac{dP}{P} \quad (4)$$

Where, Z is the compressibility factor. In this study we used the equation of state Soave-Redlich-Kwong - SRK (Soave 1972) is:

$$P = RT/(v-b) - a_c\alpha/v(v+b) \quad (5)$$

Where v is the molar volume and a_c and b are constants that depend on the nature and temperature of the gas. The a_c, b parameter can be calculated using a modified equation of the Van Der Waals equation:

$$a_c = 0,42747\frac{R^2T_C^2}{P_C} \quad (6)$$

$$b = 0,08664\frac{RT_C}{P_C} \quad (7)$$

And

$$\alpha = \left[1 + m\left(1 - T_r^{0.5}\right)\right]^2 \quad (8)$$

With $$T_r = \sqrt{\frac{T}{T_c}} \quad (9)$$

Where T_C and P_C are respectively the critical temperature and critical pressure of the gas. m was crrolated with the acentric factor by equating fugacities of saturated liquid and vapour at T_r=0.7. (Ali danesh, 1998).

$$m = 0.048 + 1.574\omega - 0.176\omega^2 \quad (10)$$

To solve the equation of state Eq.(5), the constants used are listed in Table 4

Table 4 Constants for calculating the fugacity of gas.

Gas	P_C (bar)	T_C (K)	ω (-)
CO_2	72.8	304.2	0.2667
N_2	33.5	126.2	0.0372
CH_4	45.4	190.6	0.0104
C_2H_6	48	305.41	0.0979
C_3H_8	42.4	369.77	0.1522
C_4H_{10}	37.84	425.1	0.1995

After rearrangement of the SRK equation of state, we have the compressibility factor is the solution of a cubic function:

Note: in the case of gas mixtures use peudocritical values. Ankur produced a method for calculate, see example below for calculating pseudocritical temperature and pseudocritical pressure

Table 5 example for calculating pseudocritical temperature and pseudocritical pressure

Calculation of Pseudocritical Temperature & Pressure for a Gas Mixture:							
Component description	Mole Fraction, y_i	Component Critical Temp., T_c, °K	Pseudo-critical Temp, T_{pc}, °K	Component Critical Pressure, Pc_i, atmA	Pseudo-critical Pressure, P_{pc}, atm	Component Molecular weight, M_i	Mixture Molecular weight, y_i*M_i
CH_4	0,932	190,6	177,64	45,35	42,27	16,04	14,95
C_2H_6	0,058	305,33	17,71	48,07	2,79	30,07	1,74
C_3H_8	0,01	369,83	3,70	41,92	0,42	44,1	0,44
			0,00		0,00		0,00
			0,00		0,00		0,00
			0,00		0,00		0,00
			0,00		0,00		0,00
			0,00		0,00		0,00
			0,00		0,00		0,00
	1,000	T_{pc} =	199,05	P_{pc} =	45,47	M_{mix} =	17,13

$$Z^3 - Z^2 + \left(A - B^2 - B\right)Z - A\,B = 0 \tag{11}$$

Constants A and B is determined respectively by:

$$A = \frac{a_c P}{R^2 T^2} \tag{12}$$

$$B = \frac{b\,P}{RT} \tag{13}$$

The equation (11) can be solved iteratively or algebraically. We can define new constants Eq((15)(16)) (Bonnefoy 2005). From equation general cube (14)

$$Z^3 + pZ^2 + qZ + r = 0 \tag{14}$$

$$m = q - \frac{p^3}{3} \tag{15}$$

$$n = r + \frac{2p^3 - 9pq}{27} \tag{16}$$

$$\Delta = \frac{n^2}{4} + \frac{m^3}{27} \tag{17}$$

If $\Delta > 0$, then Z is given

$$Z = \frac{-p}{3} + \left(\sqrt{\Delta} - \frac{n}{2}\right)^{\frac{1}{3}} + \left(-\sqrt{\Delta} - \frac{n}{2}\right)^{\frac{1}{3}} \tag{18}$$

If $\Delta < 0$, the compressibility factor is obtained from a different expression :

$$Z = \frac{-p}{3} + 2\sqrt{\frac{-m}{3}} \cdot \cos\left(\frac{\phi}{3}\right) \tag{19}$$

where ϕ is the angle calculated from $\cos(\phi) = -\frac{n}{|n|} \cdot \sqrt{\frac{-27n^2}{4m^3}}$ (20)

In the case of $\Delta = 0$, the fugacity is given

$$\ln\phi = -\frac{A}{B}\ln\left(1 + \frac{B}{Z}\right) - \ln\left(Z - B\right) + Z - 1 \tag{21}$$

Thus, if the acentric factor is known, the critical properties of the gas temperature and pressure, it is possible to determine the compressibility factor, *Z*, after the fugacity and, finally, the transience of gas. The solubility of gas in liquid phase will be present in section 4.

4. THE SOLUBILITIES OF THE GASES IN THE LIQUID PHASE

The gaseous components are dissolved in a liquid phase prior to be crystallized in the hydrate phase. The liquid phase can be both an hydrophilic phase, for example TBAB solution in water, or an hydrocarbon phase, such as cyclopentane when cyclopentane is used as a thermodynamic promoter.

Upon being dissolved in an aqueous phase (L_w), CO_2 molecules do partially undergo acid-base type of chemical reactions: the neutral H_2CO_3 molecules, the ionic species HCO_3^- and CO_3^{2-} are formed in the aqueous liquid phase. However, chemical species other than $CO_2\,(aq)$ do only exist in negligible amounts (26). In the *P*–*T* region of interest, the influence of the species $HCO_3^-(aq)$, $CO_3^{2-}(aq)$, H_2CO_3 on the solubility of CO_2 is negligible (Scharlin, 1996). Thus, the condition of thermodynamic equilibrium for CO_2 reduces to the phase equilibrium condition given in eq(22). Expressed in terms of the fugacity $f_j^{L_w}$, the phase equilibrium condition reads:

$$f_j^{L_w}(T,p,x^{L_w}) = f_j^{L_{hc}}(T,p,x^{L_{hc}}) = f_j^{G}(T,p,y) \tag{22}$$

In eq. (22), $f_j^{L_w}(T,p,x^{L_w})$, $f_j^{L_{hc}}(T,p,x^{L_{hc}})$ and $f_j^{G}(T,p,y)$ denote the fugacities in the liquid aqueous phase (L_w), in liquid organic phase (L_{hc}) and in the gas phase (G) respectively, for the component j.

The fugacity of components in the liquid phases L_w and L_{HC} are given by an extended form of Henry's law.

$$f_j^{L_w}(T,p,x^{L_w}) = x_j^{L_w}\gamma_j^{*,L_w}k_{H,j,w}^{L_w}(T,p) \tag{23}$$

$$f_j^{L_{hc}}(T,p,x^{L_{hc}}) = x_j^{L_{hc}}\gamma_j^{*,L_{hc}}k_{H,j,CP}^{L_{hc}}(T,p) \tag{24}$$

In eq. (23) and eq.(24), the component solubility is considered to be sufficiently low to define the activity coefficient $\gamma_j^{*,L_w \text{ or } L_{hc}}$ equal to unity in the two liquid phases and to assume

that interactions between both liquids are negligible. The liquid phase is considered incompressible. The pressure dependence of Henry's constant can be expressed by means of a Poynting correction in the form of the eq. (25).

$$k_{\mathrm{H},j,s}(T,p) = k_{\mathrm{H},j,s}(T,p_j^{\mathrm{o},\sigma}) \exp\left(\frac{V_{\mathrm{m},j}^{\infty} p}{RT}\right) \tag{25}$$

In eq.(25), $k_{\mathrm{H},j,s}(T,p_j^{\mathrm{o},\sigma})$ and $V_{\mathrm{m},j}^{\infty}$ denote the Henry's constant of gas j in solvent at saturation condition prevailing at liquid-vapor phase equilibrium of the pure solvents and partial molar volume of gas j in solvent s, respectively.

$V_{\mathrm{m},j}^{\infty}$=32 $cm^3.mol^{-1}$ is the partial molar volume of the gas in water from Holder et al (1980).

$K_{H,j}^{\infty}$, is also calculated here from the correlation of Holder et al (1980):

$$K_{H,j}^{\infty} = exp\left(A + \frac{B}{T}\right) \tag{26}$$

Where *A* and *B* are constants, given in Table 6

Table 6 Coefficients for the calculation of the Henry constant, from Holder(1980)

Gas	*A*	*B*
CO_2	14.283146	-2050.3269
N_2	17.934347	-1933.381
CH_4	15.826277	-1559.0631
C_2H_6	18.400368	-2410.4807
C_3H_8	20.958631	-3109.3918
n-C_4H_{10}	22.150557	-2739.7313

5. EXPERIMENTAL EQUILIBRIUM POINTS

5.1. MATERIALS OF EXPERIMENT

In this work, we used bottles of the individual gases CO_2, CH_4, C_2H_6, C_3H_8, C_4H_{10}, provided by Air liquide. The water is de-ionised from the MILLI-Q 185 PLUS system (IONEX). In the liquid phase contains $LiNO_3$ as a tracer (10ppm weight fraction).

Table 7 Compositions of the gas use for experiments

Impurity	CO2	N2	CH4	C_2H_6	C_3H_8	C_4H_{10}
H_2O	< 7ppm	< 3 ppm	< 5 ppm	< 5 ppm	< 5 ppm	< 5 ppm
C_2H_6	-	-	< 200 ppm	-	-	-
CnHm	< 5 ppm	< 2 ppm	< 50 ppm	< 25 ppm	< 200 ppm	-
CO	< 2 ppm	-	-	-	-	-
CO_2	-	-	< 10 ppm	< 5 ppm	< 5 ppm	< 20 ppm
O_2	< 10 ppm	< 0.5 ppm	< 10 ppm	< 10 ppm	< 10 ppm	< 10 ppm
H_2	< 1 ppm	-	< 20 ppm	< 40 ppm	< 40 ppm	-
N_2	< 25 ppm	-	< 200 ppm	< 40 ppm	< 40 ppm	< 40 ppm

5.2. PREPARATION OF GAS MIXTURES

Mixtures studied in this study are hydrocarbon and carbon dioxide (CH_4 ,C_2H_6 C_3H_8, n-C_4H_{10}, CO_2) mixtures. The compositions are detailed in Table 8.

Table 8 Theoretical request for composition of gas mixtures

Gas	*Gas 1*	*Gas 2*	*Gas 3*	*Gas 4*	*Gas 5*	*Gas 6*
CO_2	-	1	0,2	0,06	-	-
CH_4	1	-	0,8	0,91	0,95	0,86
C_2H_6	-	-	-	0,03	0,03	0,05
C_3H_8	-	-	-	-	0,02	0,06
$n\text{-}C_4H_{10}$	-	-	-	-	-	0,03

Two methods are used to prepare the gas mixture, one consist in preparing directly the mixture in the reactor, the other in preparing the gas mixture outside, in a preparation room, and to feed the reactor directly with a bottle of the gas mixture.

- Case 1: Bottles of each gas are directly connected to the reactor (Experiments No. 4, 5 in Figure 6). The mixture is made by a sequential injection of the gases into the reactor which has been previously vacuumed. The quantities of gases is controlled from the pressure monitoring and the knowledge of the exact composition is validated by gas chromatography. The mass balance is made from a method given in section. This method has been used for binary mixtures.

- Case 2: For all other gas mixtures (more than two gas), an external gas bottle has been prepared in a preparation room, also by successive injections of each gas, from less volatile to more volatile, by controlling the pressure. At each step, the composition is determined from a weighing with a balance of 0.1 g precision. The final composition is cross validated by gas chromatography.

Due to the methods, it is difficult to get exactly the compositions specified in Table 8. The final composition is given in Table 11.

5.3. EXPERIMENTAL SET-UP

The experimental apparatus (Figure 6) is designed to measure the thermodynamic equilibrium points in presence of gas mixture and to determine the composition of all phases (gas, liquid and hydrate). The reactor consists of a 2.36 liter autoclave reactor in which the pressure can reach up to 100 bars. The reactor is equipped with two vertical stirrers with four

blades, one in the liquid, one in the gas. The stirring rate can vary between 0 and 600 rpm. The temperature is controlled by a double jacket in which is circulated a fluid at constant temperature from a cryostat HUBERT CC-250. A Pyrex cell is laid inside the reactor and filled with water containing Lithium as an anion tracer. The liquid is injected in the reactor under pressure by using a HPLC pump (JASCO). Temperature is monitored by two Pt100 probes, one in the gas phase, the other in the liquid phase. The pressure is measured with an accuracy of 0.01 MPa in the range 0-10 MPa. A ROLSI sampler is mounted on the reactor. It allows to sampling online the gas and to sending the sample into a gas chromatograph (GC Varian model 38002) equipped with a TCD detector and two columns PoraBOND Q and CP-Molsieve. The peak integration is possible with software provided by Varian Galaxie. Another sampling system can exit the liquid phase through a mechanical valve and a capillary tube. The liquid is analyzed off-line by ion chromatography. The data acquisition is controlled on the personal computer.

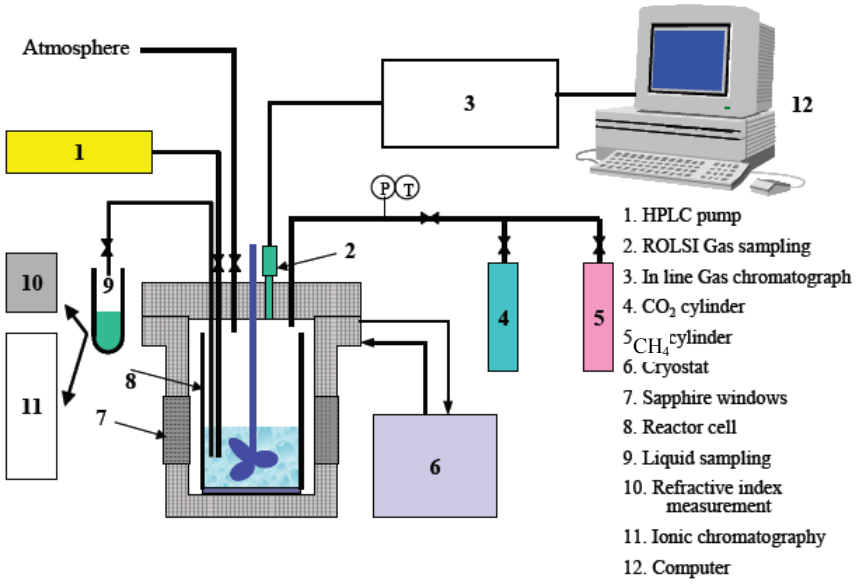

Figure 6 Experimental device

5.4. EXPERIMENTAL PROTOCOL

Initially, the reactor is cleaned with water and evacuated by a vacuum pump for 40 minutes. Then, depending on the case (see section 5.2), the pure gases are directly injected into the reactor from pure gas cylinders (CO_2 and CH_4), or from a bottle prepared previously at the good composition. In each case, the first injection of gas is repeated three times after a purge under vacuuming, to ensure that air is totally evacuated.

The temperature is initially set with the thermostat at the value of 1°C. The control of temperature takes into account a difference between the temperature of the glycol solution circulating in the jacket, and the effective temperature in the reactor which is around the value of 1.5°C higher, but depends on the room temperature.

The experiments are realized following 3 steps

Step 1: Injection of the pure gas, or gas mixture, following the procedure given in 5.2 (case 1 or case 2). The stirrer is on. The composition of the gas is controlled via gas chromatography.

Step 2: Injection of water: The stirrer is stopped. The water solution containing 10 ppm molar fraction of LiNO3 (tracer) is prepared and injected via the HPLC pump with the amount of 800 g measured by a mass balance. Pressure and temperature increase due to the gas contraction volume. Then, the pressure decreases because a fraction of the gas dissolves in the liquid phase. The temperature also decreases because to reach the operative temperature controlled by the cooling jacket. Agitation is restarted, and the evolution of the temperature and pressure in the reactor is monitored. After a delay corresponding to the induction time, ranging from minutes to hours (nucleation is a stochastic phenomenon), the crystallization starts, gas is consumed and the pressure is dropped down to the equilibrium. It is accompanied by a temperature increase due to the exothermic character of the crystallization. During formation of the solid phase, the pressure decreases because it consumes gas. The crystallization is occurring during hours and days, during which the gas phase is sampled on-line. The liquid phase is also sampled and analyzed later (off-lines).

Step 3: Dissociation of hydrates: when the system is at equilibrium (temperature and pressure are stable), the reactor is heated by steps of 1°K until a full dissociation of hydrates (Figure 8). At each stage of dissociation, a gas sample is taken with the sampler ROLSI and it is sent to the gas chromatograph (on-line) to determine the gas compositions in gas phase. The liquid is also sampled to determine the concentration of Lithium in the water, after off line analysis in an ion chromatography. During each step, the pressure in the reactor increases due to the dissociation of hydrates and reaches a constant value which is considered as the thermodynamic equilibrium. This step is repeated until total dissociation. After a

complete dissociation, the pressure in the reactor continues to increase but only in respect to the dilatation of gases and decrease of the solubility of gases.

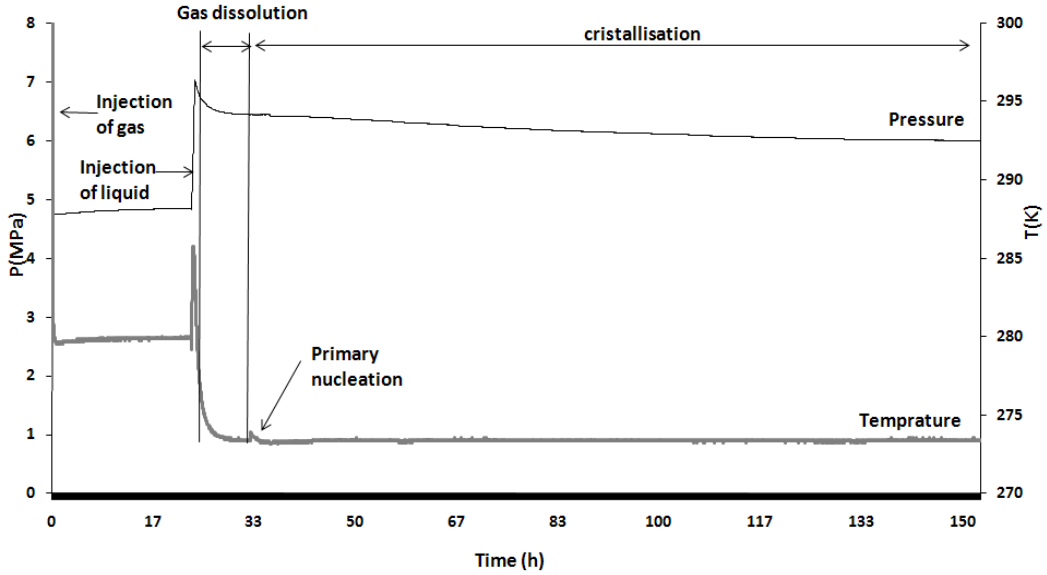

Figure 7 Evolution of pressure and temperature during the Crystallization

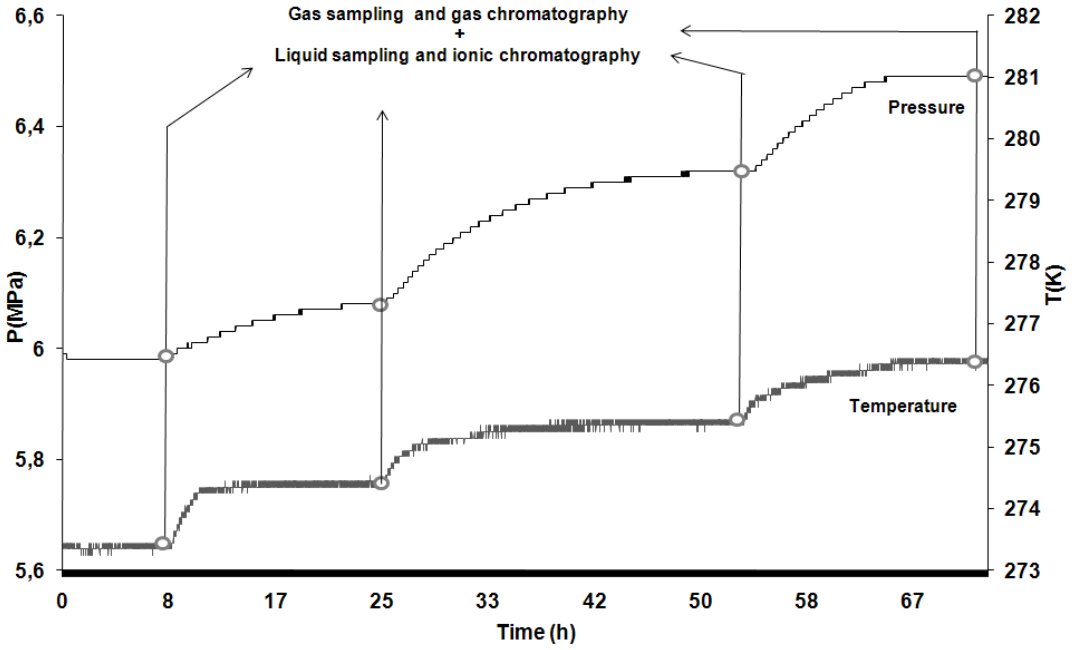

Figure 8 Evolution of pressure and temperature during the dissociation

5.5. CALIBRATION OF THE GC DETECTOR

In these studies the gas Chromatograph used is the Varian 3800 GC model, the gas chromatograph allows us to know the composition of a gas mixture. In fact, the area of a

given peak of component A in the chromatogram is proportional to the amount of material (n_A) in the sample.

$$S_A = k_A n_A = k_A n_T x_A \tag{27}$$

n_T represents the number of moles of all the species, and x_A is the molar fraction of component A. k_A is a constant of proportionality which can be determined experimentally if the amount of A is known. But, in our experiment, the amount of component can not be determined after sampling due to the sampling method. In fact, the Rolsi instrument is a valve that is opened during a period of time. During this period, the amount of material is proportional to the flow rate, and the flow rate is directly proportional to the pressure. The pressure is not a process control parameter, but is dependent from equilibrium considerations, for example the temperature.

So, we need to use a relative calibration method, by taking a gas as a reference, here the methane because it is the higher composition component, in general:

$$S_A = k_A n_A = k_A n_T x_A \tag{28}$$

$$S_{CH_4} = k_{CH_4} n_{CH_4} = k_{CH_4} n_T x_{CH_4} \tag{29}$$

$$\frac{S_A}{S_{CH_4}} = k_{A,CH_4} \frac{x_A}{x_{CH_4}} \tag{30}$$

The calibration curves are presented in the form of the straight lines with different slopes ($K_{A,CH_4} = 1/k_{A,CH_4}$) and given in Figure 9 to **Erreur ! Source du renvoi introuvable.**.

Once the K_{A,CH_4} constants have been determined, for a given gas mixture, the gas composition is given by the following equations:

$$x_{CH_4} = \frac{1}{1 + \sum_{A \neq CH_4} K_{A,CH_4} \frac{S_A}{S_{CH_4}}} \tag{31}$$

$$x_{A \neq CH_4} = \frac{S_A}{S_{CH_4}} x_{CH_4} K_{A,CH_4} \tag{32}$$

5.5.1 Calibration of CO_2

Table 9 Results of the calibration of gas chromatography (CO_2-CH_4)

$P(CO_2)$ bars	$P(CH_4)$ bars	$X(CO_2)/X(CH_4)$ from mass balance, case 1, §5.2	$S(CO_2)/S(CH_4)$ from gas chromatography	$X(CO_2)/X(CH_4)$ from GC and Eqs.(31) and (32)	Erreur (%)
19.9	5.6	4.28	6.07	4.44	2.89
15.6	5.6	3.22	4.77	3.48	5.87
10.6	5.6	2.10	3.13	2.29	5.84
10.5	7.9	1.30	1.85	1.35	2.21
6.2	5.3	1.15	1.60	1.17	0.70
5.1	5.6	0.97	1.45	1.06	4.60
6.2	10.2	0.59	0.85	0.62	1.93
10.5	17.9	0.56	0.80	0.58	1.30
10.8	19.9	0.52	0.79	0.57	3.65
10.8	23	0.44	0.68	0.50	3.65
10.8	28	0.36	0.54	0.40	2.62
10.5	29.3	0.33	0.49	0.36	1.61
6.7	20.1	0.32	0.46	0.34	1.52
6.2	18.9	0.31	0.44	0.32	0.65
10.5	35.1	0.27	0.41	0.30	2.07
10.8	36.9	0.27	0.40	0.29	1.73
6.7	29.6	0.21	0.32	0.23	1.68
6.3	29.5	0.20	0.28	0.20	0.21
6.2	29.2	0.20	0.28	0.21	0.74
6.7	40.1	0.15	0.22	0.16	0.53
6.2	39.8	1.45	0.22	0.20	1.45
The average Deviation					2.20

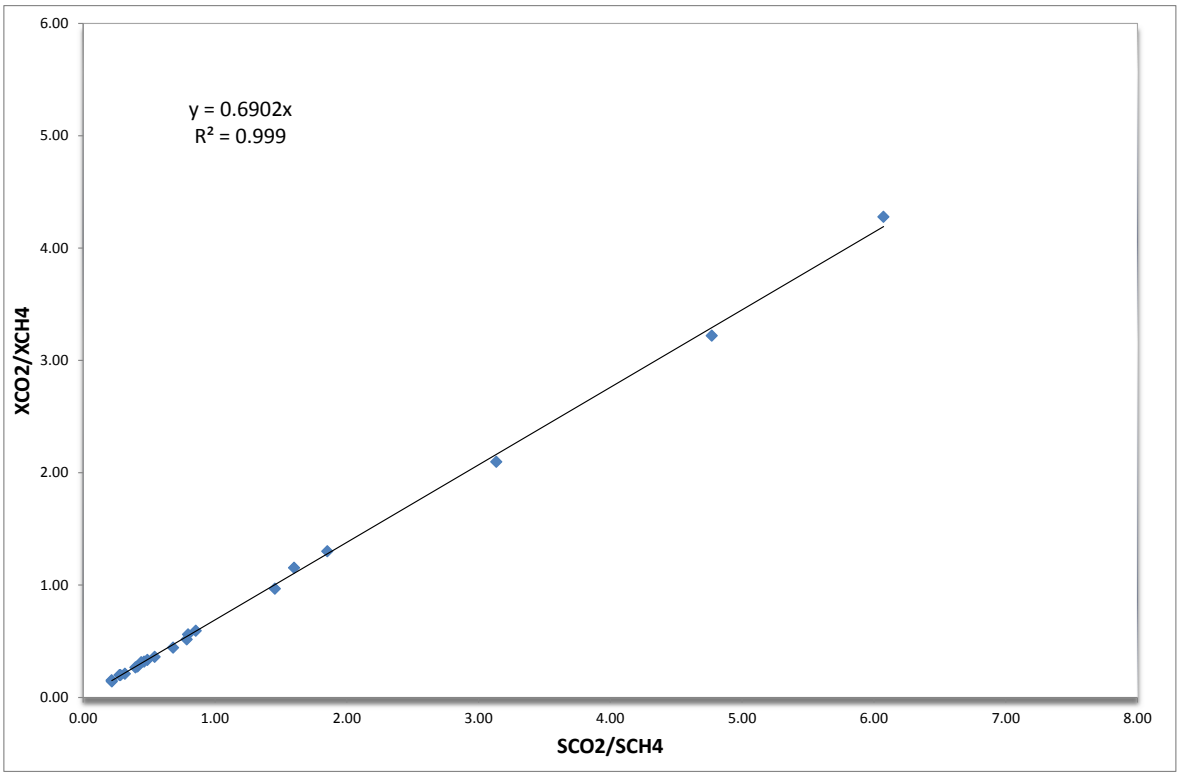

Figure 9 Calibration curve of the gas chromatograph for CO_2-CH_4

5.5.2 Calibration of C_2H_6

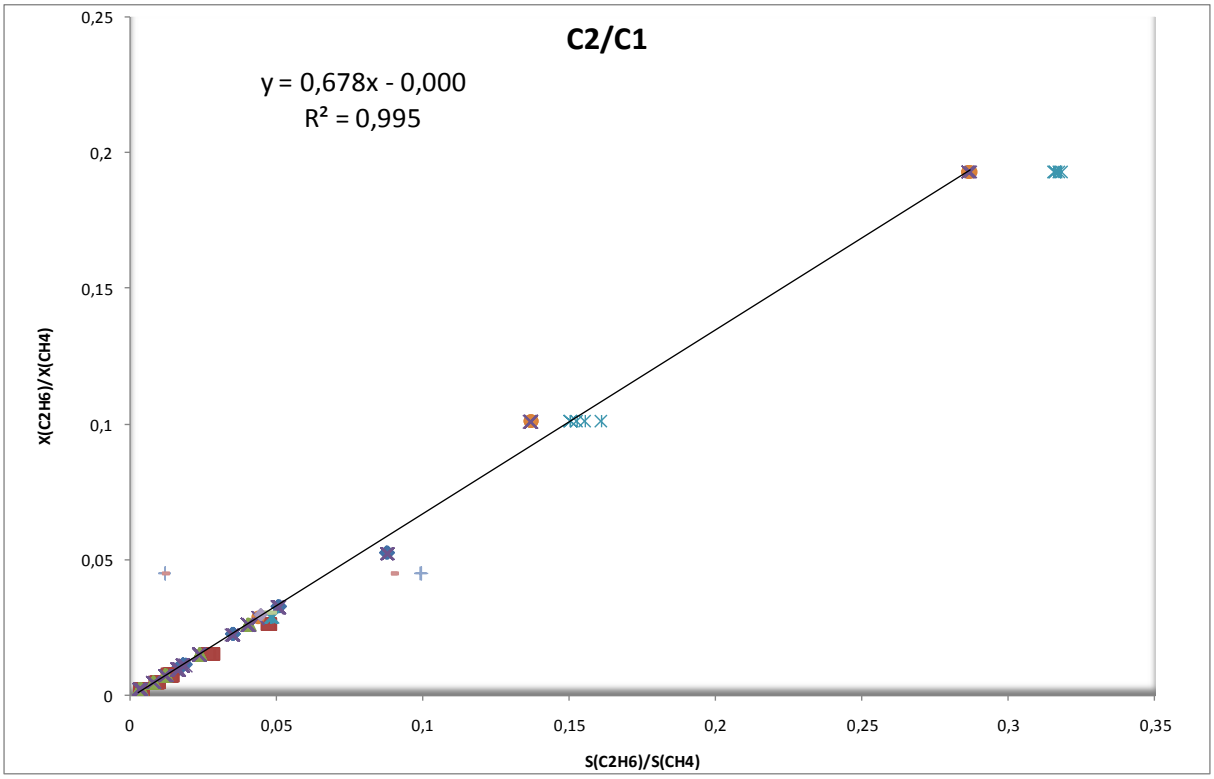

Figure 10Calibration curve of the gas chromatograph for C_2H_6-CH_4

5.5.3 Calibration of C_3H_8

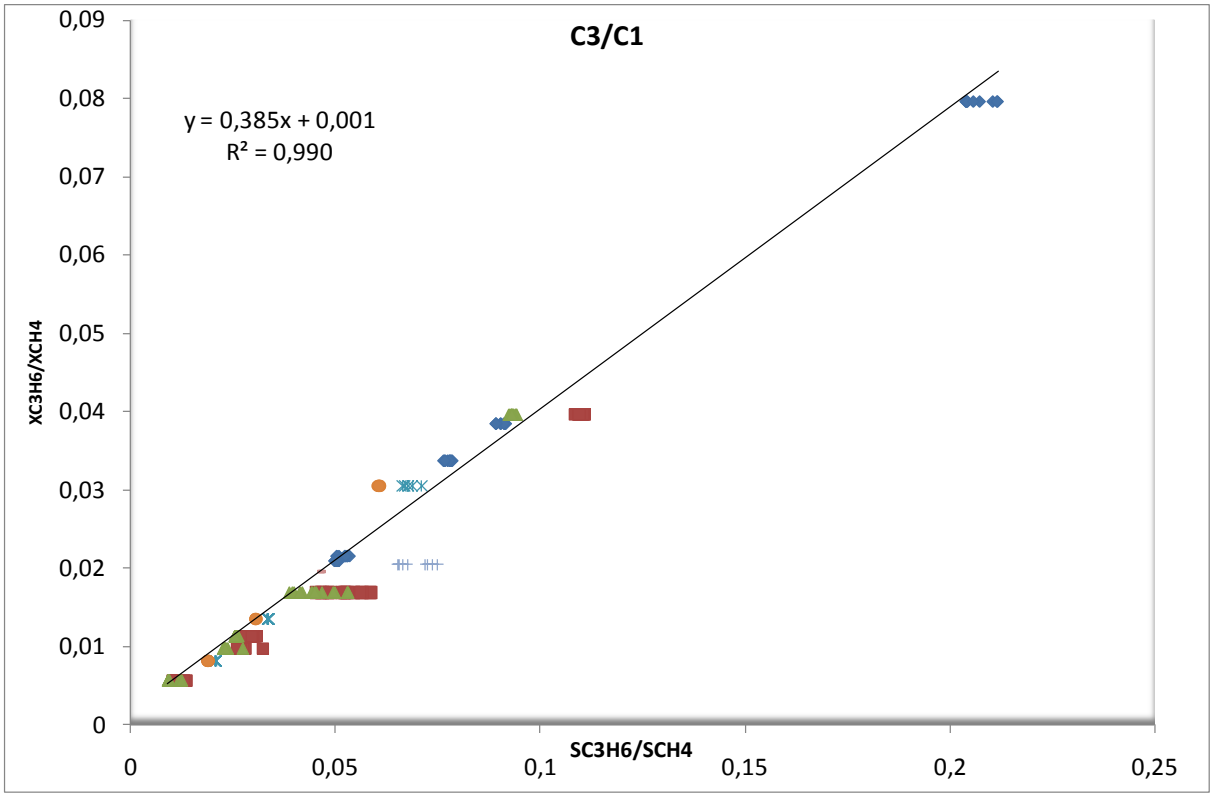

Figure 11Calibration curve of the gas chromatograph for C_3H_8-CH_4

5.5.4 Calibration of C_4H_{10}

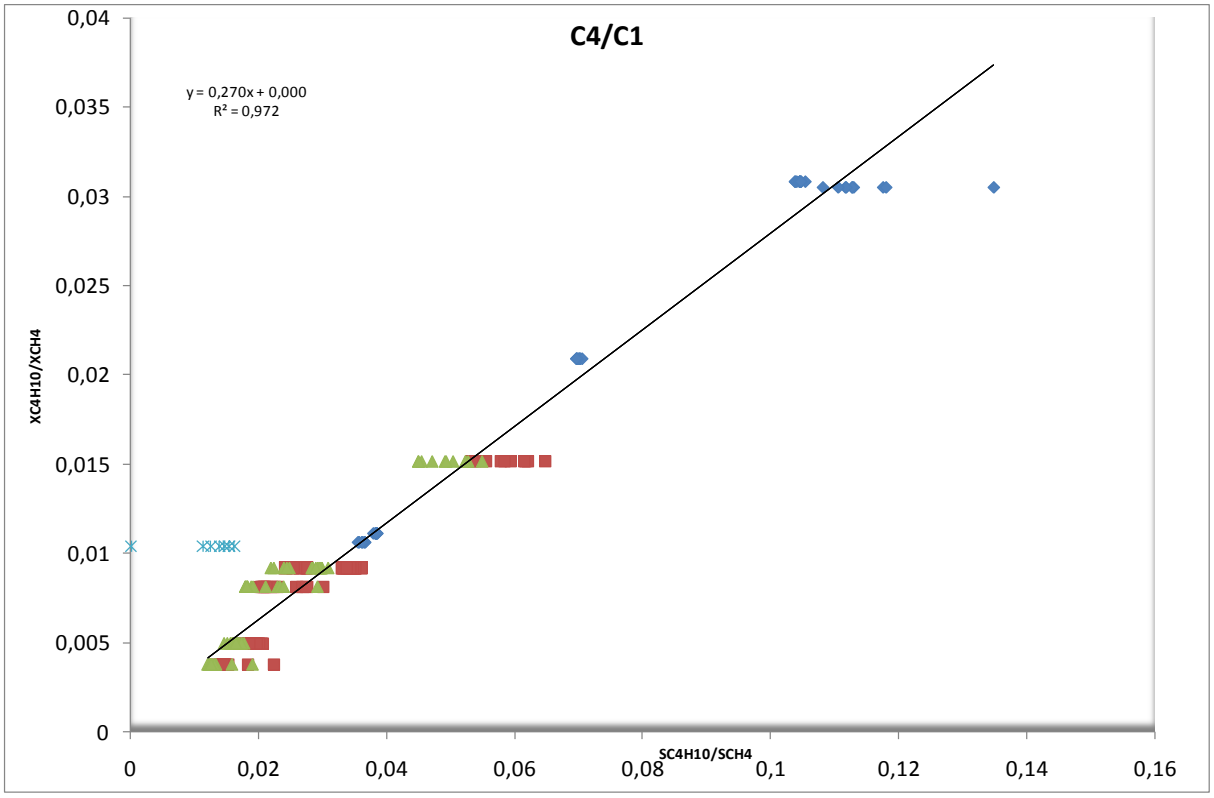

Figure 12 Calibration curve of the gas chromatograph for C_4H_{10}-CH_4

5.6. EXPERIMENTAL RESULTS

In this section, we present our method to calculate the mass balance, and evaluate the hydrate composition as a function of the gas composition at a given temperature and pressure. We give also the experimental results under the form of figures and tables.

5.6.1 Calculation of the composition in the different coexisting phases

To calculate the mole number of each gas in the different coexisting phases, a mass balance is used. Notes n_j^0 is the amount of initial and molecule total gas j in the reactor:

$$n_j^0 = n_j^G + n_j^L + n_j^H \tag{33}$$

Where exhibitors G, L and H correspond to gas phase, liquid and hydrate.

And:

- n_j^G the number of moles of gas j in the gaseous phase,

- n_j^L the number of moles of gas j in the liquid phase j,

- n_j^H the number of moles of gas j in the hydrate phase.

The initial quantity of gases in the reactor is finally distributed within the three phases. Before and during the crystallization, or at equilibrium, the composition of gas in the gas phase is determined from a gas chromatography analysis given in Eqs.(31) and (32). The total mole number in the gas phase is calculated from the classical state equation:

$$PV_0 = ZnRT_0 \tag{34}$$

Where, Z is the compressibility factor, n is the total mole number of gas molecules. P is the pressure. V_0 is the total volume of the reactor (V_0 = $V_{reactor}$ = 2.36 L). T_0 is the temperature (°K) and R is universal gas constant.

- *In the gas phase*

The number of moles in the gas phase is determined by the classical equation of gas:

$$PV_G = Zn^G RT \tag{35}$$

with:

- P is the pressure in the reactor,

- T is the temperature in the reactor,

- V_G is the volume of the gas, approximated by $V_G = V_0 - V_w$,

- Z is the compressibility factor,

- V_w The volume of water,

- n^G is the total number of moles in the gas.

where the compressibility factor (Z) is determined from the critical properties and acentric factor (ω) as explained in section 3. From P, V, T, and the composition of the mixtures gas (by chromatography), n_j^G is calculated for each gas j.

Note: The volume occupied by the gas is equal to the reactor volume minus the volume of the liquid (≈ water) and hydrate (determined from the Li concentration measurement that gives the amount of liquid water consumed).

- *In the liquid phase*

At equilibrium, the quantity of gas in the liquid is calculated from two steps, calculation of the volume of remaining water, and calculation of the dissolved components from a gas/liquid model assumption.

Calculation of the volume of water

As mentioned before, the liquid phase (water) contains a tracer $LiNO_3$. Initially the concentration of lithium $[Li^+]^0$ and the initial volume of liquid V_0^L are known (Lithium is about 10 ppm, and water is about 800ml). During crystallization and dissociation steps, the concentration of lithium is measured by ionic chromatography after sampling. So, we can calculate the volume of remaining liquid water by:

$$V_0^L \left[Li^+\right]^0 = V_{eq}^L [Li^+]^{eq} \tag{36}$$

$$\Rightarrow V_{eq}^L = \frac{V_0^L . \left[Li^+\right]^0}{\left[Li^+\right]^{eq}} \tag{37}$$

Where, $\left[Li^+\right]^{eq}$, V_0^L are concentration of lithium at equilibrium and volume of water injection is the concentration after sampling, at equilibrium.

Modeling the Liquid-vapor equilibria for each gas.

The composition of the liquid phase for each gas is calculated by:

$$f_j^L\left(T,P,y_j\right)=f_j^G\left(T,P,z_j\right) \tag{38}$$

For this calculation, Henry's law is applied leading to:

$$n_j^L=\frac{V^L\rho_w^o}{M_w}\frac{y_j\varphi_j^G P}{K_{H,j}^{\infty}exp\left(Pv_j^{\infty}/RT\right)} \tag{39}$$

with:

- ρ_w^o And M_w, the density and molecular mass of water,

- φ_j^G , The fugacity coefficient of gas j

- $K_{H,j}^{\infty}$, Henry's constant saturation pressure of the pure solvent

- V^{∞} =32 $cm^3.mol^{-1}$, the partial molar volume of the gas in water, Holder et al (1980)

- *Hydrate Phase*

The quantity of gas in the hydrate phase could be determined from a simple mass:

$$n_j^H=n_j^0-n_j^L-n_j^G \tag{40}$$

5.6.2 Calculation of equilibrium points

For calculation this work, we have all input data from monitoring (P,T), gas chromatography (molar fraction of gas), liquid chromatography (concentration of lithium), Mass balance (mass of injection water)and we can canculation of all parameter of the coexisting phases:

Initial molar of the gas in the reactor:

$$n^0=\frac{PV_0}{ZRT_0} \tag{41}$$

Initial molar of each gas can calculate:

$$n_j^0=n^0XG_j=\frac{PV_0}{ZRT_0}XG_j \tag{42}$$

Where, XG_j is concentration of gas *j* in the gas phase, they have been determined by gas chromatography and calibration curve see more section 5.5

When the systems achieve equilibrium, the concentration of gas phase are determined by gas chromatography supports to calculate of the mole number of each gas follows:

$$n_j^G = n_{eq}^G XG_j^G \tag{43}$$

Where, XG_j^G, n_{eq}^G are concentration of gas *j* in the gas phase at equilibrium and total mole number of the gas in the gas phase

$$n_{eq}^G = \frac{P_{eq} V_{eq}^G}{Z_{eq} RT_{eq}} \tag{44}$$

$$\Rightarrow n_j^G = \frac{P_{eq} V_{eq}^G}{Z_{eq} RT_{eq}} XG_j^G \tag{45}$$

Where,

P_{eq} is pressure at equilibrium

T_{eq} is temperature at equilibrium

Z_{eq} is compressibility factor of gas mixtures at equilibrium

V_{eq}^G is volume of the gas phase at equilibrium

$$V_{eq}^G = V_0 - V_w \tag{46}$$

Where, V_w The volume of water injection,

From sample results ion-chromatography, we have the value of $[Li^+]^o$, $[Li^+]^{eq}$, the volume of water consumption by hydrate can calculate as:

$$V_w^H = V_0^L - V_{eq}^L = V_0^L - \frac{V_0^L . \left[Li^+\right]^0}{\left[Li^+\right]^{eq}} \tag{47}$$

The solubility of gas in the liquid phase are calculated by eq.(39) after that we calculated mole number of each gas in hydrate phase following eq. (40).

We can calculate the hydration number n_hyd by:

$$n\_hyd = \frac{n^W}{n_G^H} \tag{48}$$

n^W is mole number of the water in hydrate phase, with $n^W = \frac{V_w^H}{M_w}$

Where, M_w is molecular mass of water

n_G^H is mole number of the gas in hydrate phase, $n_G^H = \sum_j n_j^G$

Finally, we calculated mole fraction in the hydrate phase by following:

$$XG_j^H = \frac{n_j^H}{\sum_j n_j^H} = \frac{n_j^H}{\sum_j (n_j^0 - n_j^L - n_j^G)} \tag{49}$$

From eq.(40) and eq.(49)

$$XG_j^H = \frac{n_j^H}{\sum_j (n_j^0 - n_j^L - n_j^G)} \tag{50}$$

Where, XG_j^H is mole fraction of gas j in phase hydrate

A summary of the steps calculation is presented in the figure Figure 13:

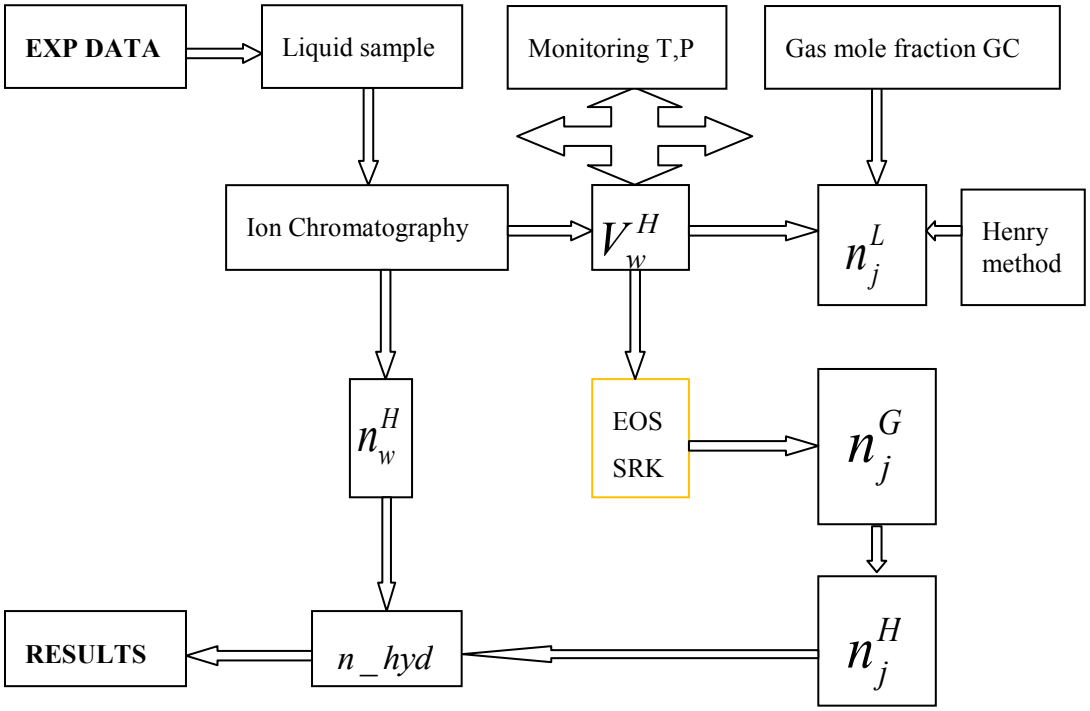

Figure 13 Step of calculation data

5.6.3 Summary of the Experimental results

Table 10 gives the different experiments that we have performed for pure gas, binary mixtures and multiple mixtures. Table 11 gives the details of the initial compositions.

Table 10 List of experiments: ranges of Pressure and Temperature, number of equilibrium points.

Mixtures	Range of Pressure (bar)	Range of Temperature (^oC)	Number of equilibrium points
CO_2	14.51 – 17.02	1.6 – 2.6	4
CH_4	43.7 - 61	0.8 – 2.8	5
CO_2/CH_4	29.1 – 56.3	2.2 – 9.5	7
$CO_2/CH_4/C_2H_6$	27.1 – 65.7	1 – 12.5	7
$CH_4/C_2H_6/C_3H_8$	31.3 - 46	2.3 - 11	9
$CH_4/C_2H_6/C_3H_8/C_4H_{10}$	37.3 – 38.2	2.9 – 18.6	21

Table 11: Initial composition of the different experiments

Number Exp	Composition of gas (%)					Quantity of gas (Mole)	Li^+	Water [g]	Reactor vol. [L]
	CO_2	CH_4	C_2H_6	C_3H_8	C_4H_{10}				
1	45.70	55.30	-	-	-	4.08	9.93	800.10	2.36
2	22.60	77.40	-	-	-	3.99	10.76	824.11	2.36
3	75.30	24.70	-	-	-	4.01	10.40	800.15	2.36
4	24.70	75.30	-	-	-	4.08	11.32	800.00	2.36
5	100	-	-	-	-	3.06	10.78	800,5	2.36
6	-	100	-	-	-	5.80	10,53	801,35	2.36
7	11.70	82.50	5.80	-	-	3.75	10.17	801.25	2.36
8	5.30	91.90	2.80	-	-	2.38	10.50	799.58	2.36
9	-	94.04	2.70	3.26	-	3.69	10.12	800.59	2.36
10	-	86.30	5.73	5.30	2.67	2.95	10.40	800.60	2.36
11	-	84.80	5.02	7.55	2.63	2.87	10.04	800.60	2.36
12	11.20	83.16	5.64	-	-	5.70	10.78	800.30	2.36

5.6.4 Experiments on pure CO_2

In this experiment we did crystallization of pure CO_2 with their initial composition is shown in Table 12.

Table 12: Experimental results for CO_2 gas

T (°C)	P_{eq} (bar)	CO_2 in the liquid (molar)	Li+ (mg/l)	CO_2 in the hydrate (molar)	CO_2 in gas phase(molar)	Hydratation number

2.2	16.2	0.646	12.65	1.18	1.24	5.6
3.3	18.2	0.711	12.5	0.95	1.4	6.4
4.1	20.1	0.79	12.2	0.71	1.57	7.3
5	22.6	0.92	11.4	0.34	1.8	7

Below is figure of evolution of pressure and temperature during crystallization and dissociation.

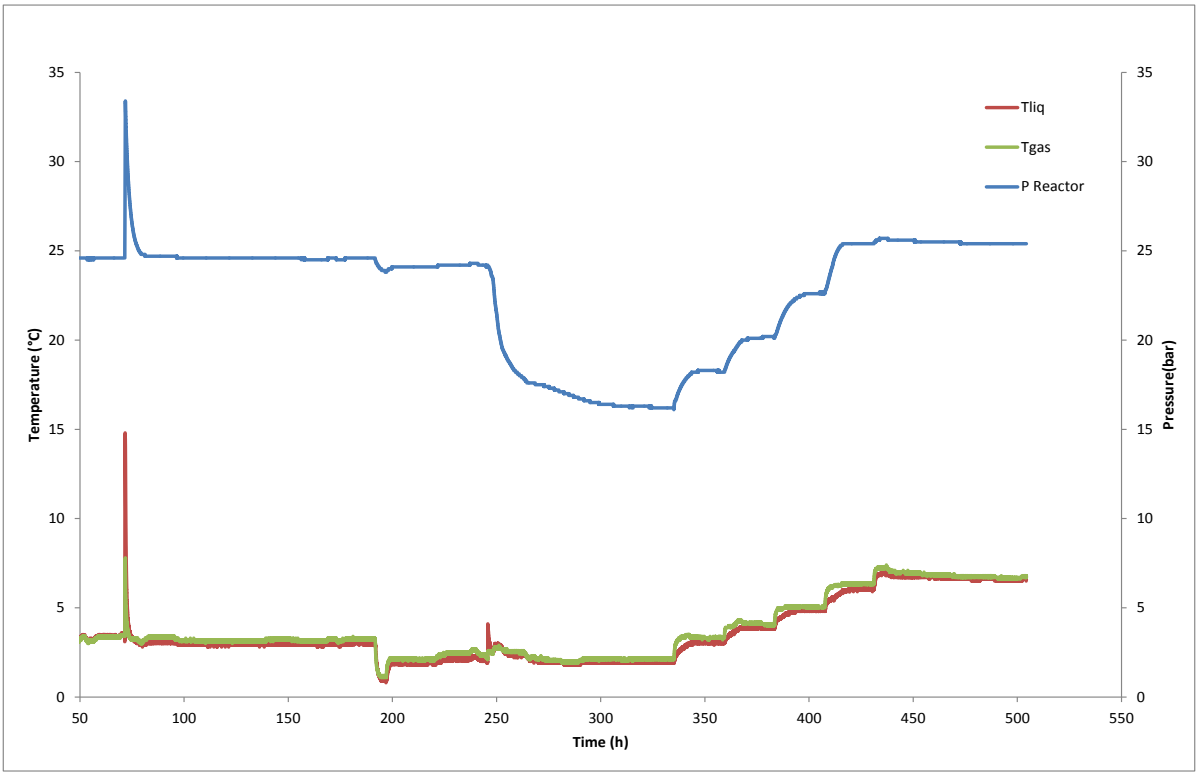

Figure 14 Evolution of the pressure and temperature in the experiment with pure CO_2

5.6.5 Experiments on pure CH_4

Table 13 Experimental results for pure CH_4 gas

T (°C)	P_{eq} (bar)	CH_4 in the Liquid (molar)	Li+ (mg/l)	CH_4 in the hydrate (molar)	CH_4 in the gas (molar)	Hydratation number
3.0	37.0	0.037	17.70	3.08	2.68	5.8
4.5	42.0	0.041	17.51	2.70	3.06	6.5
5.7	47.4	0.050	16.04	2.27	3.48	6.7

7.3	55.4	0.065	13.82	1.61	4.12	6.6
8.8	64.9	0.086	11.93	0.80	4.91	6.5

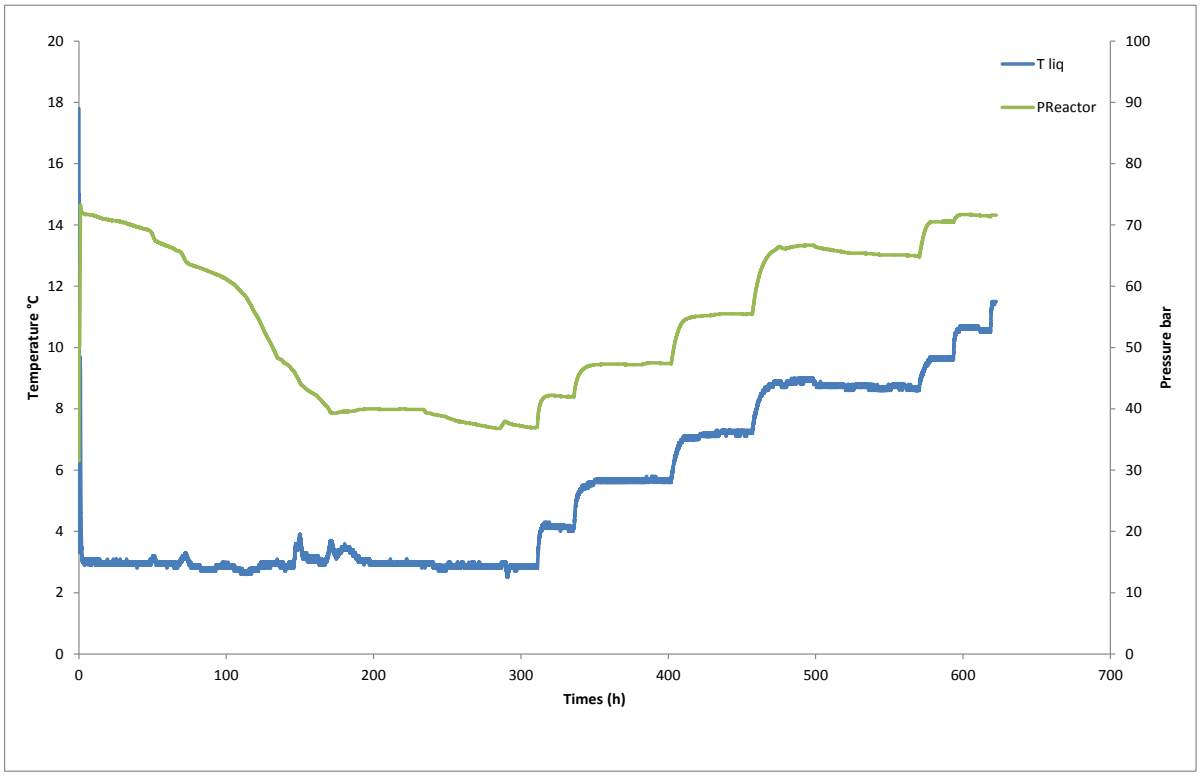

Figure 15 Evolution of the pressure and temperature in the experiment pure CH_4

5.6.6 Experiments on gas mixture (CH_4 - CO_2)

Table 14 Results of experiment 24.70% CH_4 and 75.30% CO_2

T (°C)	P_{eq} (bar)	Li+ (mg/l)	Mole fraction in the gas		Mole fraction in the hydrates		Hydratation number
			CO_2	CH_4	CO_2	CH_4	
2.2	19.2	14.11	0.655	0.345	0.77	0.23	5.6
2.9	20.5	14.46	0.776	0.224	0.67	0.33	6.4
4.0	22.6	13.71	0.659	0.341	0.77	0.23	5.9
4.5	24.4	13.15	0.665	0.335	0.77	0.23	5.8
5.5	27.1	12.51	0.670	0.33	0.77	0.23	5.8
6.5	30.1	11.81	0.678	0.322	0.76	0.24	5.8
7.3	33.1	11.16	0.682	0.318	0.73	0.27	5.8

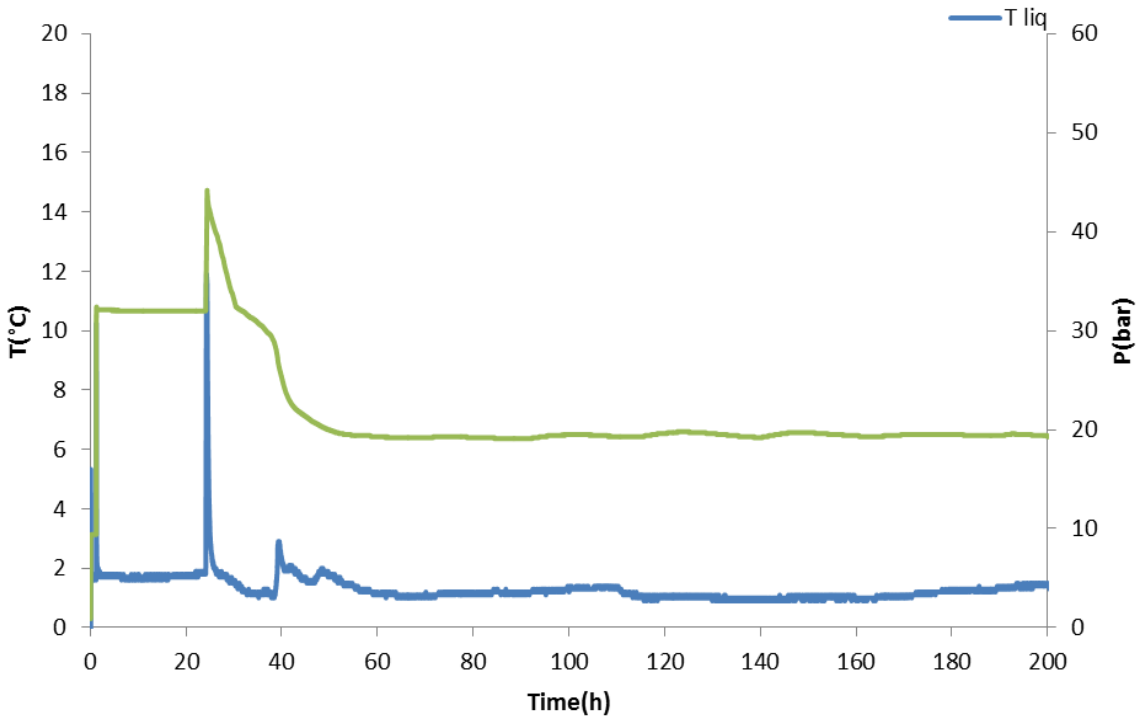

Figure 16 Evolution of the pressure and temperature in the experiment mixtures CH_4 - CO_2 during crystallization

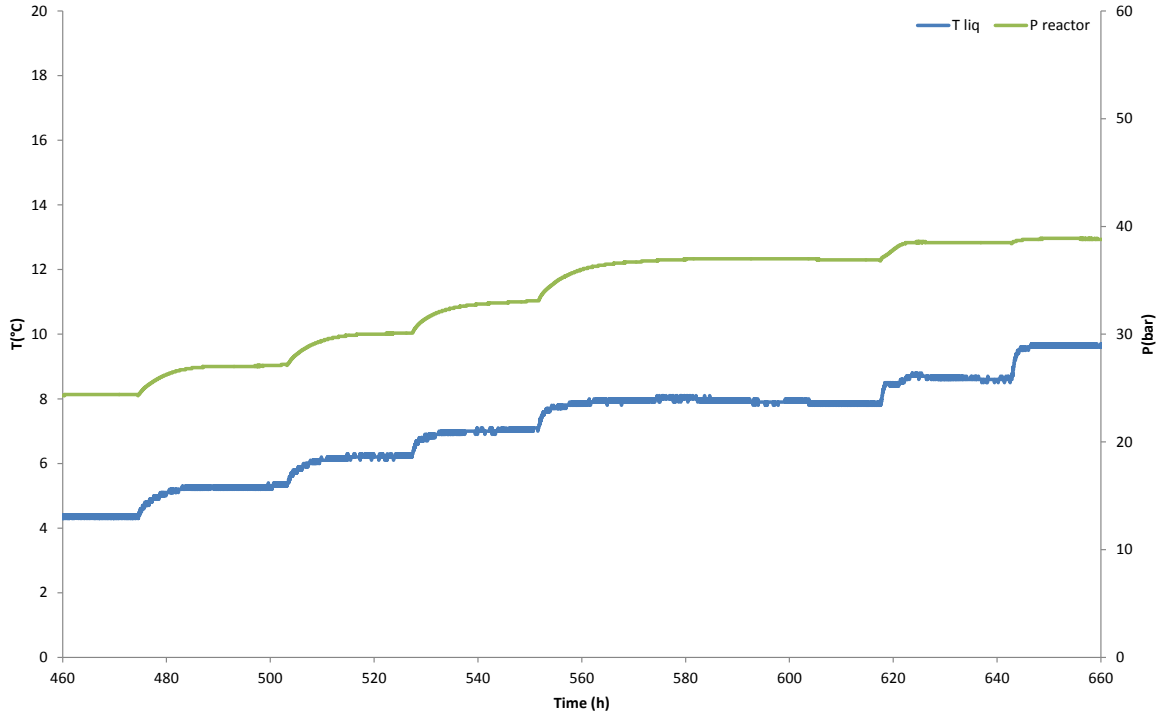

Figure 17 Evolution of the pressure and temperature in the experiment mixture CH_4 - CO_2 during dissociation

5.6.7 Experiments on gas mixture ($CO_2/CH_4/C_2H_6$)

Table 15 Results of experiment of mixtures ($CO_2/CH_4/C_2H_6$)

T (°C)	P_{eq} (bar)	Mole fraction in the gas			Li^+ (mg/l)	Mole fraction in the Hydrate			Hydratation number
		CH_4	CO_2	C_2H_6		CH_4	CO_2	C_2H_6	
1.9	35.4	0.91	0.06	0.03	16.36	0.79	0.16	0.05	5.08
3.0	38.1	0.91	0.06	0.03	17.31	0.82	0.14	0.04	6.06
4.6	42.3	0.89	0.07	0.04	16.27	0.77	0.10	0.03	6.23
6.2	45.6	0.89	0.07	0.04	15.18	0.89	0.08	0.03	6.06
7.5	51.2	0.87	0.08	0.05	13.83	0.93	0.05	0.02	6.05
9.1	59.9	0.87	0.09	0.04	12.29	0.97	0.01	0.02	7.01

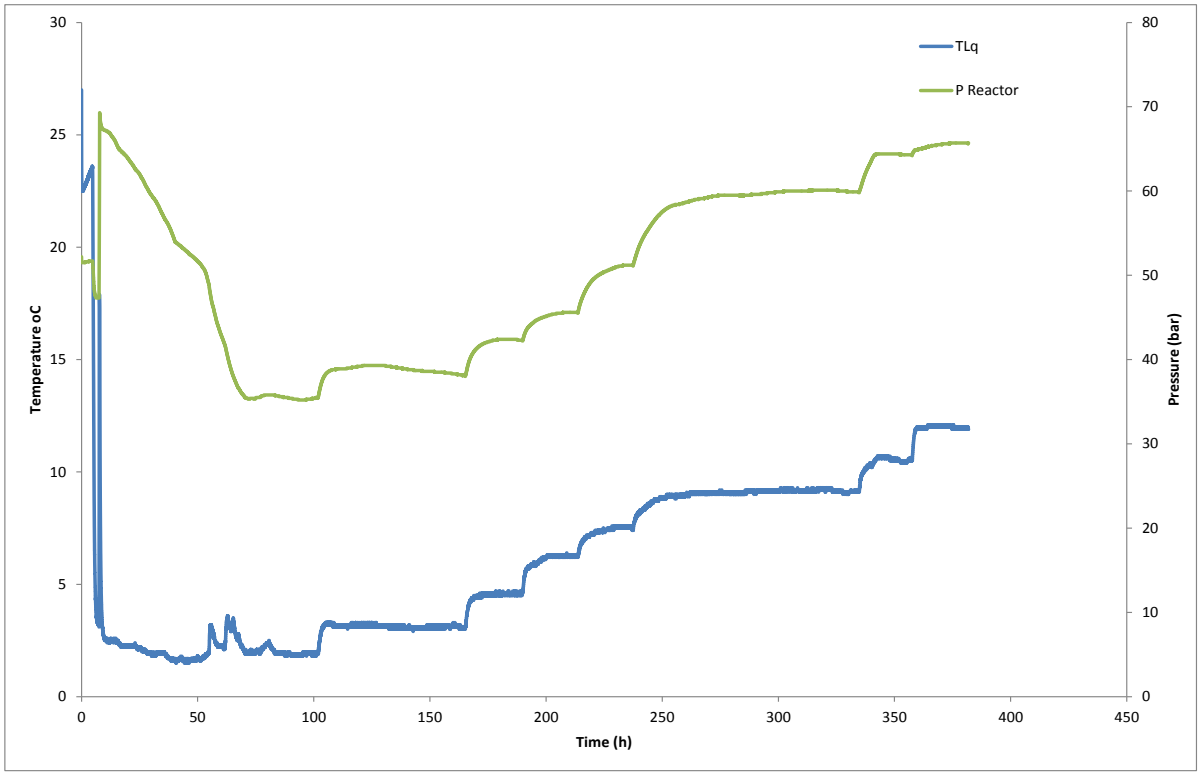

Figure 18 Evolution of the pressure and temperature in the experiment mixtures $CO_2/CH_4/C_2H_6$

5.6.8 Experiments on gas mixture ($CH_4/C_2H_6/C_3H_8$)

Table 16 Results of experimental mixtures ($CH_4/C_2H_6/C_3H_8$)

T	P_{eq}	Mole fraction in the gas			Li^+	Mole fraction in the Hydrate			Hydratation
(°C)	(bar)	CH_4	C_2H_6	C_3H_8	(mg/l)	CH_4	C_2H_6	C_3H_8	number
2.2	31.3	0.98	0.003	0.017	12.42	0.87	0.068	0.062	6.0
3.0	33.6	0.98	0.003	0.017	12.12	0.85	0.076	0.074	6.2
4.0	35.5	0.98	0.004	0.016	12.10	0.84	0.084	0.076	7.1
4.7	36.7	0.98	0.006	0.014	11.71	0.83	0.086	0.084	6.4
6.1	37.8	0.97	0.008	0.022	11.92	0.83	0.085	0.085	7.7
7.6	39.4	0.97	0.012	0.017	11.83	0.83	0.084	0.086	8.5
9.0	42.1	0.96	0.017	0.023	11.11	0.82	0.079	0.101	7.2
10	43.4	0.96	0.019	0.021	11.01	0.81	0.079	0.121	8.2
11	45	0.95	0.022	0.028	10.89	0.81	0.069	0.131	9.7

Figure 19 Evolution of the pressure and temperature in the experiment mixtures $CH_4/C_2H_6/C_3H_8$ during crystallization

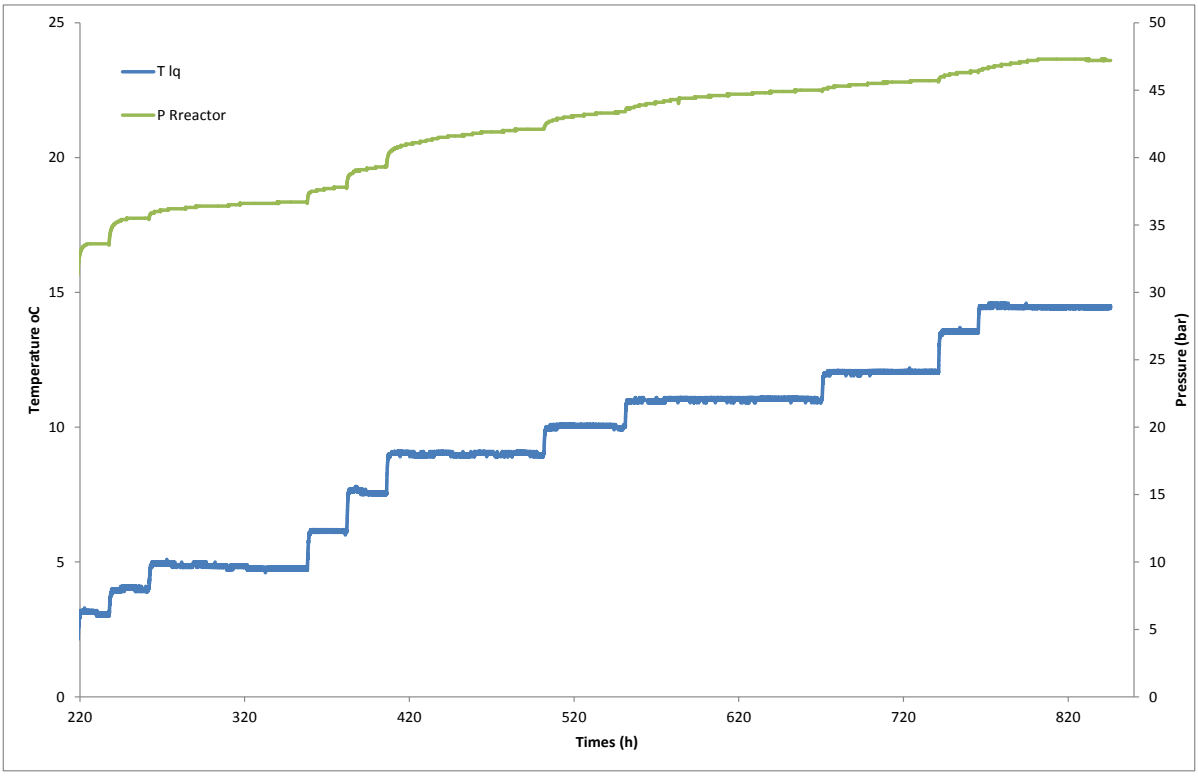

Figure 20 Evolution of the pressure and temperature in the experiment mixtures $CH_4/C_2H_6/C_3H_8$ during dissociation

5.6.9 Experiments on gas mixture ($CH_4/C_2H_6/C_3H_8/C_4H_{10}$)

Table 17 Results of experimental of mixtures 1st($CH_4/C_2H_6/C_3H_8/C_4H_{10}$)

T (°C)	P_{eq} (bar)	Mole fraction in the gas				Li^+ (mg/l)	Mole fraction in the Hydrate				Hydratation number
		CH_4	C_2H_6	C_3H_8	C_4H_{10}		CH_4	C_2H_6	C_3H_8	C_4H_{10}	
1.9	22.8	0.971	0.017	0.004	0.008	12.9	0.726	0.109	0.115	0.050	6.7
3.0	23.1	0.967	0.019	0.005	0.008	13.6	0.729	0.107	0.115	0.050	8.2
7.4	27.5	0.942	0.035	0.008	0.015	12.3	0.701	0.103	0.146	0.051	7.1
9.7	30.5	0.923	0.044	0.015	0.018	11.5	0.682	0.098	0.168	0.051	5.9
10.6	31.2	0.915	0.046	0.020	0.019	11.7	0.691	0.095	0.163	0.051	7.3
11.5	32.2	0.906	0.048	0.026	0.021	11.7	0.698	0.094	0.159	0.050	8.3
12.5	33.4	0.896	0.050	0.032	0.022	11.6	0.709	0.091	0.151	0.049	9.5
13.5	34.6	0.888	0.052	0.037	0.023	11.4	0.716	0.089	0.146	0.050	9.7
14.5	34.8	0.887	0.052	0.038	0.023	11.3	0.721	0.086	0.143	0.049	9.3
15.5	35.2	0.885	0.053	0.039	0.023	11.5	0.726	0.084	0.143	0.047	11.5
16.5	36.1	0.879	0.054	0.042	0.024	11.4	0.738	0.079	0.136	0.047	12.7
18.5	38.2	0.863	0.057	0.054	0.026	11.1	0.875	0.054	0.035	0.036	18.6

Table 18 Results of experimental of mixtures 2nd ($CH_4/C_2H_6/C_3H_8/C_4H_{10}$)

T (°C)	P_{eq} (bar)	Mole fraction in the gas				Li^+ (mg/l)	Mole fraction in the Hydrate				Hydratation number
		CH_4	C_2H_6	C_3H_8	C_4H_{10}		CH_4	C_2H_6	C_3H_8	C_4H_{10}	
2.1	21.4	0.954	0.024	0.007	0.014	12.9	0.723	0.081	0.156	0.040	7.4
3.6	21.6	0.955	0.024	0.007	0.014	12.9	0.721	0.081	0.157	0.041	7.4
4.2	21.8	0.952	0.025	0.009	0.014	12.9	0.722	0.081	0.156	0.041	7.5
5.3	22.1	0.951	0.025	0.010	0.014	12.8	0.721	0.081	0.157	0.041	7.5
6.4	22.6	0.948	0.027	0.011	0.014	12.6	0.719	0.081	0.159	0.041	7.3
7	23.6	0.939	0.030	0.015	0.016	12.6	0.717	0.078	0.163	0.042	7.6
8.9	25.3	0.926	0.035	0.022	0.017	12.3	0.713	0.076	0.168	0.043	7.8
10.8	28.2	0.905	0.042	0.032	0.021	11.9	0.708	0.069	0.182	0.041	8.4
18.1	37.2	0.845	0.050	0.078	0.027	10.5	0.913	0.043	0.023	0.021	16.9

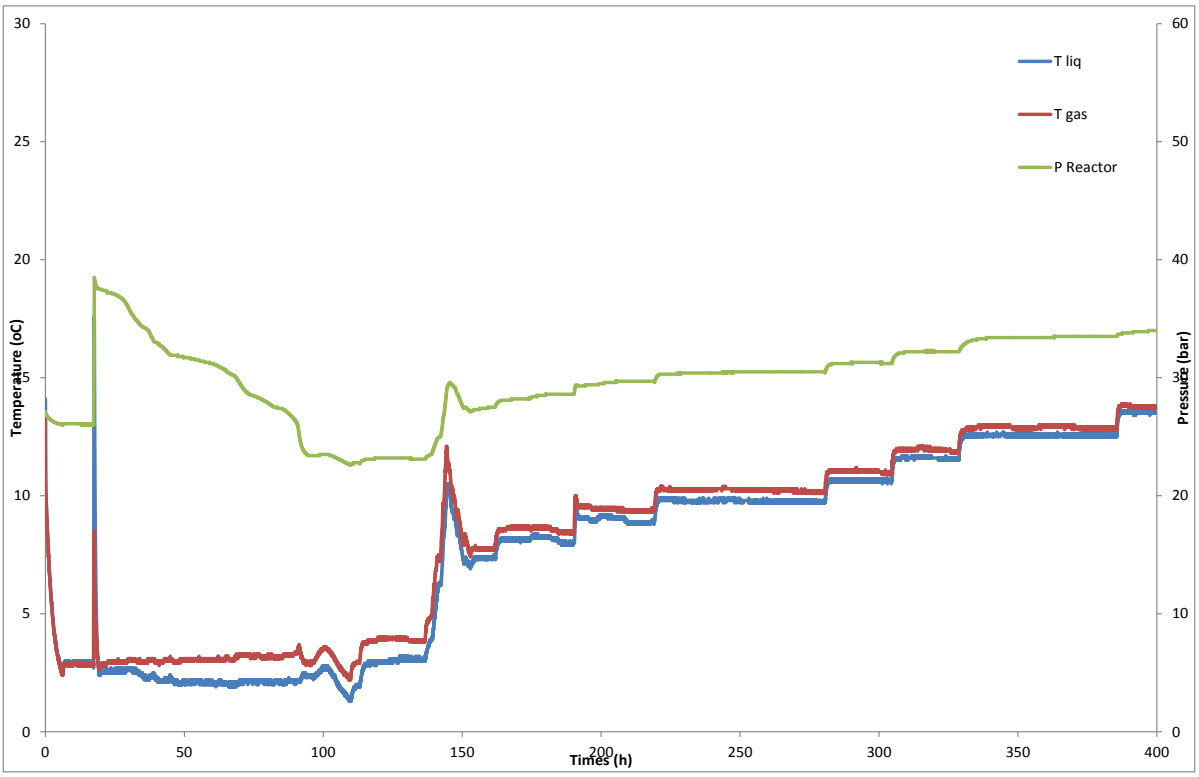

Figure 21 Evolution of the pressure and temperature in the experiment mixtures $CH_4/C_2H_6/C_3H_8/C_4H_{10}$

In this experiment we have a problem with control the temperature of the system at about 150 hour.

6. LITTERATURE EQUILIBRIUM DATA

The NIST Standard Reference Database #156 is an open access data base which gives the equilibrium data in multiphase systems with Clathrate Hydrates (CH), Vapor (V), Liquid water (L_w) or Ice (I), Liquid hydrocarbon (L_{HC}) for many pure components or mixtures. This data base extends the data from Sloan (1998, 2005): http://gashydrates.nist.gov/

In our Hydrate Team the data base has been implemented in the GasHyDyn software and completed with new experimental data from literature and from our experiments. All the following equilibrium data are extracted from this data base.

The experimental data are compared to the a model which has been optimized in the last part of this work, in the chapter devoted to thermodynamic modeling.

6.1. PURE GAS HYDRATE EQUILIBRIUM

6.1.1 CO_2 Clathrate Hydrate equilbrium data

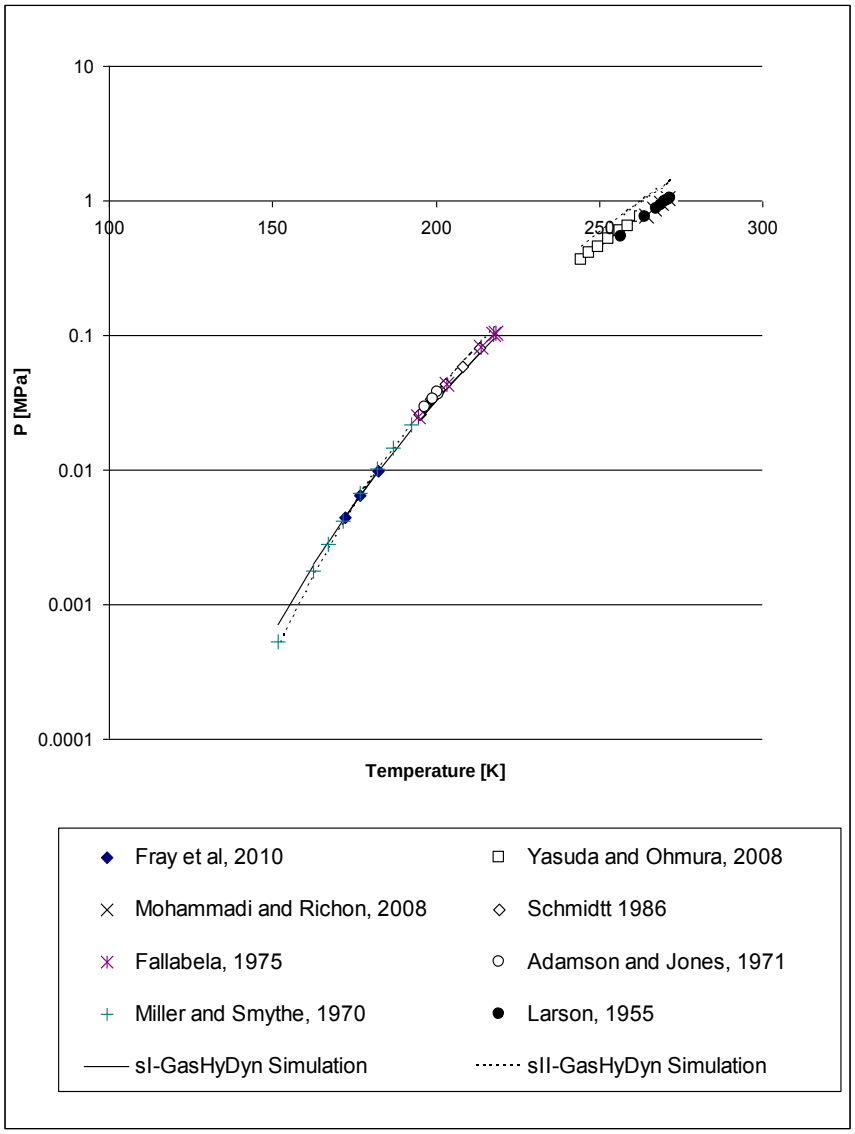

Figure 22 : CH-V Equilibrium of single CO_2 at temperature below the ice point. The simuation curve is obtained with the GasHyDyn simulator, implemented with reference parameters from Table 52 (Dharmawardhana et al, 1980) and Table 53. (page 105) and Kihara parameters given in Table 55 (page 120)

6.1.2 CH_4 Clathrate Hydrate equilbrium data

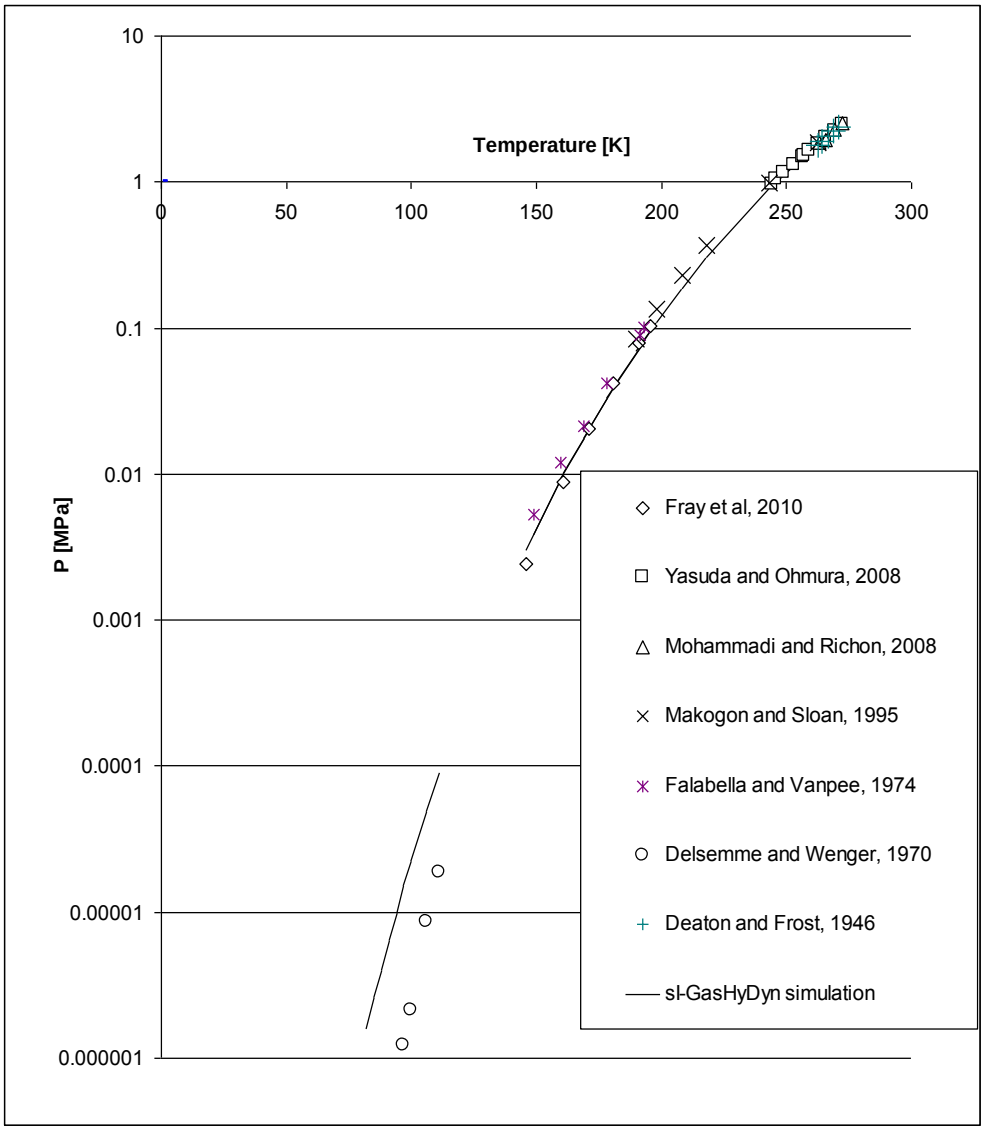

Figure 23 : CH-V Equilibrium of single CH_4 at temperature below the ice point. The simuation curve is obtained with the GasHyDyn simulator, implemented with reference parameters from Table 52 (Dharmawardhana et al, 1980) and Table 53. (page 105) and Kihara parameters given in Table 55 (page 120)

6.1.3 C_2H_6 Clathrate Hydrate equilbrium data

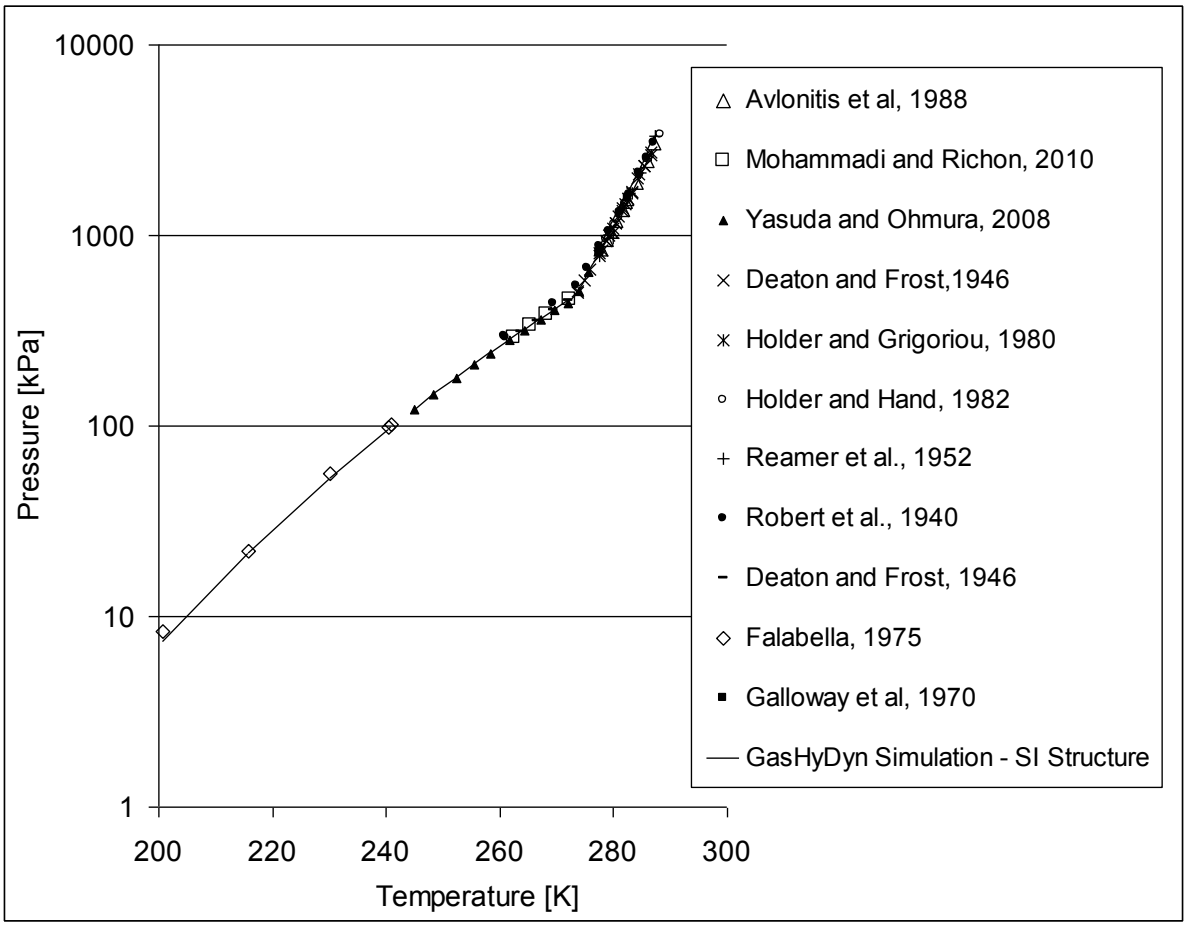

Figure 24 : CH-V Equilibrium of single C_2H_6. The simuation curve is obtained with the GasHyDyn simulator, implemented with reference parameters from Table 52 (Dharmawardhana et al, 1980) and Table 53 (Page 105) and Kihara parameters given in Table 55 (page 120)

6.1.4 C_3H_8 Clathrate Hydrate equilbrium data

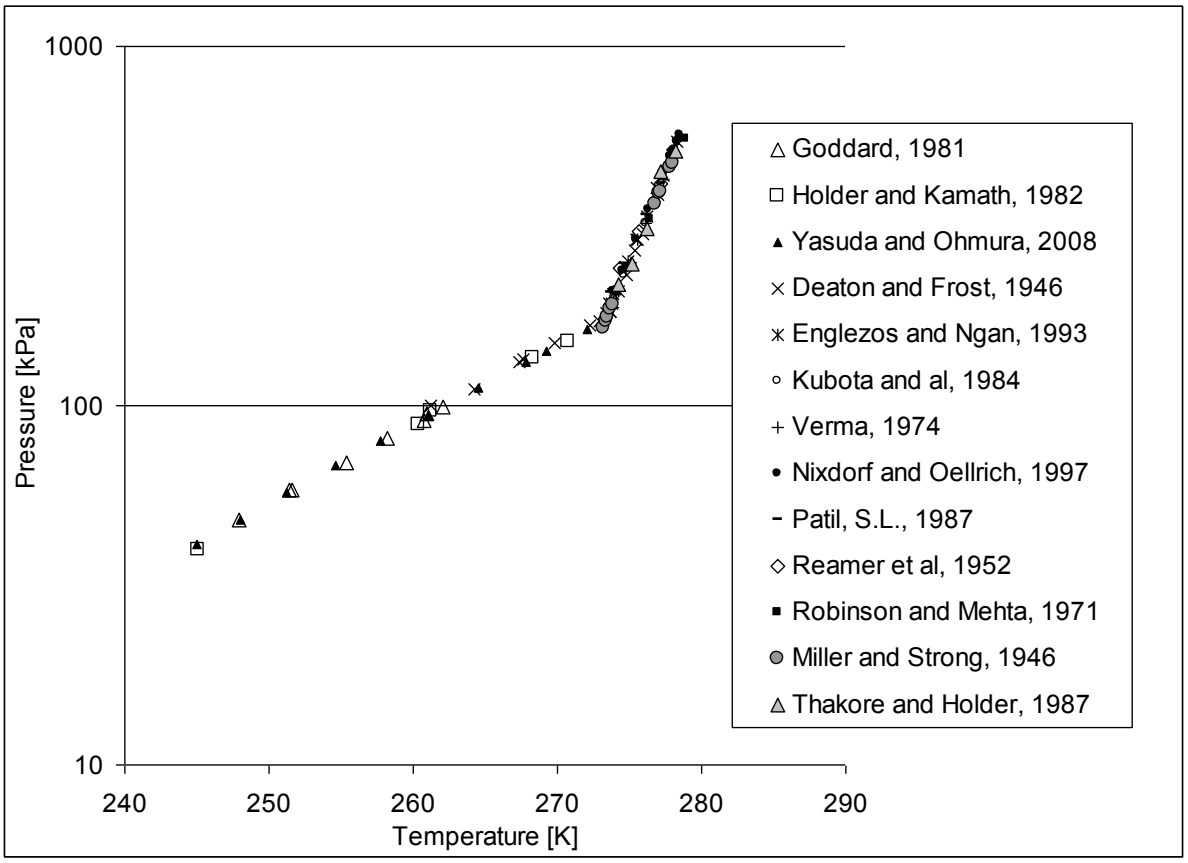

Figure 25 : CH-V Equilibrium of single C_3H_8. The simuation curve is obtained with the GasHyDyn simulator, implemented with reference parameters from Table 52 (Dharmawardhana et al, 1980) and Table 53. (page 105) and Kihara parameters given in Table 55 (page 120)

6.1.5 Kripton Clathrate Hydrate equilbrium data

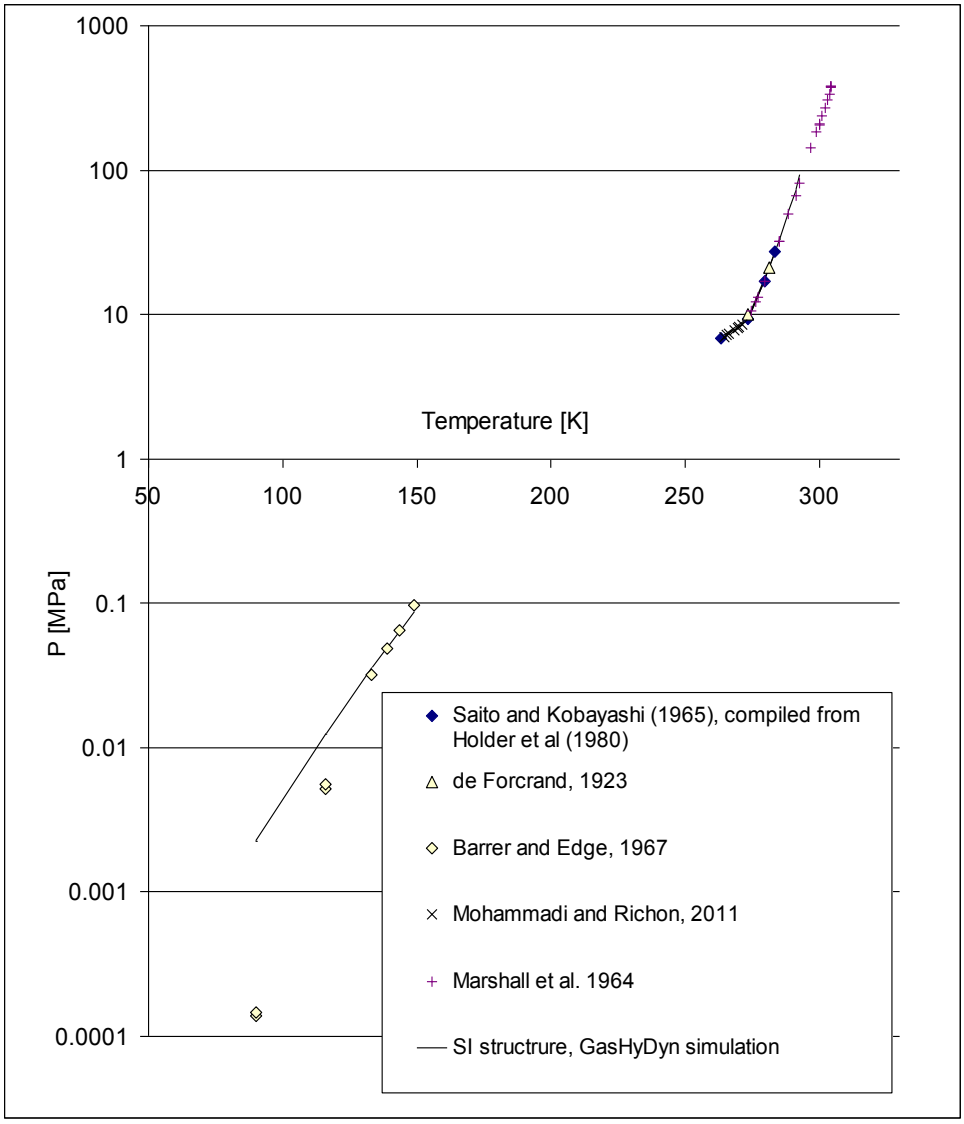

Figure 26 : CH-V Equilibrium of single Kr at temperature below the ice point. The simuation curve is obtained with the GasHyDyn simulator, implemented with reference parameters from Table 52 (Dharmawardhana et al, 1980) and Table 53. (page 105) and Kihara parameters given in Table 55 (page 120)

6.1.6 Xenon Clathrate Hydrate equilbrium data

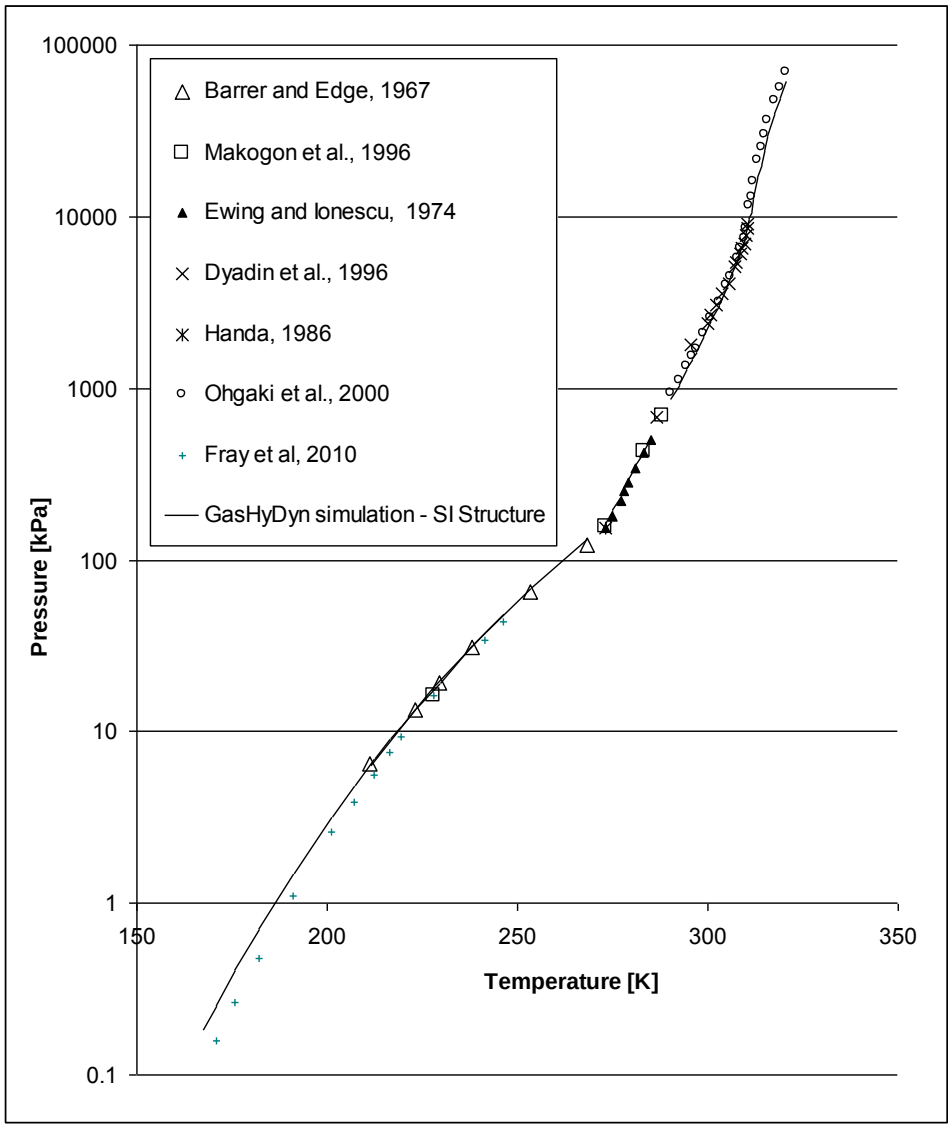

Figure 27 : CH-V Equilibrium of single Xe. The simuation curve is obtained with the GasHyDyn simulator, implemented with reference parameters from Table 52 (Dharmawardhana et al, 1980) and Table 53. (Page 105) and Kihara parameters given in Table 55 (page 120)

6.2. GAS MIXTURES

6.2.1 CO_2-N_2 Clathrate Hydrate equilibrium data

Table 19 CH_SI-V-Lw Equilibrium of CO_2-N_2 from Bouchemoua et al (2009). The simulation curve is obtained with the GasHyDyn simulator, implemented with reference parameters from Table 52 (Dharmawardhana et al, 1980) and Table 53. (page 105) and Kihara parameters given in Table 55 (page 120)

Experimental Equilibrium Data						Simulation			
T °C	P MPa	Gas composition		Hydrate composition		S	P MPa	Hydrate composition	
		CO_2	N_2	CO_2	N_2			CO_2	N_2
0.25	6.1	0.157	0.843	0.658	0.342	SI	7.5	0.632	0.368
1.35	6.2	0.164	0.836	0.657	0.343	SI	8.4	0.632	0.368
2.25	6.4	0.185	0.815	0.656	0.344	SI	8.6	0.659	0.341
3.35	6.6	0.2	0.8	0.584	0.416	SI	9.5	0.669	0.331
0.75	5.9	0.253	0.747	0.752	0.248	SI	5.4	0.768	0.232
1.55	5.9	0.255	0.745	0.73	0.27	SI	5.9	0.764	0.236
2.85	5.9	0.263	0.737	0.704	0.296	SI	6.9	0.760	0.240
3.75	6	0.265	0.735	0.703	0.297	SI	7.8	0.752	0.248
4.65	6.3	0.291	0.709	0.671	0.329	SI	8.1	0.768	0.232
4.95	6.4	0.295	0.705	0.691	0.309	SI	8.4	0.769	0.231
5.25	6.4	0.295	0.705	0.715	0.285	SI	8.8	0.764	0.236
5.45	6.5	0.301	0.699	0.695	0.305	SI	8.9	0.768	0.232
2.25	6.1	0.203	0.797	0.67	0.33	SI	8.0	0.689	0.311
2.85	6.2	0.219	0.781	0.648	0.352	SI	8.1	0.705	0.295
6.95	5.3	0.559	0.441	0.845	0.155	SI	5.7	0.911	0.089
7.95	5.6	0.585	0.415	0.819	0.181	SI	6.4	0.913	0.087
0.25	6.1	0.157	0.843	0.658	0.342	SI	7.5	0.632	0.368
Mean Deviation (%)							25.8	7.4	18.9

Table 20 : CH_SI-V-Lw Equilibrium of CO_2-N_2 from Belandria et al (2010). The simulation curve is obtained with the GasHyDyn simulator, implemented with reference parameters from Table 52 (Dharmawardhana et al, 1980) and Table 53. (page 105) and Kihara parameters given in Table 55 (page 120)

Experimental Equilibrium Data						Simulation			
T °C	P MPa	Gas composition		Hydrate composition		S	P MPa	Hydrate composition	
		CO_2	N_2	CO_2	N_2			CO_2	N_2
0.45	2.032	0.617	0.383	0.97	0.03	SI	2.216	0.947	0.053
0.45	8.149	0.171	0.829	0.657	0.343	SI	7.194	0.657	0.343
0.45	11.943	0.179	0.821	0.373	0.627	SI	6.960	0.671	0.329
0.45	2.962	0.429	0.571	0.897	0.103	SI	3.166	0.889	0.111
0.45	3.761	0.32	0.68	none	none	SI	4.192	0.829	0.171
1.45	2.543	0.728	0.272	0.739	0.261	SI	2.102	0.967	0.033
1.75	5.204	0.717	0.283	0.788	0.212	SI	2.213	0.965	0.035
2.05	2.29	0.656	0.344	0.897	0.103	SI	2.508	0.953	0.047
2.05	2.643	0.729	0.271	0.888	0.112	SI	2.254	0.966	0.034
2.05	3.256	0.449	0.551	0.879	0.121	SI	3.686	0.892	0.108
2.05	4.045	0.357	0.643	none	none	SI	4.623	0.845	0.155
2.05	7.45	0.174	0.826	0.817	0.183	SI	8.815	0.642	0.358
2.05	8.246	0.176	0.824	0.799	0.201	SI	8.739	0.646	0.354
2.05	12.745	0.16	0.84	0.382	0.618	SI	9.411	0.614	0.386
2.45	2.714	0.73	0.27	0.764	0.236	SI	2.359	0.966	0.034
2.65	5.381	0.719	0.281	0.802	0.198	SI	2.454	0.964	0.036
2.95	2.5	0.682	0.318	0.984	0.016	SI	2.688	0.957	0.043
2.95	2.865	0.731	0.269	0.79	0.21	SI	2.495	0.966	0.034
2.95	3.703	0.488	0.512	0.703	0.297	SI	3.800	0.904	0.096
2.95	4.401	0.396	0.604	0.688	0.312	SI	4.699	0.862	0.138
2.95	8.58	0.196	0.804	0.574	0.426	SI	9.081	0.668	0.332

3.55	3.703	0.488	0.512	0.703	0.297	SI	4.104	0.902	0.098
3.95	2.706	0.705	0.295	0.838	0.162	SI	2.935	0.960	0.040
4.15	3.13	0.732	0.268	0.83	0.17	SI	2.888	0.964	0.036
4.65	6.159	0.747	0.253	0.864	0.136	SI	3.008	0.966	0.034
4.95	2.974	0.729	0.271	0.89	0.11	SI	3.211	0.963	0.037
4.95	3.411	0.734	0.266	0.752	0.248	SI	3.185	0.964	0.036
4.95	4.194	0.521	0.479	0.655	0.345	SI	4.629	0.908	0.092
4.95	9.146	0.229	0.771	0.541	0.459	SI	10.702	0.688	0.312
4.95	14.26	0.127	0.873	0.513	0.487	SI	16.668	0.486	0.514
6.55	4.817	0.557	0.443	0.698	0.302	SI	5.421	0.913	0.087
6.55	10.021	0.263	0.737	0.607	0.393	SI	12.159	0.706	0.294
6.55	15.816	0.148	0.852	0.551	0.449	SI	19.252	0.504	0.496
8.05	17.628	0.176	0.824	0.584	0.416	SI	21.836	0.530	0.470
8.55	6.329	0.746	0.254	0.806	0.194	SI	5.218	0.957	0.043
Mean Deviation (%)							17.0	19.9	59.7

Table 21 : CH_SI-V-Lw Equilibrium of CO_2-N_2 from Bruusgaard and Servio (2008).The simulation curve is obtained with the GasHyDyn simulator, implemented with reference parameters from Table 52 (Dharmawardhana et al, 1980) and Table 53. (page 105) and Kihara parameters given in Table 55 (page 120)

Experimental Equilibrium Data						Simulation			
T °C	P MPa	Gas composition		Hydrate composition		S	P MPa	Hydrate composition	
		CO_2	N_2	CO_2	N_2			CO_2	N_2
2.15	1.6	1	0	none	none	SI	1.64	1.000	0.000
2.15	2	0.763	0.237	none	none	SI	2.18	0.972	0.028
2.15	2.1	0.704	0.296	none	none	SI	2.36	0.962	0.038
2.15	3	0.443	0.557	none	none	SI	3.79	0.889	0.111
2.15	3	0.448	0.552	none	none	SI	3.74	0.891	0.109

2.15	3	0.445	0.555	none	none	SI	3.77	0.890	0.110
2.15	3.1	0.436	0.564	none	none	SI	3.75	0.887	0.113
2.25	3.2	0.418	0.582	none	none	SI	4.05	0.877	0.123
2.15	3.3	0.395	0.605	none	none	SI	4.24	0.866	0.134
2.05	3.5	0.365	0.635	none	none	SI	4.53	0.849	0.151
2.15	6.5	0.17	0.83	none	none	SI	9.11	0.633	0.367
2.25	6.6	0.162	0.838	none	none	SI	9.59	0.615	0.385
4.25	2.5	0.745	0.255	none	none	SI	2.87	0.967	0.033
4.05	4.5	0.361	0.639	none	none	SI	5.98	0.833	0.167
4.25	8.7	0.17	0.83	none	none	SI	12.32	0.599	0.401
6.25	3.3	0.711	0.289	none	none	SI	3.93	0.956	0.044
5.85	5.2	0.393	0.607	none	none	SI	7.09	0.839	0.161
6.15	10.6	0.185	0.815	none	none	SI	15.50	0.590	0.410
7.85	3.8	0.787	0.213	none	none	SI	4.38	0.968	0.032
7.95	6.6	0.416	0.584	none	none	SI	9.63	0.827	0.173
7.95	15.4	0.183	0.817	none	none	SI	20.95	0.546	0.454
7.95	15.4	0.183	0.817	none	none	SI	20.95	0.546	0.454
9.75	5	0.78	0.22	none	none	SI	6.14	0.959	0.041
9.95	8.1	0.483	0.517	none	none	SI	12.56	0.829	0.171
9.85	22.1	0.189	0.811	none	none	SI	27.97	0.512	0.488
Mean Deviation (%)							28.8	none	none

Table 22 : CH_SI-V-Lw Equilibrium of CO_2-N_2 from Seo et al (2000) The simulation curve is obtained with the GasHyDyn simulator, implemented with reference parameters from Table 52 (Dharmawardhana et al, 1980) and Table 53. (page 105) and Kihara parameters given in Table 55 (page 120)

Experimental Equilibrium Data				Simulation		
T °C	P MPa	Gas composition	Hydrate composition	S	P MPa	Hydrate composition

		CO_2	N_2	CO_2	N_2			CO_2	N_2
0.85	1.394	1	0	1	0	SI	1.42	1.000	0.000
0.85	1.769	0.8205	0.1795	0.985	0.015	SI	1.74	0.981	0.019
0.85	2.354	0.5994	0.4006	0.9517	0.0483	SI	2.39	0.942	0.058
0.85	2.835	0.5048	0.4952	0.9301	0.0699	SI	2.74	0.917	0.083
0.85	3.46	0.3994	0.6006	0.9001	0.0999	SI	3.57	0.874	0.126
0.85	7.235	0.2057	0.7943	0.5836	0.4164	SI	6.54	0.709	0.291
0.85	11.2	0.1159	0.8841	0.3426	0.6574	SI	9.93	0.526	0.474
0.85	14.928	0.0498	0.9502	0.1793	0.8207	SI	14.79	0.283	0.717
0.85	17.926	0	1	0	1	SI	20.77	0.000	1.000
3.85	1.953	1	0	1	0	SI	1.99	1.000	0.000
3.85	2.6	0.8491	0.1509	0.9782	0.0218	SI	2.38	0.983	0.017
3.85	3.377	0.5867	0.4133	0.9455	0.0545	SI	3.52	0.933	0.067
3.85	5.233	0.3899	0.6101	0.8867	0.1133	SI	5.37	0.853	0.147
3.85	11.98	0.1761	0.8239	0.54	0.46	SI	11.30	0.618	0.382
3.85	15.5	0.1159	0.8841	0.3526	0.6474	SI	15.05	0.476	0.524
3.85	19.174	0.0663	0.9337	0.1928	0.8072	SI	19.53	0.313	0.687
3.85	24.041	0	1	0	1	SI	28.32	0.000	1.000
6.85	2.801	1	0	1	0	SI	2.86	1.000	0.000
6.85	3.6	0.825	0.175	0.9765	0.0235	SI	3.59	0.977	0.023
6.85	4.233	0.6999	0.3001	0.9612	0.0388	SI	4.35	0.952	0.048
6.85	5.068	0.5917	0.4083	0.9432	0.0568	SI	5.29	0.923	0.077
6.85	8.275	0.3924	0.6076	0.8641	0.1359	SI	8.50	0.826	0.174
6.85	14.974	0.251	0.749	0.64	0.36	SI	13.48	0.683	0.317
6.85	20.753	0.1709	0.8291	0.45	0.55	SI	18.34	0.547	0.453
6.85	26.69	0.0905	0.9095	0.2217	0.7783	SI	25.69	0.348	0.652
6.85	32.308	0	1	0	1	SI	38.71	0.000	1.000
Mean Deviation (%)							5.9	17.4	21.0

Table 23 : CH_SI-V-Lw Equilibrium of CO_2-N_2 from Kang et al (2001). The simulation curve is obtained with the GasHyDyn simulator, implemented with reference parameters from Table 52 (Dharmawardhana et al, 1980) and Table 53. (page 105) and Kihara parameters given in Table 55 (page 120)

Experimental Equilibrium Data						Simulation			
T °C	P MPa	Gas composition		Hydrate composition		S	P MPa	Hydrate composition	
		CO_2	N_2	CO_2	N_2			CO_2	N_2
1.8	1.565	0.9659	0.0341	none	none	SI	1.64	0.997	0.003
4.3	2.06	0.9659	0.0341	none	none	SI	2.18	0.997	0.003
7.1	2.9	0.9659	0.0341	none	none	SI	3.08	0.996	0.004
9.4	4	0.9659	0.0341	none	none	SI	4.26	0.995	0.005
10.4	5.115	0.9659	0.0341	none	none	SI	5.07	0.994	0.006
0.85	2	0.778	0.222	none	none	SI	1.84	0.975	0.025
3	2.6	0.778	0.222	none	none	SI	2.36	0.973	0.027
7.5	4.225	0.778	0.222	none	none	SI	4.22	0.967	0.033
10.3	6.45	0.778	0.222	none	none	SI	6.89	0.954	0.046
11.1	7.445	0.778	0.222	none	none	SI	9.22	0.934	0.066
0.6	3.195	0.4815	0.5185	none	none	SI	2.88	0.909	0.091
2.85	4.257	0.4815	0.5185	none	none	SI	3.80	0.902	0.098
5.85	5.867	0.4815	0.5185	none	none	SI	5.75	0.887	0.113
7.85	7.449	0.4815	0.5185	none	none	SI	8.00	0.868	0.132
8.85	8.975	0.4815	0.5185	none	none	SI	9.78	0.853	0.147
-0.3	7.24	0.1721	0.8279	none	none	SI	5.93	0.673	0.327
0.9	8.12	0.1721	0.8279	none	none	SI	7.62	0.653	0.347
4.3	10.65	0.1721	0.8279	none	none	SI	12.26	0.602	0.398
5.5	11.748	0.1721	0.8279	none	none	SI	14.77	0.579	0.421
7.4	14.22	0.1721	0.8279	none	none	SI	19.96	0.537	0.463
1.1	11.02	0.1159	0.8841	none	none	SI	10.36	0.522	0.478

2.5	13.87	0.1159	0.8841	none	none	SI	12.50	0.500	0.500
4.45	18.1	0.1159	0.8841	none	none	SI	16.36	0.465	0.535
5.8	22.23	0.1159	0.8841	none	none	SI	19.76	0.440	0.560
0.8	14.085	0.0063	0.9937	none	none	SI	19.78	0.042	0.958
1.4	15.4	0.0063	0.9937	none	none	SI	21.08	0.040	0.960
3.85	20.68	0.0063	0.9937	none	none	SI	27.31	0.036	0.964
5.1	24.12	0.0063	0.9937	none	none	SI	31.21	0.033	0.967
Mean Deviation (%)							14.0	none	none

Table 24 : CH_SI-V-Lw Equilibrium of CO_2-N_2 from Fan and Guo (1999). The simulation curve is obtained with the GasHyDyn simulator, implemented with reference parameters from Table 52 (Dharmawardhana et al, 1980) and Table 53. (page 105) and Kihara parameters given in Table 55 (page 120)

Experimental Equilibrium Data						Simulation			
T °C	P MPa	Gas composition		Hydrate composition		S	P MPa	Hydrate composition	
		CO_2	N_2	CO_2	N_2			CO_2	N_2
-0.05	1.22	0.9652	0.0348	none	none	SI	1.21	0.997	0.003
1.45	1.54	0.9652	0.0348	none	none	SI	1.57	0.997	0.003
5.15	2.42	0.9652	0.0348	none	none	SI	2.42	0.996	0.004
6.25	2.89	0.9652	0.0348	none	none	SI	2.77	0.996	0.004
7.05	2.95	0.9652	0.0348	none	none	SI	3.07	0.996	0.004
0.25	1.37	0.9099	0.0901	none	none	SI	1.46	0.991	0.009
0.95	1.53	0.9099	0.0901	none	none	SI	1.57	0.991	0.009
3.55	1.89	0.9099	0.0901	none	none	SI	2.13	0.991	0.009
5.95	3.09	0.9099	0.0901	none	none	SI	2.85	0.990	0.010
Mean Deviation (%)							4.6	none	none

Table 25 : CH_SI-V-Lw Equilibrium of CO_2-N_2 from Olsen et al (1999). The simulation curve is obtained with the GasHyDyn simulator, implemented with reference

parameters from Table 52 (Dharmawardhana et al, 1980) and Table 53. (page 105) and Kihara parameters given in Table 55 (page 120)

Experimental Equilibrium Data						Simulation			
T °C	P MPa	Gas composition		Hydrate composition		S	P MPa	Hydrate composition	
		CO_2	N_2	CO_2	N_2			CO_2	N_2
1.25	3.074	0.4358	0.5642	none	none	SI	3.44	0.889	0.111
2.85	3.753	0.4473	0.5527	none	none	SI	4.05	0.888	0.112
4.95	4.822	0.46	0.54	none	none	SI	5.29	0.883	0.117
7.05	6.561	0.469	0.531	none	none	SI	7.18	0.871	0.129
7.95	7.266	0.4748	0.5252	none	none	SI	8.21	0.864	0.136
0.95	1.986	0.655	0.345	none	none	SI	2.21	0.954	0.046
4.35	2.803	0.6859	0.3141	none	none	SI	3.17	0.955	0.045
6.55	3.777	0.7132	0.2868	none	none	SI	4.08	0.956	0.044
8.15	4.852	0.7189	0.2811	none	none	SI	5.12	0.952	0.048
8.75	5.453	0.7122	0.2878	none	none	SI	5.75	0.948	0.052
0.25	6.243	0.162	0.838	none	none	SI	7.32	0.642	0.358
0.85	6.51	0.165	0.835	none	none	SI	7.82	0.640	0.360
1.95	7.324	0.172	0.828	none	none	SI	8.78	0.639	0.361
3.15	8.458	0.179	0.821	none	none	SI	10.07	0.635	0.365
4.05	9.55	0.1826	0.8174	none	none	SI	11.31	0.627	0.373
Mean Deviation (%)							12.7	none	none

Table 26 : CH_SI-V-Lw Equilibrium of CO_2-N_2 from Le Quang Du (Ph.D. work undergoing). The simulation curve is obtained with the GasHyDyn simulator, implemented with reference parameters from Table 52 (Dharmawardhana et al, 1980) and Table 53. (page 105) and Kihara parameters given in Table 55 (page 120)

Experimental Equilibrium Data				Simulation		
T °C	P MPa	Gas composition	Hydrate composition	S	P MPa	Hydrate composition

		CO_2	N_2	CO_2	N_2			CO_2	N_2
2.3	2.46	0.667	0.333	0.970	0.030	SI	2.53	0.955	0.045
3.1	2.6	0.689	0.311	0.965	0.035	SI	2.69	0.958	0.042
3.3	2.66	0.699	0.301	0.961	0.039	SI	2.73	0.960	0.040
4.3	2.87	0.723	0.277	0.958	0.042	SI	2.99	0.962	0.038
5.2	3.13	0.747	0.253	0.955	0.045	SI	3.22	0.966	0.034
6	3.38	0.768	0.232	0.947	0.053	SI	3.48	0.968	0.032
Mean Deviation (%)							3.1	1.04	24.7

6.2.2 CO2-CH4 Clathrate Hydrate equilibrium data

Table 27 : CH_SI-V-Lw Equilibrium of CO_2-CH_4 from Bouchemoua et al (2009). The simulation curve is obtained with the GasHyDyn simulator, implemented with reference parameters from Table 52 (Dharmawardhana et al, 1980) and Table 53. (page 105) and Kihara parameters given in Table 55 (page 120)

Experimental Equilibrium Data						Simulation			
T °C	P MPa	Gas composition		Hydrate composition		S	P MPa	Hydrate composition	
		CO_2	CH_4	CO_2	CH_4			CO_2	CH_4
4	2.04	1.000	0.000	1.000	0.000	SI	2.03	1.000	0.000
4	2.36	0.639	0.361	0.767	0.233	SI	2.45	0.771	0.229
4	2.55	0.523	0.477	0.677	0.323	SI	2.63	0.678	0.322
4	2.8	0.364	0.636	0.535	0.465	SI	2.92	0.527	0.473
4	3.55	0.112	0.888	0.214	0.786	SI	3.55	0.202	0.798
4	3.9	0.000	1.000	0.000	1.000	SI	3.94	0.000	1.000
Mean Deviation (%)							2.14	1.98	1.37

Table 28 : CH_SI-V-Lw Equilibrium of CO_2-CH_4 from our work. The simulation curve is obtained with the GasHyDyn simulator, implemented with reference parameters from

Table 52 (Dharmawardhana et al, 1980) and Table 53. (page 105) and Kihara parameters given in Table 55 (page 120)

Experimental Equilibrium Data						Simulation			
T °C	P MPa	Gas composition		Hydrate composition		S	P MPa	Hydrate composition	
		CO_2	CH_4	CO_2	CH_4			CO_2	CH_4
2.2	1.92	0.655	0.345	0.760	0.240	SI	1.99	0.789	0.211
2.9	2.05	0.776	0.224	0.640	0.360	SI	2.00	0.870	0.130
4	2.26	0.659	0.341	0.760	0.240	SI	2.42	0.786	0.214
4.5	2.44	0.665	0.335	0.760	0.240	SI	2.53	0.789	0.211
5.5	2.71	0.670	0.330	0.760	0.240	SI	2.86	0.789	0.211
6.5	3.01	0.678	0.322	0.740	0.260	SI	3.20	0.791	0.209
7.3	3.31	0.682	0.318	0.730	0.270	SI	3.53	0.790	0.210
2.2	2.91	0.120	0.880	0.290	0.710	SI	2.93	0.219	0.781
2.5	2.97	0.129	0.871	0.280	0.720	SI	3.00	0.232	0.768
3.6	3.18	0.135	0.865	0.280	0.720	SI	3.33	0.239	0.761
4.5	3.47	0.147	0.853	0.260	0.740	SI	3.63	0.254	0.746
5.2	3.8	0.162	0.838	0.200	0.800	SI	3.85	0.274	0.726
2.2	2.52	0.296	0.704	none	none	SI	2.53	0.459	0.541
3.1	2.59	0.454	0.546	none	none	SI	2.49	0.620	0.380
3.9	2.81	0.407	0.593	none	none	SI	2.80	0.572	0.428
4.7	3.02	0.334	0.666	none	none	SI	3.21	0.492	0.508
5.6	3.29	0.340	0.660	none	none	SI	3.52	0.495	0.505
6.6	3.53	0.345	0.655	none	none	SI	3.93	0.495	0.505
7.3	3.87	0.350	0.650	none	none	SI	4.25	0.497	0.503
3.4	3.33	0.127	0.873	0.311	0.689	SI	3.29	0.227	0.773
4.4	3.53	0.134	0.866	0.309	0.691	SI	3.62	0.235	0.765
4.9	3.71	0.141	0.859	0.308	0.692	SI	3.80	0.244	0.756
5.8	4.03	0.151	0.849	0.304	0.696	SI	4.14	0.256	0.744

6.8	4.45	0.163	0.837	0.295	0.705	SI	4.57	0.270	0.730
7.8	4.93	0.175	0.825	0.260	0.740	SI	5.06	0.283	0.717
2.2	2.91	0.120	0.880	0.290	0.710	SI	2.93	0.219	0.781
2.5	2.97	0.129	0.871	0.280	0.720	SI	3.00	0.232	0.768
3.6	3.18	0.135	0.865	0.280	0.720	SI	3.33	0.239	0.761
4.5	3.47	0.147	0.853	0.260	0.740	SI	3.63	0.254	0.746
5.2	3.8	0.162	0.838	0.200	0.800	SI	3.85	0.274	0.726
Mean Deviation (%)							3.8	15.7	11.5

Table 29 : CH_SI-V-Lw Equilibrium of CO_2-CH_4 from Belandria et al (2011). The simulation curve is obtained with the GasHyDyn simulator, implemented with reference parameters from Table 52 (Dharmawardhana et al, 1980) and Table 53. (page 105) and Kihara parameters given in Table 55 (page 120)

Experimental Equilibrium Data						Simulation			
T °C	P MPa	Gas composition		Hydrate composition		S	P MPa	Hydrate composition	
		CO_2	CH_4	CO_2	CH_4			CO_2	CH_4
0.45	2.234	0.141	0.859	none	none	SI	2.41	0.255	0.745
0.45	2.416	0.125	0.875	none	none	SI	2.43	0.230	0.770
0.45	2.44	0.081	0.919	0.096	0.904	SI	2.55	0.156	0.844
0.45	1.844	0.345	0.655	0.549	0.451	SI	2.03	0.520	0.480
0.45	1.941	0.288	0.712	0.392	0.608	SI	2.12	0.455	0.545
0.45	2.048	0.220	0.780	0.294	0.706	SI	2.24	0.369	0.631
0.45	1.51	0.630	0.370	0.884	0.116	SI	1.67	0.775	0.225
0.45	1.607	0.545	0.455	0.801	0.199	SI	1.77	0.708	0.292
2.05	2.583	0.166	0.834	0.338	0.662	SI	2.77	0.289	0.711
2.05	2.712	0.129	0.871	none	none	SI	2.84	0.233	0.767
2.05	2.766	0.086	0.914	0.179	0.821	SI	2.98	0.162	0.838
2.05	2.123	0.384	0.616	0.650	0.350	SI	2.33	0.556	0.444

2.05	2.22	0.302	0.698	0.586	0.414	SI	2.48	0.466	0.534
2.05	2.4	0.228	0.772	0.366	0.634	SI	2.63	0.375	0.625
2.05	1.792	0.657	0.343	0.831	0.169	SI	1.96	0.790	0.210
2.05	1.865	0.565	0.435	0.752	0.248	SI	2.07	0.720	0.280
2.95	2.813	0.179	0.821	0.264	0.736	SI	3.00	0.306	0.694
2.95	3.025	0.134	0.866	0.239	0.761	SI	3.12	0.239	0.761
2.95	3.027	0.096	0.904	0.238	0.762	SI	3.23	0.178	0.822
2.95	2.318	0.405	0.595	0.644	0.356	SI	2.43	0.575	0.425
2.95	2.503	0.315	0.685	0.400	0.600	SI	2.70	0.478	0.522
2.95	2.69	0.232	0.768	0.312	0.688	SI	2.88	0.377	0.623
2.95	1.985	0.669	0.331	0.877	0.123	SI	2.14	0.797	0.203
2.95	2.174	0.579	0.421	0.784	0.216	SI	2.26	0.728	0.272
4.95	3.416	0.202	0.798	0.233	0.767	SI	3.64	0.331	0.669
4.95	3.631	0.139	0.861	0.225	0.775	SI	3.83	0.241	0.759
4.95	3.802	0.103	0.897	0.148	0.852	SI	3.95	0.185	0.815
4.95	3.037	0.323	0.677	0.457	0.543	SI	3.33	0.479	0.521
4.95	3.319	0.233	0.767	0.273	0.727	SI	3.55	0.372	0.628
4.95	2.45	0.694	0.306	none	none	SI	2.65	0.808	0.192
4.95	2.58	0.609	0.391	0.786	0.214	SI	2.77	0.745	0.255
6.05	3.565	0.202	0.798	0.266	0.734	SI	4.09	0.327	0.673
7.05	4.486	0.147	0.853	0.307	0.693	SI	4.76	0.246	0.754
7.05	4.655	0.108	0.892	0.245	0.755	SI	4.90	0.188	0.812
7.05	3.541	0.344	0.656	0.727	0.273	SI	4.14	0.492	0.508
7.05	4.109	0.235	0.765	0.339	0.661	SI	4.46	0.365	0.635
7.05	3.139	0.620	0.380	0.860	0.140	SI	3.53	0.744	0.256
7.05	3.481	0.490	0.510	0.788	0.212	SI	3.75	0.635	0.365
9.05	5.767	0.114	0.886	0.276	0.724	SI	6.08	0.191	0.809
11.05	7.19	0.115	0.885	0.107	0.893	SI	7.65	0.184	0.816
Mean Deviation (%)							7.8	18.8	21.4

Table 30 : CH_SI-V-Lw Equilibrium of CO_2-CH_4 from Seo et al (2000). The simulation curve is obtained with the GasHyDyn simulator, implemented with reference parameters from Table 52 (Dharmawardhana et al, 1980) and Table 53. (page 105) and Kihara parameters given in Table 55 (page 120)

Experimental Equilibrium Data						Simulation			
T °C	P MPa	Gas composition		Hydrate composition		S	P MPa	Hydrate composition	
		CO_2	CH_4	CO_2	CH_4			CO_2	CH_4
-0.05	2	0.284	0.716	0.915	0.085	SI	1.92	0.453	0.547
0.95	2	0.403	0.597	0.936	0.064	SI	2.03	0.579	0.421
2.25	2	0.608	0.392	0.982	0.018	SI	2.06	0.753	0.247
3.15	2	0.794	0.206	0.997	0.003	SI	2.04	0.881	0.119
0.65	2.6	0.129	0.871	0.662	0.338	SI	2.48	0.236	0.764
1.75	2.6	0.234	0.766	0.847	0.153	SI	2.54	0.384	0.616
3.15	2.6	0.415	0.585	0.927	0.073	SI	2.56	0.583	0.417
4.35	2.6	0.641	0.359	0.981	0.019	SI	2.55	0.772	0.228
4.95	2.6	0.834	0.166	0.994	0.006	SI	2.46	0.902	0.098
3.45	3.5	0.133	0.867	0.647	0.353	SI	3.29	0.236	0.764
4.45	3.5	0.252	0.748	0.733	0.267	SI	3.32	0.397	0.603
5.85	3.5	0.419	0.581	0.890	0.110	SI	3.45	0.575	0.425
6.75	3.5	0.611	0.389	0.952	0.048	SI	3.43	0.738	0.262
7.35	3.5	0.834	0.166	0.993	0.007	SI	3.30	0.896	0.104
Mean Deviation (%)							3.3	34.8	866.5

Table 31 : CH_SI-V-Lw Equilibrium of CO_2-CH_4 from Fan and Guo (1999). The simulation curve is obtained with the GasHyDyn simulator, implemented with reference parameters from Table 52 (Dharmawardhana et al, 1980) and Table 53. (page 105) and Kihara parameters given in Table 55 (page 120)

Experimental Equilibrium Data						Simulation			
T °C	P MPa	Gas composition		Hydrate composition		S	P MPa	Hydrate composition	
		CO_2	CH_4	CO_2	CH_4			CO_2	CH_4
0.35	1.1	0.965	0.035	none	none	SI	1.37	0.982	0.018
0.45	1.16	0.965	0.035	none	none	SI	1.38	0.982	0.018
0.55	1.2	0.965	0.035	none	none	SI	1.40	0.982	0.018
4.05	1.95	0.965	0.035	none	none	SI	2.07	0.981	0.019
4.45	1.94	0.965	0.035	none	none	SI	2.17	0.981	0.019
4.75	2.05	0.965	0.035	none	none	SI	2.25	0.981	0.019
7.25	3	0.965	0.035	none	none	SI	3.07	0.979	0.021
8.55	3.73	0.965	0.035	none	none	SI	3.65	0.978	0.022
9.15	4.8	0.965	0.035	none	none	SI	3.98	0.977	0.023
Mean Deviation (%)							12.2	none	none

Table 32 : CH_SI-V-Lw Equilibrium of CO_2-CH_4 from Ohgaki et al (1996). The simulation curve is obtained with the GasHyDyn simulator, implemented with reference parameters from Table 52 (Dharmawardhana et al, 1980) and Table 53. (page 105) and Kihara parameters given in Table 55 (page 120)

Experimental Equilibrium Data						Simulation			
T °C	P MPa	Gas composition		Hydrate composition		S	P MPa	Hydrate composition	
		CO_2	CH_4	CO_2	CH_4			CO_2	CH_4
7.15	3.04	1.000	0.000	1.000	0.000	SI	2.98	1.000	0.000
7.15	3.24	0.683	0.317	0.840	0.160	SI	3.46	0.792	0.208
7.15	3.38	0.585	0.415	0.800	0.200	SI	3.55	0.717	0.283

7.15	3.6	0.488	0.512	0.670	0.330	SI	3.85	0.632	0.368
7.15	3.64	0.450	0.550	0.690	0.310	SI	3.93	0.598	0.402
7.15	3.67	0.448	0.552	0.680	0.320	SI	3.93	0.596	0.404
7.15	3.71	0.429	0.571	0.610	0.390	SI	3.98	0.578	0.422
7.15	3.77	0.384	0.616	0.600	0.400	SI	4.09	0.533	0.467
7.15	3.86	0.357	0.643	0.590	0.410	SI	4.16	0.505	0.495
7.15	4.22	0.241	0.759	0.440	0.560	SI	4.49	0.372	0.628
7.15	4.31	0.215	0.785	0.390	0.610	SI	4.57	0.339	0.661
7.15	4.32	0.217	0.783	0.360	0.640	SI	4.57	0.342	0.658
7.15	4.34	0.203	0.797	0.370	0.630	SI	4.61	0.323	0.677
7.15	4.37	0.203	0.797	0.350	0.650	SI	4.61	0.323	0.677
7.15	4.37	0.183	0.817	0.360	0.640	SI	4.68	0.297	0.703
7.15	4.44	0.179	0.821	0.360	0.640	SI	4.70	0.291	0.709
7.15	4.5	0.169	0.831	0.350	0.650	SI	4.73	0.277	0.723
7.15	4.57	0.144	0.856	0.320	0.680	SI	4.82	0.242	0.758
7.15	3.98	0.302	0.698	0.530	0.470	SI	4.31	0.445	0.555
7.15	4	0.310	0.690	0.520	0.480	SI	4.29	0.454	0.546
7.15	4.01	0.311	0.689	0.550	0.450	SI	4.28	0.455	0.545
7.15	4.06	0.288	0.712	0.510	0.490	SI	4.35	0.429	0.571
7.15	4.07	0.293	0.707	0.520	0.480	SI	4.33	0.434	0.566
7.15	4.15	0.268	0.732	0.470	0.530	SI	4.41	0.405	0.595
7.15	4.2	0.245	0.755	0.450	0.550	SI	4.48	0.377	0.623
7.15	4.58	0.141	0.859	0.320	0.680	SI	4.83	0.237	0.763
7.15	4.63	0.143	0.857	0.290	0.710	SI	4.83	0.240	0.760
7.15	4.75	0.104	0.896	0.240	0.760	SI	4.96	0.181	0.819
7.15	4.85	0.090	0.910	0.230	0.770	SI	5.03	0.159	0.841
7.15	4.99	0.065	0.935	0.160	0.840	SI	5.14	0.118	0.882
7.15	5.46	0.000	1.000	0.000	1.000	SI	5.44	0.000	1.000
Mean Deviation (%)							5.9	15.4	14.4

Table 33 : CH_SI-V-Lw Equilibrium of CO_2-CH_4 from Adisasmito et al (1999). The simulation curve is obtained with the GasHyDyn simulator, implemented with reference parameters from Table 52 (Dharmawardhana et al, 1980) and Table 53. (page 105) and Kihara parameters given in Table 55 (page 120)

Experimental Equilibrium Data						Simulation			
T °C	P MPa	Gas composition		Hydrate composition		S	P MPa	Hydrate composition	
		CO_2	CH_4	CO_2	CH_4			CO_2	CH_4
0.55	2.52	0.100	0.900	none	none	SI	2.53	0.189	0.811
2.65	3.1	0.090	0.910	none	none	SI	3.15	0.168	0.832
4.65	3.83	0.080	0.920	none	none	SI	3.90	0.148	0.852
7.05	4.91	0.080	0.920	none	none	SI	5.02	0.143	0.857
10.05	6.8	0.080	0.920	none	none	SI	6.98	0.135	0.865
11.95	8.4	0.080	0.920	none	none	SI	8.71	0.130	0.870
14.05	10.76	0.090	0.910	none	none	SI	11.20	0.136	0.864
1.45	2.59	0.140	0.860	none	none	SI	2.67	0.252	0.748
3.75	3.24	0.130	0.870	none	none	SI	3.40	0.231	0.769
5.95	4.18	0.130	0.870	none	none	SI	4.28	0.225	0.775
8.45	5.38	0.130	0.870	none	none	SI	5.57	0.217	0.783
10.85	7.17	0.130	0.870	none	none	SI	7.40	0.207	0.793
12.95	9.24	0.120	0.880	none	none	SI	9.60	0.183	0.817
14.25	10.95	0.130	0.870	none	none	SI	11.30	0.189	0.811
0.65	2.12	0.250	0.750	none	none	SI	2.24	0.408	0.592
6.25	3.96	0.220	0.780	none	none	SI	4.13	0.350	0.650
10.25	6.23	0.220	0.780	none	none	SI	6.51	0.329	0.671
12.05	7.75	0.210	0.790	none	none	SI	8.16	0.304	0.696
14.45	10.44	0.250	0.750	none	none	SI	11.10	0.327	0.673
0.55	1.81	0.440	0.560	none	none	SI	1.92	0.616	0.384
3.75	2.63	0.420	0.580	none	none	SI	2.73	0.585	0.415

7.55	4.03	0.400	0.600	none	none	SI	4.24	0.547	0.453
9.95	5.43	0.390	0.610	none	none	SI	5.70	0.519	0.481
11.95	6.94	0.390	0.610	none	none	SI	7.42	0.499	0.501
14.25	9.78	0.390	0.610	none	none	SI	10.41	0.465	0.535
2.45	1.99	0.500	0.500	none	none	SI	2.25	0.664	0.336
5.35	2.98	0.470	0.530	none	none	SI	3.15	0.626	0.374
7.75	4.14	0.400	0.600	none	none	SI	4.34	0.545	0.455
8.65	4.47	0.410	0.590	none	none	SI	4.76	0.550	0.450
11.95	6.84	0.440	0.560	none	none	SI	7.29	0.546	0.454
14.25	9.59	0.450	0.550	none	none	SI	10.23	0.517	0.483
1.45	1.66	0.730	0.270	none	none	SI	1.75	0.842	0.158
3.25	2.08	0.700	0.300	none	none	SI	2.13	0.818	0.182
5.05	2.58	0.680	0.320	none	none	SI	2.70	0.798	0.202
7.05	3.28	0.680	0.320	none	none	SI	3.43	0.790	0.210
8.85	4.12	0.670	0.330	none	none	SI	4.33	0.772	0.228
0.55	1.45	0.790	0.210	none	none	SI	1.54	0.883	0.117
2.75	1.88	0.780	0.220	none	none	SI	1.97	0.873	0.127
4.65	2.37	0.760	0.240	none	none	SI	2.47	0.855	0.145
6.45	2.97	0.750	0.250	none	none	SI	3.07	0.843	0.157
8.45	3.79	0.740	0.260	none	none	SI	3.97	0.827	0.173
9.55	4.37	0.850	0.150	none	none	SI	4.41	0.898	0.102
Mean Deviation (%)							4.5	none	none

Table 34 : CH_SI-V-Lw Equilibrium of CO_2-CH_4 from Hachikubo et al (2002). The simulation curve is obtained with the GasHyDyn simulator, implemented with reference parameters from Table 52 (Dharmawardhana et al, 1980) and Table 53. (page 105) and Kihara parameters given in Table 55 (page 120)

Experimental Equilibrium Data				Simulation		
T	P	Gas composition	Hydrate composition	S	P	Hydrate composition

°C	MPa						MPa		
		CO_2	CH_4	CO_2	CH_4			CO_2	CH_4
0.78	1.349	1.000	0.000	1.000	0.000	SI	1.41	1.000	0.000
3.65	1.806	1.000	0.000	1.000	0.000	SI	1.94	1.000	0.000
4.9	2.204	1.000	0.000	1.000	0.000	SI	2.25	1.000	0.000
-9.98	0.774	1.000	0.000	1.000	0.000	SI	0.79	1.000	0.000
-5.04	0.921	1.000	0.000	1.000	0.000	SI	0.96	1.000	0.000
-1.92	1.029	1.000	0.000	1.000	0.000	SI	1.09	1.000	0.000
4.13	2.187	1.000	0.000	1.000	0.000	SI	2.06	1.000	0.000
-4.75	2.324	0.000	1.000	0.000	1.000	SI	2.23	0.000	1.000
-1.87	2.527	0.000	1.000	0.000	1.000	SI	2.45	0.000	1.000
-1.9	1.271	0.770	0.230	none	none	SI	1.25	0.873	0.127
-1.74	1.434	0.500	0.500	none	none	SI	1.52	0.676	0.324
-1.78	2.022	0.250	0.750	none	none	SI	1.87	0.413	0.587
Mean Deviation (%)							4.6	none	none

Table 35: CH_SI-V-Lw Equilibrium of CO_2-CH_4 from Unruh and Katz (1949). The simulation curve is obtained with the GasHyDyn simulator, implemented with reference parameters from Table 52 (Dharmawardhana et al, 1980) and Table 53. (page 105) and Kihara parameters given in Table 55 (page 120)

Experimental Equilibrium Data						Simulation			
T °C	P MPa	Gas composition		Hydrate composition		S	P MPa	Hydrate composition	
		CO_2	CH_4	CO_2	CH_4			CO_2	CH_4
5.75	3.46	0.300	0.700	none	none	SI	3.69	0.449	0.551
5.75	3.43	0.360	0.640	none	none	SI	3.45	0.516	0.484
7.75	4.24	0.320	0.680	none	none	SI	4.56	0.461	0.539
9.75	5.17	0.280	0.720	none	none	SI	5.91	0.404	0.596
11.55	6.47	0.230	0.770	none	none	SI	7.50	0.332	0.668
2.35	1.99	0.600	0.400	none	none	SI	2.09	0.747	0.253
6.05	3.08	0.440	0.560	none	none	SI	3.48	0.594	0.406

3.25	3.2	0.125	0.875	none	none	SI	3.25	0.224	0.776
5.25	3.95	0.085	0.915	none	none	SI	4.13	0.155	0.845
7.85	5.1	0.070	0.930	none	none	SI	5.52	0.125	0.875
10.65	6.89	0.055	0.945	none	none	SI	7.61	0.094	0.906
6.45	3	0.710	0.290	none	none	SI	3.13	0.814	0.186
9.05	4.27	0.610	0.390	none	none	SI	4.57	0.723	0.277
10.65	5.27	0.520	0.480	none	none	SI	5.88	0.633	0.367
12.35	6.89	0.410	0.590	none	none	SI	7.70	0.514	0.486
12.55	7	0.410	0.590	none	none	SI	8.00	0.510	0.490
Mean Deviation (%)							8.2	none	None

6.2.3 CH_4-N_2 Clathrate Hydrate equilibrium data

Table 36 : CH_SI-V-Lw Equilibrium of N_2-CH_4 from Jhaveri and Robinson (1965). The simulation curve is obtained with the GasHyDyn simulator, implemented with reference parameters from Table 52 (Dharmawardhana et al, 1980) and Table 53. (page 105) and Kihara parameters given in Table 55 (page 120)

Experimental Equilibrium Data						Simulation			
T °C	P MPa	Gas composition		Hydrate composition		S	P MPa	Hydrate composition	
		N_2	CH_4	N_2	CH_4			N_2	CH_4
0.05	2.64	0.000	1.000	0.000	1.000	SI	2.66	0.000	1.000
0.05	3.62	0.160	0.840	0.065	0.935	SI	3.12	0.034	0.966
0.05	4.31	0.310	0.690	0.098	0.902	SI	3.71	0.078	0.922
0.05	5.35	0.530	0.470	0.200	0.800	SI	5.09	0.177	0.823
0.05	6.55	0.645	0.355	0.350	0.650	SI	6.30	0.259	0.741
0.05	7.75	0.725	0.275	0.425	0.575	SI	7.51	0.339	0.661
0.05	10.64	0.815	0.185	0.620	0.380	SI	9.52	0.466	0.534
0.05	11.65	0.880	0.120	0.710	0.290	SI	11.71	0.597	0.403

0.05	12.77	0.900	0.100	0.765	0.235	SI	12.56	0.646	0.354
4.25	3.86	0.000	1.000	0.000	1.000	SI	4.03	0.000	1.000
4.25	5.2	0.440	0.560	0.180	0.820	SI	6.84	0.138	0.862
4.25	8.11	0.630	0.370	0.310	0.690	SI	9.52	0.262	0.738
4.25	10.34	0.740	0.260	0.470	0.530	SI	12.26	0.378	0.622
4.25	12.06	0.780	0.220	0.560	0.440	SI	13.63	0.433	0.567
4.25	13.32	0.925	0.075	0.810	0.190	SI	21.66	0.735	0.265
4.25	14.59	0.940	0.060	0.860	0.140	SI	22.92	0.780	0.220
4.25	16.21	1.000	0.000	1.000	0.000	SI	29.49	1.000	0.000
6.65	5.14	0.000	1.000	0.000	1.000	SI	5.16	0.000	1.000
6.65	7.14	0.350	0.650	0.091	0.909	SI	7.75	0.103	0.897
6.65	8.37	0.460	0.540	0.224	0.776	SI	9.18	0.155	0.845
6.65	15.55	0.750	0.250	0.550	0.450	SI	16.52	0.405	0.595
6.65	20.67	0.840	0.160	0.680	0.320	SI	21.23	0.549	0.451
6.65	25.23	0.914	0.086	0.802	0.198	SI	27.05	0.715	0.285
6.65	32.42	1.000	0.000	1.000	0.000	SI	37.90	1.000	0.000
Mean Deviation (%)							16.3	20.1	23.7

Table 37 : CH_SI-V-Lw Equilibrium of N_2-CH_4 from Jhaveri and Robinson (1965). The simulation curve is obtained with the GasHyDyn simulator, implemented with reference parameters from Table 52 (Dharmawardhana et al, 1980) and Table 53. (page 105) and Kihara parameters given in Table 55 (page 120)

Experimental Equilibrium Data						Simulation			
T °C	P MPa	Gas composition		Hydrate composition		S	P MPa	Hydrate composition	
		N_2	CH_4	N_2	CH_4			N_2	CH_4
9.65	7.4	0.127	0.873	none	none	SI	8.16	0.032	0.968
11.45	9.31	0.127	0.873	none	none	SI	10.03	0.033	0.967
14.55	14.52	0.127	0.873	none	none	SI	14.59	0.037	0.963

16.35	17.11	0.127	0.873	none	none	SI	18.39	0.039	0.961
17.25	17.49	0.127	0.873	none	none	SI	20.70	0.040	0.960
17.85	19.53	0.127	0.873	none	none	SI	22.39	0.041	0.959
18.35	19.99	0.127	0.873	none	none	SI	23.94	0.042	0.958
19.75	22.94	0.127	0.873	none	none	SI	28.78	0.044	0.956
20.25	24.66	0.127	0.873	none	none	SI	30.70	0.045	0.955
22.05	31.31	0.127	0.873	none	none	SI	38.91	0.047	0.953
0.05	3.9	0.269	0.731	none	none	SI	3.53	0.064	0.936
10.15	8.95	0.269	0.731	none	none	SI	10.32	0.078	0.922
13.65	13.22	0.269	0.731	none	none	SI	15.76	0.087	0.913
16.75	19.55	0.269	0.731	none	none	SI	23.46	0.095	0.905
19.15	25.99	0.269	0.731	none	none	SI	32.07	0.102	0.898
21.25	34.33	0.269	0.731	none	none	SI	42.05	0.108	0.892
0.05	4.96	0.498	0.503	none	none	SI	4.83	0.158	0.842
4.05	6.13	0.498	0.503	none	none	SI	7.33	0.168	0.832
6.55	7.77	0.498	0.503	none	none	SI	9.65	0.176	0.824
9.15	10.49	0.498	0.503	none	none	SI	13.02	0.186	0.814
14.15	17.9	0.498	0.503	none	none	SI	24.01	0.210	0.790
16.65	24.99	0.498	0.503	none	none	SI	32.83	0.222	0.778
18.65	50.25	0.498	0.503	none	none	SI	42.15	0.230	0.770
0.05	7.96	0.728	0.272	none	none	SI	7.57	0.343	0.657
3.95	10.16	0.728	0.272	none	none	SI	11.53	0.361	0.639
6.85	12.64	0.728	0.272	none	none	SI	15.91	0.377	0.623
9.75	17.04	0.728	0.272	none	none	SI	22.47	0.395	0.605
10.05	17.5	0.728	0.272	none	none	SI	23.28	0.397	0.603
11.95	20.72	0.728	0.272	none	none	SI	29.18	0.409	0.591
13.65	25.15	0.728	0.272	none	none	SI	35.77	0.419	0.581
14.85	28.49	0.728	0.272	none	none	SI	41.24	0.425	0.575
0.05	8.62	0.760	0.240	none	none	SI	8.19	0.383	0.617

1.45	9.15	0.760	0.240	none	none	SI	9.51	0.390	0.610
5.65	12.96	0.760	0.240	none	none	SI	15.12	0.412	0.588
8.95	17.44	0.760	0.240	none	none	SI	22.14	0.433	0.567
11.95	24.34	0.760	0.240	none	none	SI	31.51	0.451	0.549
14.45	31.99	0.760	0.240	none	none	SI	42.35	0.465	0.535
15.95	35.96	0.760	0.240	none	none	SI	50.46	0.472	0.528
0.05	12.55	0.892	0.108	none	none	SI	12.21	0.626	0.374
4.05	15.86	0.892	0.108	none	none	SI	18.80	0.646	0.354
5.95	19.39	0.892	0.108	none	none	SI	23.20	0.656	0.344
7.75	22.52	0.892	0.108	none	none	SI	28.37	0.665	0.335
8.95	25.82	0.892	0.108	none	none	SI	32.42	0.671	0.329
10.05	28.79	0.892	0.108	none	none	SI	36.68	0.676	0.324
Mean Deviation (%)							21.1	none	none

6.2.4 CH_4-C_2H_6 Clathrate Hydrate equilibrium data

Table 38 : CH_SI-V-Lw Equilibrium of CH_4-C_2H_6 from Deaton and Frost (1946). The simulation curve is obtained with the GasHyDyn simulator, implemented with reference parameters from Table 52 (Dharmawardhana et al, 1980) and Table 53. (page 105) and Kihara parameters given in Table 55 (page 120)

Experimental Equilibrium Data						Simulation			
T °C	P MPa	Gas composition		Hydrate composition		S	P MPa	Hydrate composition	
		CH_4	C_2H_6	CH_4	C_2H_6				CH_4
4.45	1.289	0.564	0.436	none	none	SI	1.08	0.284	0.716
7.25	1.758	0.564	0.436	none	none	SI	1.46	0.294	0.706
10.05	2.434	0.564	0.436	none	none	SI	1.99	0.305	0.695
1.65	1.524	0.904	0.096	none	none	SI	1.74	0.570	0.430
4.45	2.096	0.904	0.096	none	none	SI	2.34	0.586	0.414

7.25	2.889	0.904	0.096	none	none	SI	3.18	0.603	0.397
10.05	3.965	0.904	0.096	none	none	SI	4.37	0.623	0.377
1.65	1.841	0.95	0.05	none	none	SI	2.18	0.708	0.292
4.45	2.53	0.95	0.05	none	none	SI	2.93	0.723	0.277
7.25	3.447	0.95	0.05	none	none	SI	3.97	0.740	0.260
10.05	4.771	0.95	0.05	none	none	SI	5.45	0.760	0.240
1.65	2.158	0.971	0.029	none	none	SI	2.50	0.804	0.196
4.45	2.958	0.971	0.029	none	none	SI	3.34	0.817	0.183
7.25	4.034	0.971	0.029	none	none	SI	4.50	0.830	0.170
1.65	2.365	0.978	0.022	none	none	SI	2.61	0.843	0.157
4.45	3.227	0.978	0.022	none	none	SI	3.50	0.854	0.146
7.25	4.413	0.978	0.022	none	none	SI	4.71	0.866	0.134
9.45	5.668	0.978	0.022	none	none	SI	6.00	0.876	0.124
10.05	6.088	0.978	0.022	none	none	SI	6.42	0.879	0.121
1.65	2.861	0.988	0.012	none	none	SI	2.82	0.908	0.092
4.45	3.806	0.988	0.012	none	none	SI	3.76	0.915	0.085
7.25	5.088	0.988	0.012	none	none	SI	5.03	0.922	0.078
Mean Deviation (%)							11.0	none	none

Table 39 : CH_SI-V-Lw Equilibrium of CH_4-C_2H_6 from Holder and Grigoriou (1980). The simulation curve is obtained with the GasHyDyn simulator, implemented with reference parameters from Table 52 (Dharmawardhana et al, 1980) and Table 53. (page 105) and Kihara parameters given in Table 55 (page 120)

Experimental Equilibrium Data						Simulation			
T °C	P MPa	Gas composition		Hydrate composition		S	P MPa	Hydrate composition	
		CH_4	C_2H_6	CH_4	C_2H_6			CH_4	C_2H_6
10.75	1.81	0.016	0.984	none	none	SI	1.81	0.034	0.966
12.55	2.31	0.016	0.984	none	none	SI	2.32	0.038	0.962

13.45	2.71	0.016	0.984	none	none	SI	2.64	0.041	0.959
14.65	3.08	0.016	0.984	none	none	SI	3.14	0.046	0.954
6.25	0.99	0.047	0.953	none	none	SI	1.01	0.063	0.937
8.35	1.34	0.047	0.953	none	none	SI	1.29	0.069	0.931
10.15	1.71	0.047	0.953	none	none	SI	1.62	0.076	0.924
12.15	2.17	0.047	0.953	none	none	SI	2.10	0.085	0.915
13.25	2.51	0.047	0.953	none	none	SI	2.43	0.090	0.910
14.45	2.99	0.047	0.953	none	none	SI	2.88	0.097	0.903
8.45	1.42	0.177	0.823	none	none	SI	1.28	0.160	0.840
10.15	1.77	0.177	0.823	none	none	SI	1.56	0.168	0.832
11.65	2.14	0.177	0.823	none	none	SI	1.87	0.174	0.826
13.05	2.66	0.177	0.823	none	none	SI	2.20	0.181	0.819
13.85	3	0.177	0.823	none	none	SI	2.45	0.185	0.815
10.75	1.81	0.016	0.984	none	none	SI	1.81	0.034	0.966
12.55	2.31	0.016	0.984	none	none	SI	2.32	0.038	0.962
13.45	2.71	0.016	0.984	none	none	SI	2.64	0.041	0.959
14.65	3.08	0.016	0.984	none	none	SI	3.14	0.046	0.954
6.25	0.99	0.047	0.953	none	none	SI	1.01	0.063	0.937
8.35	1.34	0.047	0.953	none	none	SI	1.29	0.069	0.931
10.15	1.71	0.047	0.953	none	none	SI	1.62	0.076	0.924
Mean Deviation (%)							6.3	none	none

6.2.5 CO2-C2H6 Clathrate Hydrate equilibrium data

Table 40 : CH_SI-V-Lw Equilibrium of CH_4-C_2H_6 from Adisasmito and Sloan (1992). The simulation curve is obtained with the GasHyDyn simulator, implemented with reference parameters from Table 52 (Dharmawardhana et al, 1980) and Table 53. (page 105) and Kihara parameters given in Table 55 (page 120)

Experimental Equilibrium Data	Simulation

T °C	P MPa	Gas composition		Hydrate composition		S	P MPa	Hydrate composition	
		CO_2	C_2H_6	CO_2	C_2H_6			CO_2	CO_2 H_6
0.55	0.57	0.220	0.780	none	none	SI	0.49	0.192	0.808
2.45	0.70	0.202	0.798	none	none	SI	0.60	0.189	0.811
4.35	0.87	0.189	0.811	none	none	SI	0.75	0.189	0.811
6.15	1.09	0.193	0.807	none	none	SI	0.92	0.198	0.802
7.95	1.41	0.246	0.754	none	none	SI	1.13	0.230	0.770
9.75	1.75	0.256	0.744	none	none	SI	1.39	0.241	0.759
11.95	2.39	0.317	0.683	none	none	SI	1.83	0.275	0.725
3.35	0.85	0.428	0.572	none	none	SI	0.73	0.299	0.701
5.25	1.08	0.417	0.583	none	none	SI	0.89	0.300	0.700
7.05	1.35	0.406	0.594	none	none	SI	1.08	0.300	0.700
8.85	1.72	0.400	0.600	none	none	SI	1.32	0.303	0.697
10.65	2.19	0.402	0.598	none	none	SI	1.63	0.309	0.691
12.65	2.83	0.389	0.611	none	none	SI	2.05	0.309	0.691
14.65	3.83	0.398	0.602	none	none	SI	2.64	0.321	0.679
Mean Deviation (%)							19.9	none	none

6.2.6 CH4-C3H8 Clathrate Hydrate equilibrium data

Table 41 : CH-V-Lw Equilibrium of CH_4-C_3H_8 from Verma et al (1974). The simuation curve is obtained with the GasHyDyn simulator, implemented with reference parameters from Table 52 (Dharmawardhana et al, 1980) and Table 53. (page 105) and Kihara parameters given in Table 55 (page 120)

Experimental Equilibrium Data						Simulation			
T °C	P MPa	Gas composition		Hydrate composition		S	P MPa	Hydrate composition	
		CH_4	C_3H_8	CH_4	C_3H_8			CH_4	C_3H_8

1.75	0.263	0.2375	0.7625	none	none	SI	0.34	0.119	0.881
3.25	0.35	0.2375	0.7625	none	none	SI	0.40	0.127	0.873
4.65	0.443	0.2375	0.7625	none	none	SI	0.48	0.135	0.865
5.95	0.56	0.2375	0.7625	none	none	SI	0.56	0.142	0.858
7.05	0.689	0.2375	0.7625	none	none	SI	0.65	0.149	0.851
8.25	0.83	0.2375	0.7625	none	none	SI	0.75	0.156	0.844
1.25	0.27	0.371	0.629	none	none	SI	0.35	0.159	0.841
2.75	0.343	0.371	0.629	none	none	SI	0.42	0.167	0.833
3.95	0.419	0.371	0.629	none	none	SI	0.49	0.174	0.826
5.45	0.536	0.371	0.629	none	none	SI	0.58	0.182	0.818
7.05	0.691	0.371	0.629	none	none	SI	0.71	0.191	0.809
9.15	0.945	0.371	0.629	none	none	SI	0.92	0.202	0.798
Mean Deviation (%)							12.6	none	None
1.75	0.26	0.238	0.763	none	none	SII	0.19	0.324	0.676
3.25	0.35	0.238	0.763	none	none	SII	0.25	0.353	0.647
4.65	0.44	0.238	0.763	none	none	SII	0.30	0.379	0.621
5.95	0.56	0.238	0.763	none	none	SII	0.37	0.403	0.597
7.05	0.69	0.238	0.763	none	none	SII	0.44	0.422	0.578
8.25	0.83	0.238	0.763	none	none	SII	0.52	0.441	0.559
1.25	0.27	0.371	0.629	none	none	SII	0.17	0.382	0.618
2.75	0.34	0.371	0.629	none	none	SII	0.22	0.408	0.592
3.95	0.42	0.371	0.629	none	none	SII	0.26	0.427	0.573
5.45	0.54	0.371	0.629	none	none	SII	0.32	0.450	0.550
7.05	0.69	0.371	0.629	none	none	SII	0.40	0.472	0.528
9.15	0.95	0.371	0.629	none	none	SII	0.52	0.498	0.502
Mean Deviation (%)							36.3	none	None

Table 42 : CH-V-Lw Equilibrium of CH_4-C_3H_8 from Deaton and Frost (1946). The simulation curve is obtained with the GasHyDyn simulator, implemented with reference parameters from Table 52 (Dharmawardhana et al, 1980) and Table 53. (page 105) and Kihara parameters given in Table 55 (page 120)

Experimental Equilibrium Data						Simulation			
T °C	P MPa	Gas composition		Hydrate composition		S	P MPa	Hydrate composition	
		CH_4	C_3H_8	CH_4	C_3H_8			CH_4	C_3H_8
1.65	0.27	0.362	0.638	none	none	SI	0.37	0.159	0.841
4.45	0.44	0.362	0.638	none	none	SI	0.51	0.174	0.826
7.25	0.69	0.362	0.638	none	none	SI	0.72	0.189	0.811
1.65	0.37	0.712	0.288	none	none	SI	0.61	0.274	0.726
4.45	0.54	0.712	0.288	none	none	SI	0.85	0.288	0.712
7.25	0.80	0.712	0.288	none	none	SI	1.18	0.302	0.698
10.05	1.15	0.712	0.288	none	none	SI	1.67	0.318	0.682
1.65	0.55	0.883	0.117	none	none	SI	1.08	0.412	0.588
4.45	0.78	0.883	0.117	none	none	SI	1.49	0.431	0.569
7.25	1.11	0.883	0.117	none	none	SI	2.10	0.453	0.547
10.05	1.56	0.883	0.117	none	none	SI	2.99	0.481	0.519
1.65	0.81	0.952	0.048	none	none	SI	1.73	0.592	0.408
4.45	1.14	0.952	0.048	none	none	SI	2.38	0.618	0.382
7.25	1.59	0.952	0.048	none	none	SI	3.31	0.649	0.351
10.05	2.23	0.952	0.048	none	none	SI	4.66	0.685	0.315
1.65	1.15	0.974	0.026	none	none	SI	2.17	0.720	0.280
4.45	1.59	0.974	0.026	none	none	SI	2.96	0.745	0.255
7.25	2.19	0.974	0.026	none	none	SI	4.08	0.773	0.227
10.05	3.01	0.974	0.026	none	none	SI	5.67	0.804	0.196
1.65	1.63	0.990	0.010	none	none	SI	2.67	0.868	0.132
4.45	2.25	0.990	0.010	none	none	SI	3.59	0.883	0.117

4.45	2.26	0.990	0.010	none	none	SI	3.59	0.883	0.117
7.25	3.12	0.990	0.010	none	none	SI	4.87	0.900	0.100
9.95	4.36	0.990	0.010	none	none	SI	6.61	0.917	0.083
Mean Deviation (%)							71.76	none	none
1.65	0.27	0.362	0.638	none	none	SII	0.18	0.385	0.615
4.45	0.44	0.362	0.638	none	none	SII	0.28	0.432	0.568
7.25	0.69	0.362	0.638	none	none	SII	0.41	0.472	0.528
1.65	0.37	0.712	0.288	none	none	SII	0.21	0.504	0.496
4.45	0.54	0.712	0.288	none	none	SII	0.30	0.531	0.469
7.25	0.80	0.712	0.288	none	none	SII	0.42	0.554	0.446
10.05	1.15	0.712	0.288	none	none	SII	0.59	0.573	0.427
1.65	0.55	0.883	0.117	none	none	SII	0.29	0.561	0.439
4.45	0.78	0.883	0.117	none	none	SII	0.40	0.578	0.422
7.25	1.11	0.883	0.117	none	none	SII	0.55	0.593	0.407
10.05	1.56	0.883	0.117	none	none	SII	0.76	0.606	0.394
1.65	0.81	0.952	0.048	none	none	SII	0.30	0.574	0.426
4.45	1.14	0.952	0.048	none	none	SII	0.56	0.608	0.392
7.25	1.59	0.952	0.048	none	none	SII	0.76	0.618	0.382
10.05	2.23	0.952	0.048	none	none	SII	1.04	0.627	0.373
1.65	1.15	0.974	0.026	none	none	SII	0.51	0.614	0.386
4.45	1.59	0.974	0.026	none	none	SII	0.70	0.624	0.376
7.25	2.19	0.974	0.026	none	none	SII	0.91	0.631	0.369
10.05	3.01	0.974	0.026	none	none	SII	1.31	0.640	0.360
1.65	1.63	0.990	0.010	none	none	SII	0.74	0.641	0.359
4.45	2.25	0.990	0.010	none	none	SII	1.01	0.649	0.351
4.45	2.26	0.990	0.010	none	none	SII	1.01	0.649	0.351
7.25	3.12	0.990	0.010	none	none	SII	1.38	0.657	0.343
9.95	4.36	0.990	0.010	none	none	SII	1.87	0.664	0.336
Mean Deviation (%)							50.5	none	none

Table 43 : CH-V-Lw Equilibrium of CH_4-C_3H_8 from Mc Leod and Campbell (1961). The simulation curve is obtained with the GasHyDyn simulator, implemented with reference parameters from Table 52 (Dharmawardhana et al, 1980) and Table 53. (page 105) and Kihara parameters given in Table 55 (page 120)

Experimental Equilibrium Data						Simulation			
T °C	P MPa	Gas composition		Hydrate composition		S	P MPa	Hydrate composition	
		CH_4	C_3H_8	CH_4	C_3H_8			CH_4	C_3H_8
17.35	6.93	0.965	0.035	none	none	SI	14.89	0.868	0.132
30.55	62.47	0.965	0.035	none	none	SI	86.02	0.899	0.101
31.25	68.98	0.965	0.035	none	none	SI	92.61	0.895	0.105
25.95	34.51	0.965	0.035	none	none	SI	50.26	0.913	0.087
23.45	20.86	0.965	0.035	none	none	SI	36.27	0.912	0.088
28.45	48.37	0.965	0.035	none	none	SI	68.09	0.908	0.092
30.55	62.29	0.965	0.035	none	none	SI	86.02	0.899	0.101
21.35	13.89	0.965	0.035	none	none	SI	27.05	0.905	0.095
20.15	10.45	0.965	0.035	none	none	SI	22.70	0.897	0.103
17.55	6.93	0.965	0.035	none	none	SI	15.35	0.871	0.129
19.95	7.41	0.945	0.055	none	none	SI	20.47	0.846	0.154
19.65	7.41	0.945	0.055	none	none	SI	19.61	0.843	0.157
27.45	34.58	0.945	0.055	none	none	SI	57.76	0.871	0.129
29.55	48.37	0.945	0.055	none	none	SI	73.46	0.863	0.137
31.75	62.23	0.945	0.055	none	none	SI	92.51	0.848	0.152
25.35	23.62	0.945	0.055	none	none	SI	44.48	0.874	0.126
23.05	13.89	0.945	0.055	none	none	SI	32.63	0.870	0.130
17.35	6.93	0.965	0.035	none	none	SI	14.89	0.868	0.132
Mean Deviation (%)							85	none	none
17.35	6.93	0.965	0.035	none	none	SII	2.68	0.651	0.349

30.55	62.47	0.965	0.035	none	none	SII	19.73	0.690	0.310
31.25	68.98	0.965	0.035	none	none	SII	22.49	0.693	0.307
25.95	34.51	0.965	0.035	none	none	SII	8.33	0.671	0.329
23.45	20.86	0.965	0.035	none	none	SII	5.75	0.664	0.336
28.45	48.37	0.965	0.035	none	none	SII	12.99	0.680	0.320
30.55	62.29	0.965	0.035	none	none	SII	19.73	0.690	0.310
21.35	13.89	0.965	0.035	none	none	SII	4.26	0.659	0.341
20.15	10.45	0.965	0.035	none	none	SII	3.65	0.657	0.343
17.55	6.93	0.965	0.035	none	none	SII	2.75	0.652	0.348
19.95	7.41	0.945	0.055	none	none	SII	3.05	0.649	0.351
19.65	7.41	0.945	0.055	none	none	SII	2.94	0.648	0.352
27.45	34.58	0.945	0.055	none	none	SII	8.36	0.665	0.335
29.55	48.37	0.945	0.055	none	none	SII	12.11	0.671	0.329
31.75	62.23	0.945	0.055	none	none	SII	18.75	0.679	0.321
25.35	23.62	0.945	0.055	none	none	SII	6.08	0.660	0.340
23.05	13.89	0.945	0.055	none	none	SII	4.47	0.655	0.345
17.35	6.93	0.965	0.035	none	none	SII	2.68	0.651	0.349
Mean Deviation (%)							68	none	none

Table 44 : CH-V-Lw Equilibrium of CH_4-C_3H_8 from Thakore and Holder (1987). The simulation curve is obtained with the GasHyDyn simulator, implemented with reference parameters from Table 52 (Dharmawardhana et al, 1980) and Table 53. (page 105) and Kihara parameters given in Table 55 (page 120)

Experimental Equilibrium Data						Simulation			
T °C	P MPa	Gas composition		Hydrate composition		S	P MPa	Hydrate composition	
		CH_4	C_3H_8	CH_4	C_3H_8			CH_4	C_3H_8
2	0.42	0.765	0.235	none	none	SI	0.73	0.304	0.696

2	0.39	0.727	0.273	none	none	SI	0.66	0.283	0.717
2	0.37	0.700	0.300	none	none	SI	0.62	0.271	0.729
2	0.30	0.516	0.484	none	none	SI	0.45	0.206	0.794
2	0.28	0.420	0.580	none	none	SI	0.30	0.161	0.839
2	0.28	0.366	0.634	none	none	SI	0.38	0.162	0.838
2	0.27	0.352	0.648	none	none	SI	0.38	0.158	0.842
2	0.25	0.190	0.810	none	none	SI	0.34	0.102	0.898
2	0.25	0.083	0.917	none	none	SI	0.32	0.053	0.947
2	0.25	0.081	0.919	none	none	SI	0.32	0.052	0.948
2	0.25	0.054	0.946	none	none	SI	0.31	0.037	0.963
2	0.25	0.046	0.954	none	none	SI	0.31	0.032	0.968
2	0.25	0.037	0.963	none	none	SI	0.31	0.026	0.974
2	0.25	0.021	0.979	none	none	SI	0.31	0.015	0.985
2	0.26	0.000	1.000	none	none	SI	0.31	0.000	1.000
5	1.31	0.956	0.044	none	none	SI	2.63	0.643	0.357
5	1.14	0.947	0.053	none	none	SI	2.43	0.602	0.398
5	0.85	0.894	0.106	none	none	SI	1.67	0.453	0.547
5	0.63	0.768	0.232	none	none	SI	1.04	0.321	0.679
5	0.50	0.530	0.470	none	none	SI	0.66	0.225	0.775
5	0.49	0.510	0.490	none	none	SI	0.64	0.219	0.781
5	0.48	0.502	0.498	none	none	SI	0.63	0.217	0.783
5	0.48	0.468	0.532	none	none	SI	0.61	0.207	0.793
5	0.48	0.412	0.588	none	none	SI	0.58	0.191	0.809
5	0.46	0.394	0.606	none	none	SI	0.57	0.186	0.814
5	0.46	0.390	0.610	none	none	SI	0.56	0.185	0.815
5	0.48	0.030	0.970	none	none	SI	0.46	0.028	0.972
5	0.48	0.026	0.974	none	none	SI	0.46	0.024	0.976
5	0.51	0.000	1.000	none	none	SI	0.46	0.000	1.000
Mean Deviation (%)							41.4	none	none

2	0.67	0.903	0.097	none	none	SII	0.32	0.571	0.429
2	0.42	0.765	0.235	none	none	SII	0.23	0.523	0.477
2	0.39	0.727	0.273	none	none	SII	0.22	0.512	0.488
2	0.37	0.700	0.300	none	none	SII	0.22	0.504	0.496
2	0.30	0.516	0.484	none	none	SII	0.20	0.448	0.552
2	0.28	0.420	0.580	none	none	SII	0.19	0.415	0.585
2	0.28	0.366	0.634	none	none	SII	0.19	0.393	0.607
2	0.27	0.352	0.648	none	none	SII	0.19	0.387	0.613
2	0.25	0.190	0.810	none	none	SII	0.21	0.297	0.703
2	0.25	0.083	0.917	none	none	SII	0.23	0.188	0.812
2	0.25	0.081	0.919	none	none	SII	0.23	0.184	0.816
2	0.25	0.054	0.946	none	none	SII	0.24	0.141	0.859
2	0.25	0.046	0.954	none	none	SII	0.25	0.126	0.874
2	0.25	0.037	0.963	none	none	SII	0.25	0.107	0.893
2	0.25	0.021	0.979	none	none	SII	0.26	0.067	0.933
2	0.26	0.000	1.000	none	none	SII	0.28	0.000	1.000
5	1.31	0.956	0.044	none	none	SII	0.61	0.612	0.388
5	1.14	0.947	0.053	none	none	SII	0.57	0.607	0.393
5	0.85	0.894	0.106	none	none	SII	0.43	0.583	0.417
5	0.63	0.768	0.232	none	none	SII	0.34	0.550	0.450
5	0.50	0.530	0.470	none	none	SII	0.29	0.491	0.509
5	0.49	0.510	0.490	none	none	SII	0.29	0.484	0.516
5	0.48	0.502	0.498	none	none	SII	0.29	0.483	0.517
5	0.48	0.468	0.532	none	none	SII	0.29	0.474	0.526
5	0.48	0.412	0.588	none	none	SII	0.30	0.457	0.543
5	0.46	0.394	0.606	none	none	SII	0.30	0.451	0.549
5	0.46	0.390	0.610	none	none	SII	0.30	0.450	0.550
5	0.48	0.030	0.970	none	none	SII	0.47	0.138	0.862
5	0.48	0.026	0.974	none	none	SII	0.48	0.125	0.875

Mean Deviation (%)	27.4	none	none

6.2.7 C2H6-C3H8 Clathrate Hydrate equilibrium data

Table 45 : CH-V-Lw Equilibrium of C_2H_6-C_3H_8 from Mooijer-van den Heuvel (2004). The simulation curve is obtained with the GasHyDyn simulator, implemented with reference parameters from Table 52 (Dharmawardhana et al, 1980) and Table 53. (page 105) and Kihara parameters given in Table 55 (page 120)

Experimental Equilibrium Data						Simulation			
T °C	P MPa	Gas composition		Hydrate composition		S	P MPa	Hydrate composition	
		CH_4	C_3H_8	CH_4	C_3H_8			CH_4	C_3H_8
3.88	0.54	0.299	0.701	none	none	SI	0.47	0.190	0.810
4.28	0.58	0.299	0.701	none	none	SI	0.49	0.191	0.809
4.63	0.63	0.299	0.701	none	none	SI	0.52	0.192	0.808
4.84	0.66	0.299	0.701	none	none	SI	0.53	0.193	0.807
5.02	0.67	0.299	0.701	none	none	SI	0.54	0.193	0.807
3.91	0.81	0.501	0.499	none	none	SI	0.53	0.356	0.644
4.75	0.81	0.501	0.499	none	none	SI	0.59	0.360	0.640
4.81	0.86	0.501	0.499	none	none	SI	0.60	0.360	0.640
4.88	0.86	0.501	0.499	none	none	SI	0.60	0.360	0.640
4.97	0.96	0.501	0.499	none	none	SI	0.61	0.361	0.639
5.03	0.91	0.501	0.499	none	none	SI	0.61	0.361	0.639
3.88	0.54	0.299	0.701	none	none	SI	0.47	0.190	0.810
Mean Deviation (%)							25.5	none	none
3.88	0.54	0.299	0.701	none	none	SII	0.63	0.016	0.984
4.28	0.58	0.299	0.701	none	none	SII	0.69	0.017	0.983
4.63	0.63	0.299	0.701	none	none	SII	0.76	0.018	0.982

4.84	0.66	0.299	0.701	none	none	SII	0.80	0.019	0.981
5.02	0.67	0.299	0.701	none	none	SII	0.84	0.019	0.981
3.91	0.81	0.501	0.499	none	none	SII	0.94	0.038	0.962
4.75	0.81	0.501	0.499	none	none	SII	1.19	0.044	0.956
4.81	0.86	0.501	0.499	none	none	SII	1.21	0.044	0.956
4.88	0.86	0.501	0.499	none	none	SII	1.24	0.045	0.955
4.97	0.96	0.501	0.499	none	none	SII	1.27	0.046	0.954
5.03	0.91	0.501	0.499	none	none	SII	1.30	0.046	0.954
Mean Deviation (%)							29.4	none	none

6.2.8 CO2-CH4-C2H6 Clathrate Hydrate equilibrium data

Table 46 CH-V-Lw Equilibrium of CO_2-CH_4-C_2H_6 from our work. The simulation curve is obtained with the GasHyDyn simulator, implemented with reference parameters from Table 52 (Dharmawardhana et al, 1980) and Table 53. (page 105) and Kihara parameters given in Table 55 (page 120)

Experimental Equilibrium Data								Simulation				
T °C	P MPa	Gas composition			Hydrate composition				P MPa	Hydrate composition		
		CO_2	CH_4	C_2H_6	CO_2	CH_4	C_2H_6			CO_2	CH_4	C_2H_6
2.75	3.54	0.059	0.916	0.026	0.144	0.769	0.087	SI	2.72	0.097	0.739	0.164
3.65	3.81	0.065	0.906	0.030	0.144	0.769	0.087	SI	2.90	0.103	0.717	0.180
5.15	4.23	0.071	0.892	0.038	0.141	0.774	0.085	SI	3.22	0.106	0.683	0.210
6.55	4.56	0.073	0.884	0.043	0.141	0.777	0.082	SI	3.64	0.107	0.669	0.224
7.80	5.12	0.078	0.876	0.046	0.135	0.777	0.089	SI	4.11	0.112	0.662	0.226
9.25	5.99	0.090	0.865	0.045	0.049	0.804	0.148	SI	4.83	0.127	0.661	0.211
Mean Deviation (%)									21.7	48.18	11.4	119.2
2.75	3.54	0.059	0.916	0.026	0.144	0.769	0.087	S2	2.45	0.071	0.833	0.096

3.65	3.81	0.065	0.906	0.030	0.144	0.769	0.087	S2	2.65	0.076	0.819	0.105
5.15	4.23	0.071	0.892	0.038	0.141	0.774	0.085	S2	3.03	0.081	0.798	0.121
6.55	4.56	0.073	0.884	0.043	0.141	0.777	0.082	S2	3.46	0.082	0.790	0.128
7.80	5.12	0.078	0.876	0.046	0.135	0.777	0.089	S2	3.94	0.086	0.785	0.129
9.25	5.99	0.090	0.865	0.045	0.049	0.804	0.148	S2	4.63	0.098	0.780	0.122
Mean Deviation (%)									26.5	53.3	3.9	32.1

Table 47 CH-V-Lw Equilibrium of CO_2-CH_4-C_2H_6 from Kvenvolden et al (1984). The simulation curve is obtained with the GasHyDyn simulator, implemented with reference parameters from Table 52 (Dharmawardhana et al, 1980) and Table 53. (page 105) and Kihara parameters given in Table 55 (page 120)

Experimental Equilibrium Data								Simulation				
T °C	P MPa	Gas composition			Hydrate composition				P MPa	Hydrate composition		
		CO_2	CH_4	C_2H_6	CO_2	CH_4	C_2H_6			CO_2	CH_4	C_2H_6
-4	3.79	0.002	0.997	0.001	none	none	none	SI	2.25	0.004	0.984	0.011
-4	3.62	0.002	0.991	0.007	none	none	none	SI	2.14	0.005	0.932	0.063
-4	3.50	0.003	0.995	0.003	none	none	none	SI	2.22	0.006	0.970	0.024
-4	3.22	0.002	0.995	0.002	none	none	none	SI	2.23	0.005	0.973	0.023
-4	2.78	0.003	0.994	0.003	none	none	none	SI	2.22	0.007	0.970	0.024
-4	2.04	0.003	0.995	0.003	none	none	none	SI	2.23	0.005	0.971	0.024
-4	1.20	0.005	0.992	0.003	none	none	none	SI	2.21	0.010	0.962	0.027
Mean Deviation (%)									37.4	none	none	none
-4	3.79	0.002	0.997	0.001	none	none	none	SII	1.79	0.003	0.990	0.007
-4	3.62	0.002	0.991	0.007	none	none	none	SII	1.74	0.003	0.959	0.038
-4	3.50	0.003	0.995	0.003	none	none	none	SII	1.77	0.004	0.981	0.015
-4	3.22	0.002	0.995	0.002	none	none	none	SII	1.78	0.003	0.983	0.014
-4	2.78	0.003	0.994	0.003	none	none	none	SII	1.78	0.004	0.981	0.014
-4	2.04	0.003	0.995	0.003	none	none	none	SII	1.77	0.004	0.982	0.014

-4	1.20	0.005	0.992	0.003	none	none	none	SII	1.77	0.007	0.977	0.017
Mean Deviation (%)									42.2	none	none	none

6.2.9 CH4-C2H6-C3H8 Clathrate Hydrate equilibrium data

Table 48 CH-V-Lw Equilibrium of CH_4-C_2H_6-C_3H_8 our work. The simulation curve is obtained with the GasHyDyn simulator, implemented with reference parameters from Table 52 (Dharmawardhana et al, 1980) and Table 53. (page 105) and Kihara parameters given in Table 55 (page 120)

Experimental Equilibrium Data								Simulation				
T °C	P MPa	Gas composition			Hydrate composition				P MPa	Hydrate composition		
		CH_4	C_2H_6	C_3H_8	CH_4	C_2H_6	C_3H_8			CH_4	C_2H_6	C_3H_8
2.45	3.13	0.980	0.003	0.017	0.870	0.070	0.060	SI	2.58	0.784	0.018	0.198
3.15	3.36	0.979	0.004	0.017	0.855	0.079	0.067	SI	2.78	0.786	0.023	0.191
4.15	3.55	0.978	0.005	0.017	0.840	0.087	0.073	SI	3.07	0.788	0.028	0.184
4.95	3.67	0.976	0.007	0.018	0.833	0.089	0.078	SI	3.31	0.784	0.039	0.177
6.30	3.78	0.973	0.009	0.018	0.832	0.088	0.080	SI	3.75	0.778	0.050	0.172
7.70	3.94	0.968	0.012	0.020	0.828	0.087	0.085	SI	4.27	0.769	0.064	0.167
9.10	4.21	0.962	0.018	0.021	0.813	0.083	0.104	SI	4.81	0.755	0.086	0.159
10.10	4.34	0.958	0.020	0.022	0.808	0.081	0.111	SI	5.33	0.750	0.092	0.158
11.15	4.50	0.953	0.023	0.024	0.804	0.071	0.124	SI	5.88	0.742	0.101	0.157
Mean Deviation (%)									15.0	7.3	44.2	113.8
2.45	3.13	0.980	0.003	0.017	0.870	0.070	0.060	SII	0.66	0.628	0.000	0.372
3.15	3.36	0.979	0.004	0.017	0.855	0.079	0.067	SII	0.71	0.630	0.001	0.369
4.15	3.55	0.978	0.005	0.017	0.840	0.087	0.073	SII	0.80	0.633	0.001	0.366
4.95	3.67	0.976	0.007	0.018	0.833	0.089	0.078	SII	0.86	0.635	0.001	0.364
6.30	3.78	0.973	0.009	0.018	0.832	0.088	0.080	SII	0.99	0.638	0.001	0.361
7.70	3.94	0.968	0.012	0.020	0.828	0.087	0.085	SII	1.13	0.640	0.002	0.358

9.10	4.21	0.962	0.018	0.021	0.813	0.083	0.104	SII	1.30	0.642	0.003	0.355
10.10	4.34	0.958	0.020	0.022	0.808	0.081	0.111	SII	1.42	0.643	0.003	0.354
11.15	4.50	0.953	0.023	0.024	0.804	0.071	0.124	SII	1.55	0.644	0.003	0.353
Mean Deviation (%)									73.3	23.3	97.9	338.9

6.2.10 CH4-C2H6-C3H8 C4H10(-1) Clathrate Hydrate equilibrium data

Table 49 CH-V-Lw Equilibrium of CH_4-C_2H_6-C_3H_8 C_4H_{10}(-1) our work. The simulation curve is obtained with the GasHyDyn simulator, implemented with reference parameters from Table 52 (Dharmawardhana et al, 1980) and Table 53. (page 105) and Kihara parameters given in Table 55 (page 120)

Experimental Equilibrium Data										Simulation					
T °C	P MPa	Gas composition				Hydrate composition					P MPa	Hydrate composition			
		CH_4	C_2H_6	C_3H_8	C_3H_8 -1	CH_4	C_2H_6	C_3H_8	C_3H_8 -1			CH_4	C_2H_6	C_3H_8	C_3H_8 -1
2.40	2.28	0.971	0.017	0.004	0.008	0.721	0.111	0.118	0.051	SI	2.80	0.833	0.117	0.050	0.000
3.45	2.31	0.967	0.019	0.005	0.008	0.723	0.109	0.118	0.050	SI	3.04	0.818	0.125	0.057	0.000
7.60	2.75	0.942	0.035	0.008	0.015	0.696	0.104	0.149	0.051	SI	4.21	0.748	0.182	0.069	0.000
9.15	2.97	0.930	0.041	0.012	0.017	0.677	0.103	0.169	0.052	SI	4.76	0.723	0.193	0.084	0.000
9.90	3.05	0.923	0.044	0.015	0.018	0.679	0.099	0.171	0.051	SI	4.99	0.704	0.194	0.101	0.000
10.80	3.12	0.915	0.046	0.020	0.019	0.686	0.097	0.167	0.050	SI	5.34	0.688	0.191	0.122	0.000
11.70	3.22	0.906	0.048	0.026	0.021	0.692	0.096	0.163	0.049	SI	5.70	0.670	0.186	0.144	0.000
12.65	3.34	0.896	0.050	0.032	0.022	0.703	0.093	0.155	0.048	SI	6.13	0.654	0.182	0.164	0.000
13.65	3.46	0.888	0.052	0.037	0.023	0.711	0.091	0.150	0.048	SI	6.79	0.650	0.178	0.173	0.000
Mean Deviation (%)											62.1	7.3	73.6	34.8	100
2.40	2.28	0.971	0.017	0.004	0.008	0.721	0.111	0.118	0.051	SII	1.11	0.671	0.010	0.304	0.014
3.45	2.31	0.967	0.019	0.005	0.008	0.723	0.109	0.118	0.050	SII	1.17	0.667	0.009	0.310	0.013
7.60	2.75	0.942	0.035	0.008	0.015	0.696	0.104	0.149	0.051	SII	1.55	0.660	0.012	0.314	0.014
9.15	2.97	0.930	0.041	0.012	0.017	0.677	0.103	0.169	0.052	SII	1.65	0.655	0.010	0.323	0.012
9.90	3.05	0.923	0.044	0.015	0.018	0.679	0.099	0.171	0.051	SII	1.64	0.650	0.009	0.331	0.010
10.80	3.12	0.915	0.046	0.020	0.019	0.686	0.097	0.167	0.050	SII	1.62	0.646	0.008	0.338	0.009

11.70	3.22	0.906	0.048	0.026	0.021	0.692	0.096	0.163	0.049	SII	1.66	0.643	0.006	0.344	0.007
12.65	3.34	0.896	0.050	0.032	0.022	0.703	0.093	0.155	0.048	SII	1.70	0.641	0.005	0.348	0.006
13.65	3.46	0.888	0.052	0.037	0.023	0.711	0.091	0.150	0.048	SII	1.81	0.640	0.005	0.349	0.006
Mean Deviation (%)											47.6	6.47	91.7	120.7	79.8

Table 50 CH-V-Lw Equilibrium of CH_4-C_2H_6-C_3H_8 C_4H_{10}(-1) from our work. The simulation curve is obtained with the GasHyDyn simulator, implemented with reference parameters from Table 52 (Dharmawardhana et al, 1980) and Table 53. (page 105) and Kihara parameters given in Table 55 (page 120)

Experimental Equilibrium Data										Simulation					
T °C	P MPa	Gas composition				Hydrate composition					P MPa	Hydrate composition			
		CH_4	C_2H_6	C_3H_8	C_3H_8 -1	CH_4	C_2H_6	C_3H_8	C_3H_8 -1			CH_4	C_2H_6	C_3H_8	C_3H_8 -1
2.75	2.14	0.954	0.024	0.007	0.014	0.718	0.082	0.159	0.041	SI	2.68	0.769	0.151	0.080	0.000
4.30	2.16	0.955	0.024	0.007	0.014	0.717	0.082	0.160	0.041	SI	3.16	0.780	0.146	0.074	0.000
4.85	2.18	0.952	0.025	0.009	0.014	0.718	0.082	0.159	0.041	SI	3.28	0.768	0.144	0.088	0.000
5.90	2.21	0.951	0.025	0.010	0.014	0.716	0.082	0.160	0.042	SI	3.64	0.767	0.141	0.091	0.000
6.80	2.26	0.948	0.027	0.011	0.014	0.715	0.082	0.162	0.042	SI	3.92	0.757	0.143	0.100	0.000
7.45	2.36	0.939	0.030	0.015	0.016	0.713	0.079	0.166	0.042	SI	3.95	0.726	0.154	0.121	0.000
9.20	2.53	0.926	0.035	0.022	0.017	0.709	0.077	0.172	0.042	SI	4.53	0.692	0.156	0.151	0.000
11.05	2.82	0.905	0.042	0.032	0.021	0.704	0.070	0.186	0.040	SI	5.12	0.651	0.164	0.185	0.000
18.15	3.72	0.845	0.050	0.078	0.027	0.926	0.043	0.020	0.011	SI	12.34	0.668	0.128	0.203	0.000
Mean Deviation (%)											79.9	8.4	101.3	130.6	100
2.75	2.14	0.954	0.024	0.007	0.014	0.718	0.082	0.159	0.041	SII	0.95	0.651	0.008	0.324	0.016
4.30	2.16	0.955	0.024	0.007	0.014	0.717	0.082	0.160	0.041	SII	1.13	0.656	0.009	0.319	0.016
4.85	2.18	0.952	0.025	0.009	0.014	0.718	0.082	0.159	0.041	SII	1.12	0.652	0.008	0.328	0.013
5.90	2.21	0.951	0.025	0.010	0.014	0.716	0.082	0.160	0.042	SII	1.21	0.652	0.007	0.329	0.012
6.80	2.26	0.948	0.027	0.011	0.014	0.715	0.082	0.162	0.042	SII	1.27	0.650	0.007	0.333	0.011
7.45	2.36	0.939	0.030	0.015	0.016	0.713	0.079	0.166	0.042	SII	1.24	0.645	0.006	0.340	0.009
9.20	2.53	0.926	0.035	0.022	0.017	0.709	0.077	0.172	0.042	SII	1.32	0.640	0.005	0.347	0.007
11.05	2.82	0.905	0.042	0.032	0.021	0.704	0.070	0.186	0.040	SII	1.41	0.637	0.005	0.353	0.006

18.15	3.72	0.845	0.050	0.078	0.027	0.926	0.043	0.020	0.011	SII	2.33	0.638	0.003	0.356	0.003
Mean Deviation (%)											47.1	11.7	91.7	275.6	72.6

7. THERMODYNAMICS OF CLATHRATES HYDRATES

The van der Waals and Platteeuw model (1959) describes the hydrate phase by means of statistical thermodynamics based on the following assumptions:

- Each cavity contains at most one guest (gas) molecule
- The interaction between guest and water molecules can be described by a pair potential function of the pair gas-molecule, and the cavity can be treated as perfectly spherical
- The free energy contribution of the water molecules is independent of the modes of occupancy of guest molecules. This assumption means that the gas molecules do not deform cavities
- There is no interaction between the guests molecules in different cavities, gas molecules interact only with the nearest water molecules.

From the previous hypotheses, statistical thermodynamics allows for the description of the different parameters of the system and link them to quantities like temperature, volume and chemical potential.

In the case of hydrates, in thermodynamic equilibrium, the equality of chemical potentials of water in the liquid phase and in the hydrate phase can be written. This relationship can be rewritten by introducing reference states. For the hydrate, the reference state used in the van der Waals and Platteeuw model is a hypothetical phase β which corresponds to the empty cavities:

$$\Delta\mu_w^{H-\beta} = \Delta\mu_w^{L-\beta} \tag{51}$$

Where $\Delta\mu_w^{H-\beta}$ and $\Delta\mu_w^{L-\beta}$ are the differences of the chemical potentials between water in hydrate or liquid phase and water in the reference phase, respectively. $\Delta\mu_w^{H-\beta}$ is then determined from statistical thermodynamics whereas $\Delta\mu_w^{L-\beta}$ is determined by means of relations from classical thermodynamics.

7.1. MODELLING OF $\Delta\mu_w^{H-\beta}$

$$\Delta\mu_w^{H-\beta} = RT\sum_i \nu_i \ln\left(1-\sum_j \theta_j^i\right) \tag{52}$$

In Eq.(52) ν_i is the number of cavities of type i per mole of water (see table 1) and θ_j^i is the occupancy factor ($\theta_j^i \in [0,1]$) of the cavities of type i by the gas molecule j. This last parameter is very important to define the thermodynamic equilibrium and to determine the hydrate properties.

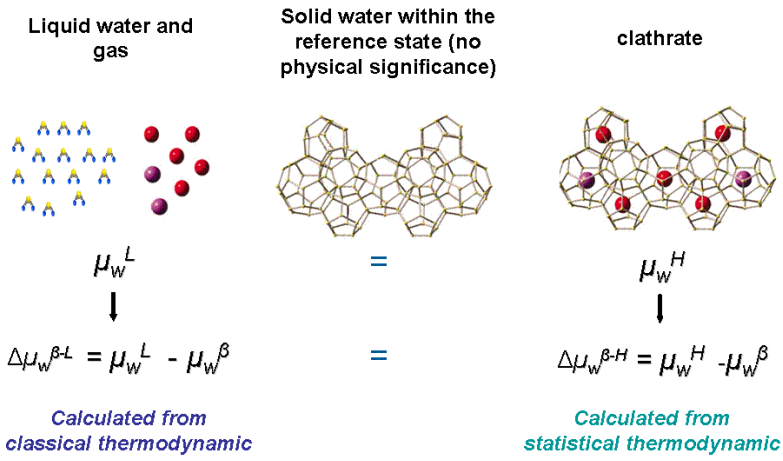

Figure 28 : Schematic of the principle to referring at a hypothetical reference state in order to write the equilibrium between the clathrate hydrate phase and the liquid phase.

The occupancy factor is described by a model based on ideas considering the analogy between the gas adsorption in the 3-dimensional hydrate structure and the 2-dimensional Langmuir adsorption:

- The guest molecule is adsorbed at the surface
- The adsorption energy is independent from the presence of other adsorbed molecules
- The maximum amount of adsorbed gas corresponds to one molecule per site (one molecule par cavity)

The expression of the occupancy factor θ_j^i is given by:

$$\theta_j^i = \frac{C_{f,ji} f_j(T,P)}{1+\sum_j C_{f,ji} f_j(T,P)} \tag{53}$$

Eq.(52) Can be rewritten as:

$$\Delta\mu_{\mathrm{w}}^{\mathrm{H}-\beta} = RT\sum_{i}\nu_i \ln\left(1-\sum_{j}C_{f,ji}f_j(T,P)\right) \tag{54}$$

Where $C_{f,ji}$ is the Langmuir constant of component j in the cavity i. It describes the interaction potential between the encaged guest molecule and the surrounding water molecules evaluated by assuming a spherically symmetrical cage that can be described by a spherical symmetrical potential:

$$C_j^i = \frac{4\pi}{kT}\int_0^{\infty}\exp\left(-\frac{w(r)}{kT}\right)r^2dr \tag{55}$$

Where $w(r)$ is the interaction potential between the cavity and the gas molecule according to the distance r between the guest molecule and the water molecules over the structure. The interaction potential can be determined by different models such as e.g. the van der Waals and Platteeuw model (1959), the Parrish and Prausnitz model (1972) or the so-called Kihara model. The latter, being the most precise (MacKoy and Sinagoglu, 1963), $w(r)$ can be expressed as:

$$w(r) = 2z\varepsilon\left[\frac{\sigma^{12}}{R^{11}r}\left(\delta^{10}+\frac{a}{R}\delta^{11}\right)-\frac{\sigma^{6}}{R^{5}r}\left(\delta^{4}+\frac{a}{R}\delta^{5}\right)\right] \tag{56}$$

$$\delta^N = \frac{1}{N}\left[\left(1-\frac{r}{R}-\frac{a}{R}\right)^{-N}-\left(1+\frac{r}{R}-\frac{a}{R}\right)^{-N}\right] \tag{57}$$

The gas parameters ε, σ and a are the so-called Kihara parameters and can be calculated from experimental data by fitting the model equations to corresponding hydrate equilibrium experimental data. In this description, the interaction potential becomes only dependent on the properties of gases (*via* the Kihara parameters), and dependent of geometrical properties of the cavities (*via* their coordination number z and radius R, Table 1, p 14)

Comment on the geometric description of the cavity

Theoretically, in Eq.(55), the interaction potential $w(r)$ needs to be integrated from 0 to infinity. It means that the gas molecule interacts with the overall structure, not only with its first hydration shell (i.e. the water molecules of the cavity inside which the gas molecule is encapsulated), but also interacts with other molecules localized away from it. In fact, John

and Holder (1982) have showed that 2nd and 3rd hydration shells contribute significantly to the Langmuir constant with a resulting change of this Langmuir constant by 1-2 orders of magnitudes (Sparks and Tester, 1992). Also, even with a rigorous integration of the interaction potential over all the hydration shells, the John and Holder model (1982) can give rigorous results only for spherical molecules (such has Kr, Ar, CH_4…). John et al (1985) have introduced a correction factor to take into account the asymmetry of the encapsulated molecules. All these refinement methods tend to give a physical signification to the interaction potential $w(r)$ and Kihara parameters but results in a time consuming calculation. For this reason, we have retained an integration of the cell potential over the first hydration shell.

Another comment concerns the size of the cavities. Hester et al (2007) did an experimental investigation of lattice parameters for sI and sII structure and different gases (Figure 3a and Figure 4). From one gas to another one, it is showed the lattice parameter can differ from 1%. It has been demonstrated previously via statistical mechanics that a minor change in the lattice parameter (0.5%) can lead to a major change in the predicted hydrate formation (e.g. > 15% at >100MPa for methane). So, from a theoretical point of view, the sizes of the cavities need to be adapted to the component. But, this adaptation can be shifted to the kihara parameter by modifying artificially the ε parameter. So, in modeling, a unique cell dimension can be retained for all gases, and the adjustment of the model will be obtained by fitting the kihara parameters once again.

Kihara parameters for pure substances can be evaluated from measurement of the viscosity, calculated from second viriel coefficient, or from both (Tee et al , 1996), or evaluated from Henry constants (Uno et al, 1975). The Table 51 gives the correlations to evaluate the kihara parameters, assuming a (6,12) Lennard-Jones potential, and interaction between pair of molecules.

These Kihara parameters can not be used directly to model the gas hydrate equilibrium. In fact, in the gas hydrate modeling, the kihara potential is assumed to be the one from MacKoy and Sinagoglu (1963) in Eq.(56) and (57). Also, and more important, and in respect to the previous comment: the interaction potential (Eq.(55)) is a pseudo pair potential between a molecule on one hand, and pseudo other molecule on the other hand consisting on the overall structure.

So, the so-called Kihara parameters need to be re-optimised on experimental data, following a procedure given in section 8

Table 51 Correlations to calculate the ε, σ, and a.kihara parameters as a function of the pitzer acentric factor ω, and critical coordinates Pc, Tc and Vc

		$a^* = \frac{2a}{\sigma - 2a}$	$\sigma\left(\frac{Pc}{Tc}\right)^{1/3}$	$\sigma(Vc)^{1/3}$	$\frac{\varepsilon}{kTc}$
Tee et al, 1996	based on viscosity	0.1501 + 2.3724 ω	2.2802+0.2487ω		0.9736-0.4317ω
	based on second virial coefficient	0.1527 + 1.9809ω	2.2639+0.2487ω		1.0042+3.0454ω
	based on second virial coefficient and viscosity	0.1495 + 1.8428 ω	2.2631-0.3278ω		1.0070+2.2450 ω
		0.1495+1.8428ω		0.7864-0.0527ω	1.0030+2.2329ω
Uno et al, 1975	based on gas solubility	0.240 + 2.20 ω		0.676+0.0788ω	1.03+1.61ω

7.2. MODELLING OF $\Delta\mu_w^{\varphi-\beta}$

The chemical potential of water in the aqueous phase is calculated by means of the Gibbs-Duhem equation of classical thermodynamics which expresses the variation of the free enthalpy with temperature and pressure. The reference conditions are the temperature $T_0 = 273.15$ K and the pressure $P_0 = 1$ bar. The difference of the chemical potential of water between the reference phase (liquid in our case, but it could be ice or vapour phase) and the (hypothetical) empty hydrate phase β, $\Delta\mu_w^{\varphi-\beta}$, can be written as follows:

$$\Delta\mu_{\mathrm{w}}^{\mathrm{L}-\beta} = T\frac{\Delta\mu_{\mathrm{w}}^{\mathrm{L}-\beta}\Big|_{T^0,P^0}}{T^0} - T\int_{T^0}^{T}\frac{\Delta h_{\mathrm{w}}^{\mathrm{L}-\beta}\Big|_{P^0}}{T^2}dT + \int_{P^0}^{P}\Delta v_{\mathrm{w}}^{\mathrm{L}-\beta}\Big|_{T}dP - RT\ln a_{\mathrm{w}}^{\mathrm{L}}\Big|_{T,P} \qquad (58))$$

- The activity of water in the liquid phase, $a_{\mathrm{w}}^{\mathrm{L}}$, is given as the product of the mole fraction of water in the liquid phase, x_{w}, and the activity coefficient of water in that phase, $\gamma_{\mathrm{w}}^{\mathrm{L}}$,

hence $a_{\mathrm{w}}^{\mathrm{L}} = x_{\mathrm{w}}\gamma_{\mathrm{w}}^{\mathrm{L}}$. In a good approximation, the aqueous phase can be regarded as ideal and the activity coefficient therefore be set to a fixed value of 1, resulting in $a_{\mathrm{w}}^{\mathrm{L}} \cong x_{\mathrm{w}}$. However, in the presence of polar molecules or even salts, the system usually shows strong deviations from ideality. In that event, $\gamma_{\mathrm{w}}^{\mathrm{L}}$ needs an appropriate description, as provided e.g. by a simple Pitzer-Debye-Hückel model accounting for the long term electrostatic interactions only, or a more elaborate model like the eNRTL (Chen et al, 1982; Chen and Evans, 1986) or the Pitzer model (1973, 1980) to describe also the short range electrostatic forces. Nevertheless, in this section, there is no need for introducing an additional model to describe $\gamma_{\mathrm{w}}^{\mathrm{L}}$ since the liquid phases encountered in these experiments can in very good approximation be treated as pure liquid water. From a practical point of view, $a_{\mathrm{w}}^{\mathrm{L}}$ is a second order parameter compared to the three following : $\Delta v_{\mathrm{w}}^{\mathrm{L}-\beta}\Big|_{T}$, $\Delta h_{\mathrm{w}}^{\mathrm{L}-\beta}\Big|_{P^0}$ and $\Delta \mu_{\mathrm{w}}^{\mathrm{L}-\beta}\Big|_{T^0,P^0}$.

- The value of $\Delta v_{\mathrm{w}}^{\mathrm{L}-\beta}\Big|_{T}$ is a first order parameter. It has been measured with high accuracy by von Stackelberg (1951) from X ray diffraction. Since that data are believed to be very reliable, the parameter $\Delta v_{\mathrm{w}}^{\mathrm{L}-\beta}\Big|_{T}$ in our model calculations has been taken from this source.
- The value of $\Delta h_{\mathrm{w}}^{\mathrm{L}-\beta}\Big|_{P^0}$ is a first order parameter as well. A refinement of the model is given by Sloan (1998, 2007) that takes into account the temperature dependence of $\Delta h_{\mathrm{w}}^{\mathrm{L}-\beta}\Big|_{P^0}$ using the well-known classical thermodynamic relationship

$$\Delta h_{\mathrm{w}}^{\mathrm{L}-\beta}\Big|_{P^0} = \Delta h_{\mathrm{w}}^{\mathrm{L}-\beta}\Big|_{T^0,\,P^0} + \int_{T^0}^{T} \Delta c_{p,\,\mathrm{w}}^{\mathrm{L}-\beta}\Big|_{P^0} dT \tag{59}$$

assuming a linear dependence of $\Delta c_{p,\,\mathrm{w}}^{\mathrm{L}-\beta}\Big|_{P^0}$ on temperature according to:

$$\Delta c_{p,\,\mathrm{w}}^{\mathrm{L}-\beta}\Big|_{P^0} = \Delta c_{p,\,\mathrm{w}}^{\mathrm{L}-\beta}\Big|_{T^0,P^0} + b_{p,\,\mathrm{w}}^{\mathrm{L}-\beta}\left(T - T^0\right) \tag{60}$$

The model becomes first order dependent on $\Delta h_{\mathrm{w}}^{\mathrm{L}-\beta}\Big|_{T^0,P^0}$ (hereafter referred as $\Delta h_{\mathrm{w}}^{\mathrm{L}-\beta,0}$) and second order dependent on $\Delta c_{p,\,\mathrm{w}}^{\mathrm{L}-\beta}\Big|_{T^0,P^0}$ (hereafter abbreviated as $\Delta c_{p,\,\mathrm{w}}^{\mathrm{L}-\beta,0}$) and $b_{p,\,\mathrm{w}}^{\mathrm{L}-\beta}$.

- The last first order parameter of the equation is $\Delta\mu_{\mathrm{w}}^{\mathrm{L}-\beta}\big|_{T^0,P^0}$ (hereafter referred to as $\Delta\mu_{\mathrm{w}}^{\mathrm{L}-\beta,0}$)

Table 52 Mascroscopic parameters of hydrates and Ice (Sloan, 1998; Sloan et al, 2007)

Structure I		**Structure II**		
$\Delta\mu_{\mathrm{w}}^{\mathrm{L}-\beta,0}$ J/mol	$\Delta h_{\mathrm{w}}^{\mathrm{I}-\beta,0}$ J/mol	$\Delta\mu_{\mathrm{w}}^{\mathrm{L}-\beta,0}$ J/mol	$\Delta h_{\mathrm{w}}^{\mathrm{I}-\beta,0}$ J/mol	
699	0	820	0	van der Waals and Platteeuw (1959)
1255.2	753	795	837	Child (1964)
1297	1389	937	1025	Dharmawardhana et al (1980).....model 1(*)
1120	931	1714	1400	John et al (1985) .....model 2(*)
1287	931	1068	764	Handa and Tse (1986).....model 3(*)
$\Delta h_{\mathrm{w}}^{\mathrm{L}-\beta,0} = \Delta h_{\mathrm{w}}^{\mathrm{I}-\beta,0} - 6011$, where 6011 is the enthalpy of fusion of Ice (J/mol)				
(*) model refers to the model in which the $\Delta\mu_{\mathrm{w}}^{\mathrm{L}-\beta,0}$ and $\Delta h_{\mathrm{w}}^{\mathrm{L}-\beta,0}$ reference parameters are implemented as described in the next part of the work.				

Table 53 Reference properties of hydrates from Sloan (Sloan, 1998; Sloan et al, 2007)

	Unit	Structure I	Structure II
$\Delta h_{\mathrm{w}}^{\mathrm{L}-\beta,0}$	J mol	$\Delta h_{\mathrm{w}}^{\mathrm{I}-\beta}\big\|_{T^0,P^0,\mathrm{SI}}$ -6011	$\Delta h_{\mathrm{w}}^{\mathrm{I}-\beta}\big\|_{T^0,P^0,\mathrm{SII}}$ -6011
$\Delta v_{\mathrm{w}}^{\mathrm{L}-\beta}\big\|_{T^0}$	10^{-6} m^3/mol	4.5959	4.99644

$\Delta c_{p,\mathrm{w}}^{\mathrm{L}-\beta,0}$	J/(mol K^{-1})	-38.12	-38.12
$b_{p,\mathrm{w}}^{\mathrm{L}-\beta}$	J/(mol K^{-2})	0.141	0.141

8. ADJUSTMENT OF MODELS PARAMETERS

The phase equilibrium between the water in the hydrate and the water in the liquid phase is described by Eq.(51).

The calculation implies to choice a set of set of Kihara parameters ε_j, σ_j, and a_j for each of components *j*, and to select the correct set of reference parameters.

Then, at a given temperature (resp. a given Pressure), and assuming a value of the pressure (resp. the temperature), it allows to calculating the interaction potential in Eq.(57), then the constants of Langmuir (Eq.(55)), and finally $\Delta\mu_{\mathrm{w}}^{\mathrm{H}-\beta}$ in Eq.(54). Also, it allows to calculating $\Delta\mu_w^{\varphi-\beta}$ following Eq.(58). The calculated equilibrium pressure P_{calc} (resp. the calculated equilibrium temperature T_{calc}) corresponds the value at which $\Delta\mu_{\mathrm{w}}^{\mathrm{H}-\beta}=\Delta\mu_{\mathrm{w}}^{\mathrm{L}-\beta}$.

A special attention (**first step**) has to be paid when assigning value for $\Delta\mu_{\mathrm{w}}^{\mathrm{L}-\beta}\big|_{T^0,P^0}$ and $\Delta h_{\mathrm{w}}^{\mathrm{L}-\beta}\big|_{T^0,P^0}$ since the corresponding data found in the literature vary strongly from one author to the other, mainly due to the difficulties arising when determining these quantities experimentally. The values can be found in the open literature as cited by Sloan (1998, 2007) and some of them are reported in Table 52 The other quantities $\Delta h_{\mathrm{w}}^{\mathrm{L}-\beta,0}$, $\Delta v_{\mathrm{w}}^{\mathrm{L}-\beta}\big|_T$, $\Delta c_{p,\mathrm{w}}^{\mathrm{L}-\beta,0}$, and $b_{p,\mathrm{w}}^{\mathrm{L}-\beta}$ are taken from Table 53.

The **second step** is to choice the Kihara parameters in order to fit with equilibrium data. The number of Kihara parameters is 3: ε_j, σ_j, and a_j.

Mehta and Sloan (1996) propose to fix the kihara *a* value first, for example by using the correlation established by Tee et al (1996). In fact, *a* is a geometric parameter, the volume of the molecule supposed to be spherical. It can be assumed it is a conservative value between the different models describing the interaction potential.

Then, for a given set of Kihara parameters ε_j and σ_j, it is possible to evaluate the deviation between the model and a set of experimental data.:

$$F(\varepsilon_j,\sigma_j)=\sum_{l=1}^{N}\left|\frac{P_{calc}}{P_{\exp}}-1\right|\rightarrow \min \text{ (resp. } F(\varepsilon_j,\sigma_j)=\sum_{l=1}^{N}\left|\frac{T_{calc}}{T_{\exp}}-1\right|\rightarrow \min \text{)} \qquad (61)$$

In Eq.(61), the index *l* assigns the specific data point and the summation has to be performed over all *N* data of the set. It presents a simplified version of the deviation function, based on deviation between the (Pressure, Temperature) coordinates at equilibrium. Eq.(61) can be enriched to additional data such as deviation to composition is the data are available.

In the end, the Kihara parameters remain adjustable parameters. As it has been claimed by John et al (1985) and reported by Mehta and Sloan (1996): the wrong kihara parameters, wrong cell potential, wrong Langmuir constants (and we can add from Herri et al (2011) the wrong reference parameters) could still lead to the right dissociation pressures.

8.1. DETERMINATION OF THE REFERENCE PARAMETERS

As we mentioned before, the values for $\Delta\mu_w^{L-\beta}\big|_{T^0,P^0}$ and $\Delta h_w^{L-\beta}\big|_{T^0,P^0}$ vary strongly from one author to the other (Table 53). A previous work consists in determining the best values to use and it implies to test them against experimental results.

1) Choice of a set of macroscopic parameters as literature input from Table 52 and Table 53.

2) Under the assumption of a SI and SII structure, respectively, retrieve the best Kihara parameters by adjusting ε and σ (*a* value is not varied and taken from Sloan, 1998, 2005, by example by using the correlation established by Tee et al (1996) given in Table 51). The best value of kihara parameter minimizes the mean standard deviation between the experimental data and the corresponding data calculated from the model (see §8.2).

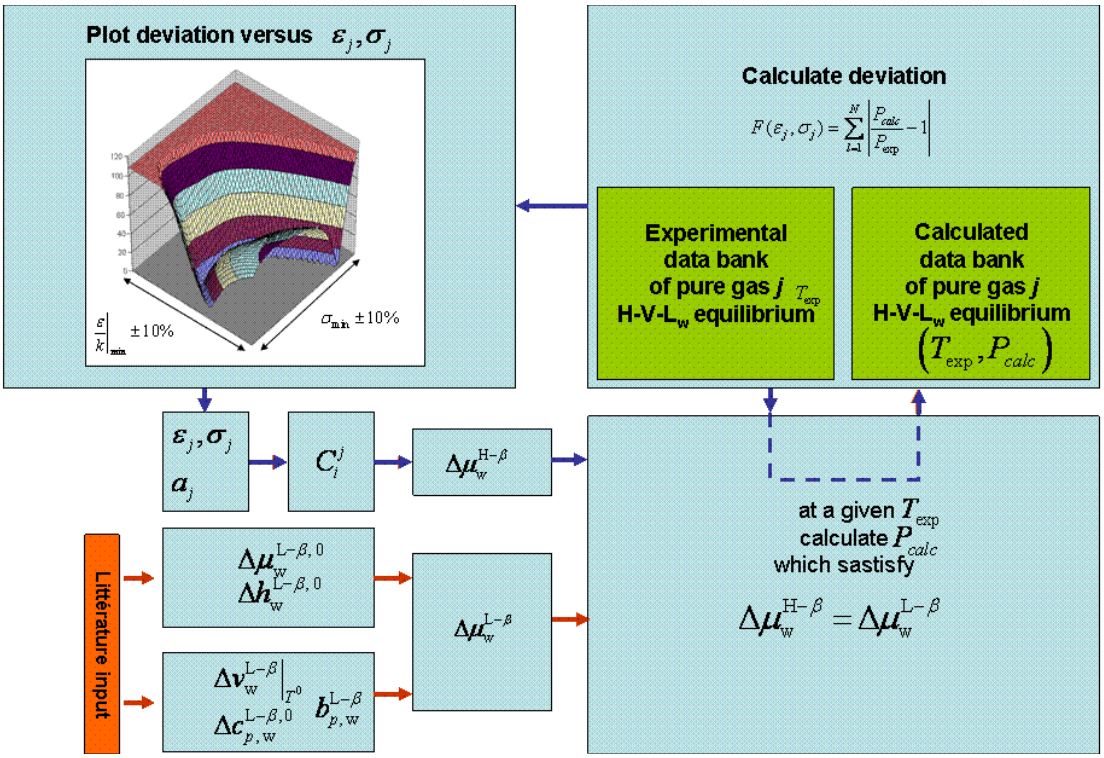

Figure 29 : Procedure to optimise the kihara parameters Herri et al (2011) have determined the sensibility of the kihara parameters to the values for $\Delta\mu_w^{L-\beta}\Big|_{T^0,P^0}$ and $\Delta h_w^{L-\beta}\Big|_{T^0,P^0}$.

The Table 53 shows the best kihara parameters to predict complex H-L_w-V equilibrium, not only on pure CO_2, N_2 and CH_4 gas, but also on CO_2-N_2 , CH_4-N_2 and CO_2-CH_4 gas mixtures, giving not only the (Pressure, Temperature, Gas mixture composition) at equilibrium but also the Hydrate composition at equilibrium. It can be observed that the kihara parameters are dependent on the values of $\Delta\mu_w^{L-\beta}\Big|_{T^0,P^0}$ and $\Delta h_w^{L-\beta}\Big|_{T^0,P^0}$. Also, Herri et al (2011) showed that a better simulation is performed as the model is implemented with values of $\Delta\mu_w^{L-\beta}\Big|_{T^0,P^0}$ and $\Delta h_w^{L-\beta}\Big|_{T^0,P^0}$ from Handa and Tse (1986).

Table 54 Kihara parameters after optimisation on experimental data (Herri et al, 2011) and compared to litterature

	Kihara parameters regressed from experimental results from Herri et al(2011) and implemented in model 1,2,3 with macroscopic parameters from Table 52 (1)Dharmawardhana et al, (1980)- (2) John et al (1985) – (3) Handa and Tse (1986)								
	CO_2			CH_4			N_2		
	$\frac{\varepsilon}{k}$	σ	a	$\frac{\varepsilon}{k}$	σ	a	$\frac{\varepsilon}{k}$	σ	a
Model 1	170.00	2.9855	0.6805	157.85	3.1439	0.3834	126.98	3.0882	0.3526
Model 2	164.56	2.9824	0.6805	154.47	3.1110	0.3834	166.38	3.0978	0.3526
Model 3	171.41	2.9830	0.6805	158.71	3.1503	0.3834	138.22	3.0993	0.3526
	Kihara parameters from literature								
Sloan (1998)	168.77	2.9818	0.6805	154.54	3.1650	0.3834	125.15	3.0124	0.3526
Sloan et al, 2007	175.405	2.97638	0.6805	155.593	3.14393	0.3834	127.426	3.13512	0.3526

8.2. DETERMINATION OF THE KIHARA PARAMETERS

The reference parameters $\Delta\mu_{\mathrm{w}}^{\mathrm{L}-\beta}\big|_{T^0,P^0}$ and $\Delta h_{\mathrm{w}}^{\mathrm{L}-\beta}\big|_{T^0,P^0}$ are taken from Handa and Tse (1986) in Table 52. The other reference parameters $\Delta h_{\mathrm{w}}^{\mathrm{L}-\beta,0}$, $\Delta v_{\mathrm{w}}^{\mathrm{L}-\beta}\big|_{T^0}$, $\Delta c_{p,\mathrm{w}}^{\mathrm{L}-\beta,0}$ and $b_{p,\mathrm{w}}^{\mathrm{L}-\beta}$ are taken from Table 53. $\Delta\mu_{\mathrm{w}}^{\mathrm{L}-\beta}$ can be calculated (Eq. (58)) provided the water activity can be calculated.

$\Delta\mu_{\mathrm{w}}^{\mathrm{H}-\beta}$ can be calculated (§7.1) provided the kihara parameters are known. As it has been mentioned in the previous section (§8.1), the determination of the kihara parameters implies to optimise them so that the condition of equilibrium is achieved (Eq.(51)) following the procedure summarized on Figure 29. It implies to minimize the deviation between experimental results from a data bank and simulated results.

8.2.1 CO_2 Kihara parameters

In the work of Herri and Chassefière (2012), the Kihara parameters have been retrieved for pure CO_2 clathrate hydrate by assuming a SI structure. It corresponds to the values of Kihara parameters which minimise the deviation given in Eq.(61). It is an optimal situation because the equilibrium data are numerous. The study compares 32 experimental results from Yasuda and Ohmura (2008), Adisasmito et al. (1991), Falabella (1975), Miller and Smythe (1970) which cover a range of temperature from 151.52K to 282.9K and a pressure range from 0.535kPa to 4370kPa.

In Figure 30, we can see that the ε/k and σ values which minimize the deviation are located in a deep valley. The Figure 31 plots the ε/k and σ values in the valley, and the corresponding deviation. We can see that the deviation presents a clear minimum which can be considered as the best values of ε/k and σ (reported in Table 55).

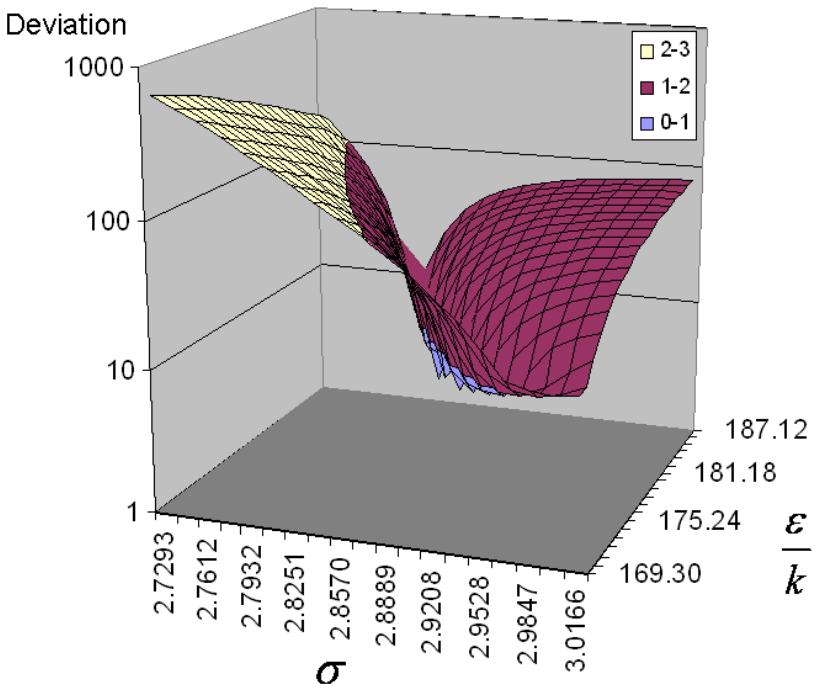

Figure 30 : Deviation (in %, from Eq.(61)) between experimental equilibrium data of pure CO_2 hydrate Experimental data are from Adisasmito et al. (1991), Falabella (1975), Miller and Smythe (1970) which cover a range of temperature from 151.52K to 282.9K and a pressure range from 0.535kPa to 4370kPa.

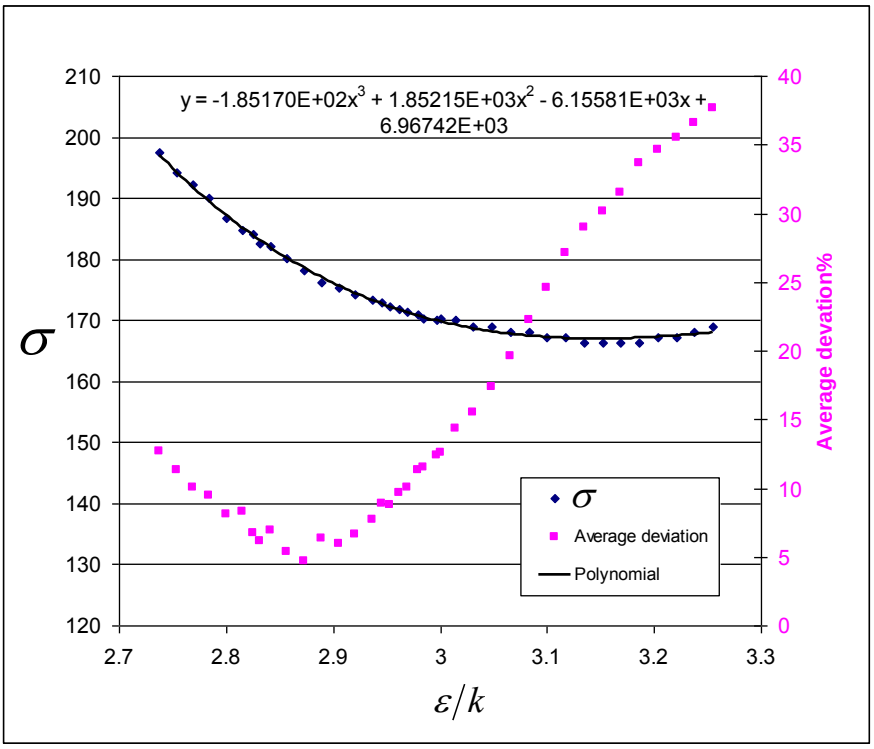

Figure 31 ε/k versus σ at the minimum deviation with experimental data. Pressure and temperature equilibrium data for CO_2 hydrate are taken fromYasuda and Ohmura (2008), Adisasmito et al. (1991), Falabella (1975), Miller and Smythe (1970) which cover a range of temperature from 151.52K to 282.9K and a pressure range from 0.535kPa to 4370kPa

8.2.2 CH_4 Kihara parameters

The Kihara parameters have been retrieved for pure CH_4 clathrate hydrate (Herri and Chassefière, 2012) by assuming a SI structure. The equilibrium data are numerous. The study compares from a set of 27 experimental results from Fray et al (2010), Yasuda and Ohmura (2008), Adisasmito et al. (1991) which cover a range of temperature from 145.75 to 286.4K and a pressure range from 2.4kPa to 10570kPa. On Figure 32, the deviation presents a clear minimum which can be considered as the best values of ε/k and σ (reported in Table 55).

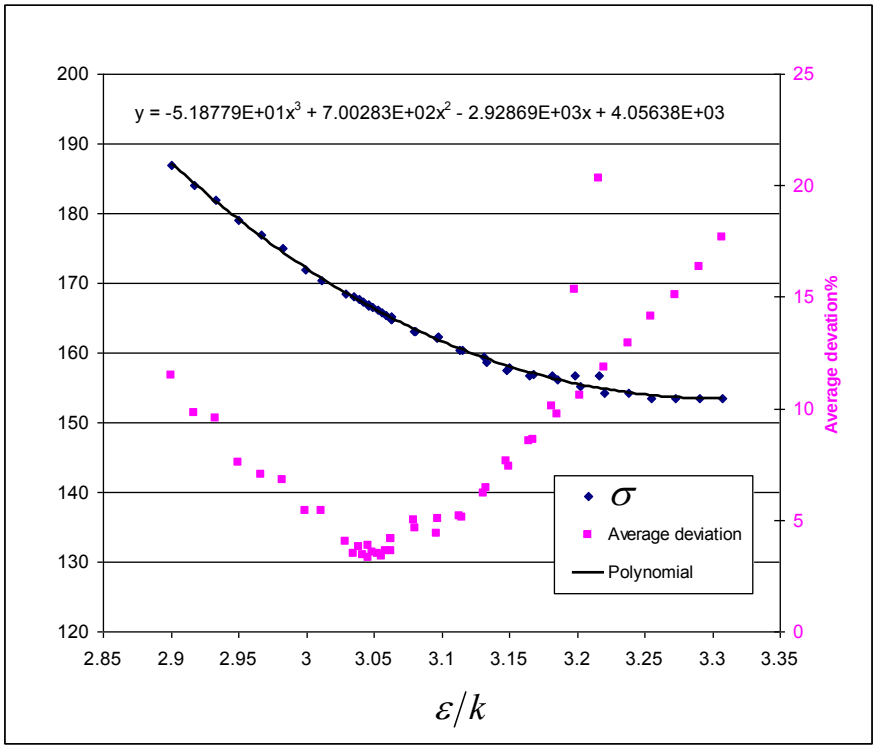

Figure 32 : ε/k versus σ at the minimum deviation with experimental data. Pressure and temperature equilibrium data for CH_4 hydrate are taken from Fray et al (2010), Yasuda and Ohmura (2008), Adisasmito et al. (1991) which cover a range of temperature from 145.75 to 286.4K and a pressure range from 2.4kPa to 10570kPa.

8.2.3 C_2H_6 Kihara parameters

The Kihara parameters have been retrieved for pure ethane clathrate hydrate by assuming a SI structure. The equilibrium data are numerous (**Figure 24**, page 56) and 61 experimental results have been retained for the optimisation, from Robert et al. (1940), Deaton and Frost (1946), Reamer et al. (1952), Falabella (1975), Yasuda and Ohmura (2008), Mohammadi and Richon (2010), which cover a wide range of temperature from 200.08 to 287.4K and a pressure range from 8.3kPa to 3298kPa. On **Figure 33**, the deviation presents a clear minimum which can be considered as the best values of ε/k and σ (reported in Table 55).

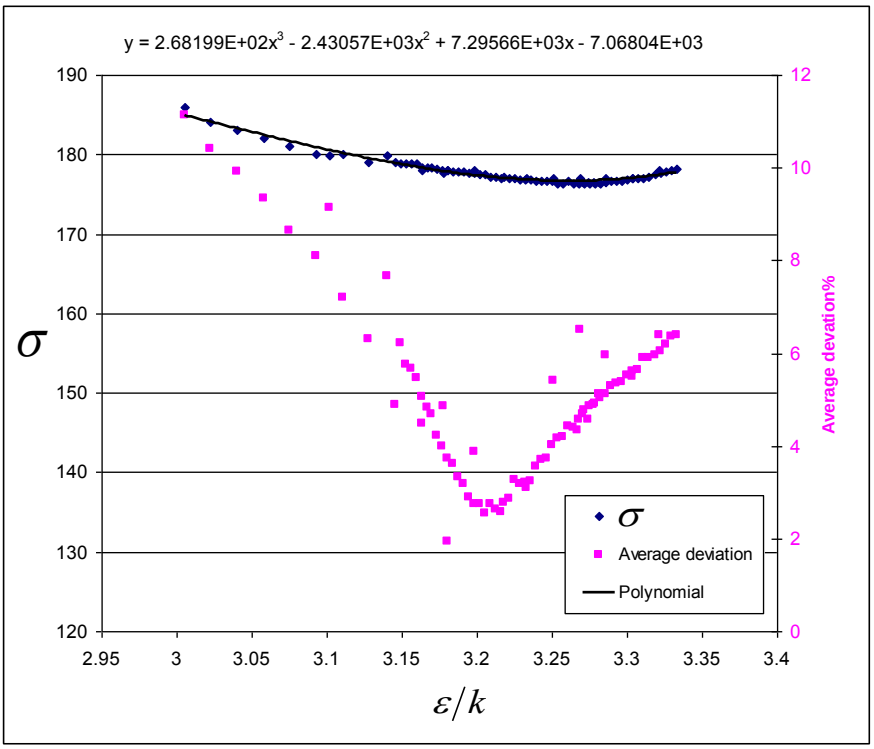

Figure 33 : $_{\varepsilon/k}$ versus σ at the minimum deviation with experimental data. Pressure and temperature equilibrium data for C_2H_6 hydrate are taken , from Robert et al. (1940), Deaton and Frost (1946), Reamer et al. (1952), Falabella (1975), Yasuda and Ohmura (2008), Mohammadi and Richon (2010), which cover a wide range of temperature from 200.08 to 287.4K and a pressure range from 8.3kPa to 3298kPa.

8.2.4 C_3H_8 Kihara parameters

The Kihara parameters have been retrieved for pure propane clathrate hydrate by assuming a SII structure. The equilibrium data are numerous (Figure 25, page 57) but does not cover a wide temperature range. 41 experimental results have been retained for the optimisation of the kihara parameters from from Yasuda and Ohmura (2008), Deaton and Frost (1946) and Nixdorf and Oellrich (1997) which cover a range of temperature from 245 to 278.5K and a pressure range from 41kPa to 567kPa. On Figure 33, the deviation does not present a minimum, and the kihara parameters can not be retrived.

The experimental data bank needs to be extended to equilibrium data on two components gas mixtures, with a second gas which kihara parameters is well known, for example CO_2, CH_4, Kr, Xe.

So, the he Kihara parameters have been firstly retrieved for binary methane-propane clathrate hydrate, from the experimental data (12 equilibrium points in the range of temperature of [274.9K-282.3K], range of pressure of [0.26MPa-0.95MPa] and range of CH_4 gas fraction [0.24-0.37]) of Verma et al (1971) and assuming a SII structure. The Figure 38 shows that the best ε/k and σ parameters does not present a clear minimum on the average deviation curve. Also, we obserse that ε/k and σ parameters are very close to the ones determined on the single propane clathrate hydrate. The comparison between the curves does not allow retrieving a best set of kihara parameters.

The Figure 37 shows another optimisation of the propane kihara parameters based on a Xe-C_3H_8 gas mixture. The literature data concerns only one equilibrium point from Tohidi et al (1993) but it gives the pressure, temperature, gas composition in the gas phase and also the gas composition in the hydrate phase. It is so possible to calculate a mean deviation not only based on the deviation between the experimental and calculated pressure, but also on compositions in the hydrate phase. The mean deviation is important (25%) and does not present a minimum. But the $(\varepsilon/k, \sigma)$ curves of the pure propane and Xe-propane mixture present a single point in common at $\sigma \approx 3.41$.

To confirm this value, we show on Figure 38 the optimisation of the propane kihara parameters based on a CO_2-C_3H_8 gas mixture, from experimental data of Adisasmito and Sloan (1993) who give 55 equilibrium points in the range of temperature of [273.7K-282.0K], range of pressure of [0.22MPa-3.64MPa] and range of CO_2 gas fraction [0.1-0.99]). The

average deviation is a mean deviation between the calculated and experimental pressures at the temperature and gas composition in the gas phase given by Adisasmito and Sloan (1993). The mean deviation is important (15%) and does not present a minimum. But the (ε/k , σ) curves of the pure propane and CO_2-propane mixture present also a single point in common at the same value of $\sigma \approx 3.41$, which confirm the value obtained from the optimisation on the Xe-C_3H_8 gas mixture.

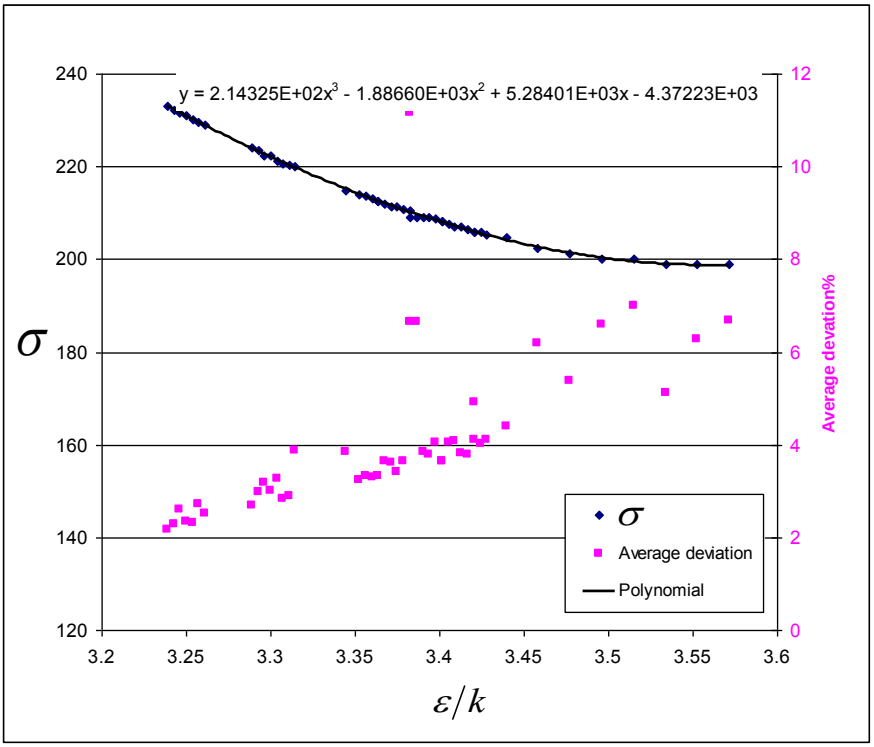

Figure 34 : $_{\varepsilon/k}$ versus σ at the minimum deviation with experimental data. Pressure and temperature equilibrium data for C_3H_8 hydrate are taken from Yasuda and Ohmura (2008), Deaton and Frost (1946) and Nixdorf and Oellrich (1997) which cover a wide range of temperature from 245 to 278.5K and a pressure range from 41kPa to 567kPa

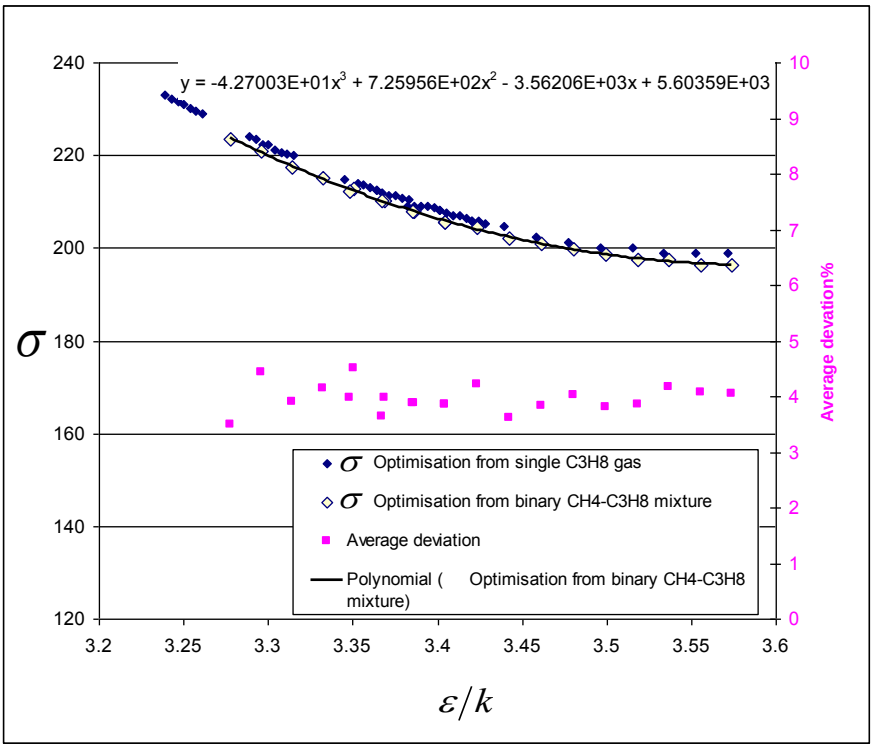

Figure 35 : $_{\varepsilon/k}$ versus σ at the minimum deviation with experimental data. Pressure and temperature equilibrium data for CH_4-C_3H_8 hydrate are taken from Verma et al (1974).

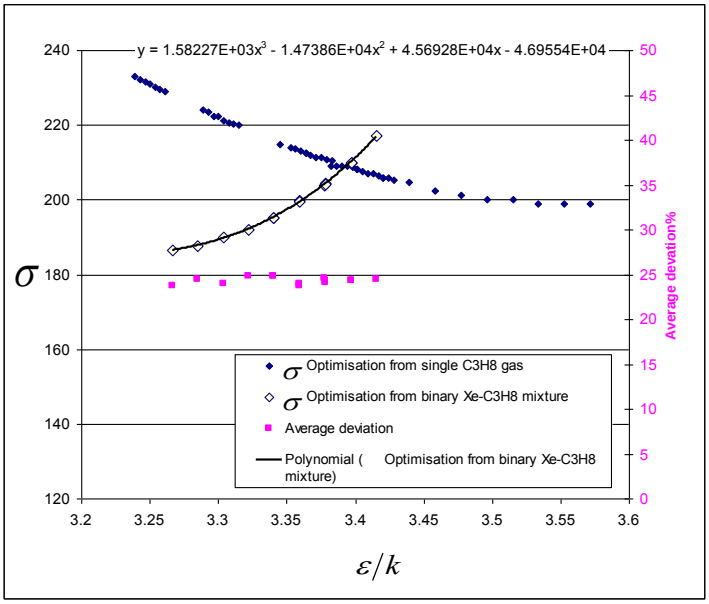

Figure 36 : $_{\varepsilon/k}$ versus σ at the minimum deviation with experimental data. Pressure and temperature equilibrium data for Xe-C_3H_8 hydrate is taken from Tohidi et al (1993).

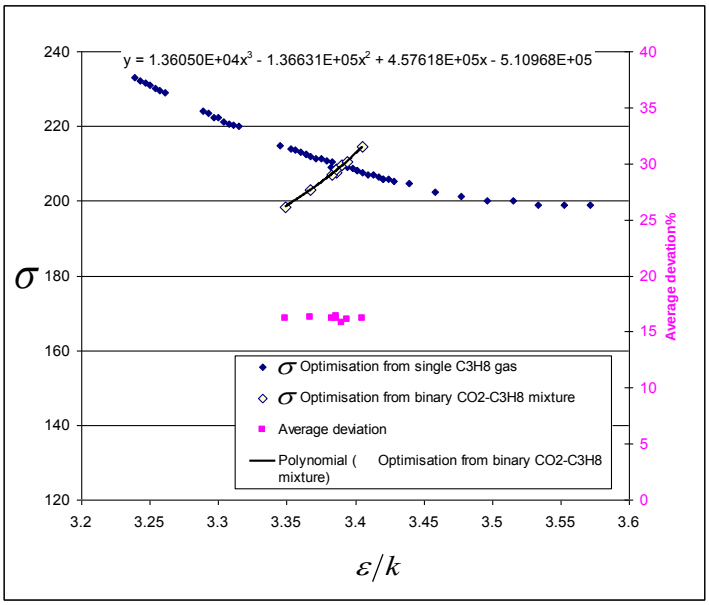

Figure 37 : $_{\varepsilon/k}$ versus σ at the minimum deviation with experimental data. Pressure and temperature equilibrium data for CO_2-C_3H_8 hydrate is taken from Adisasmito and Sloan (1993).

8.2.5 Kr Kihara parameters

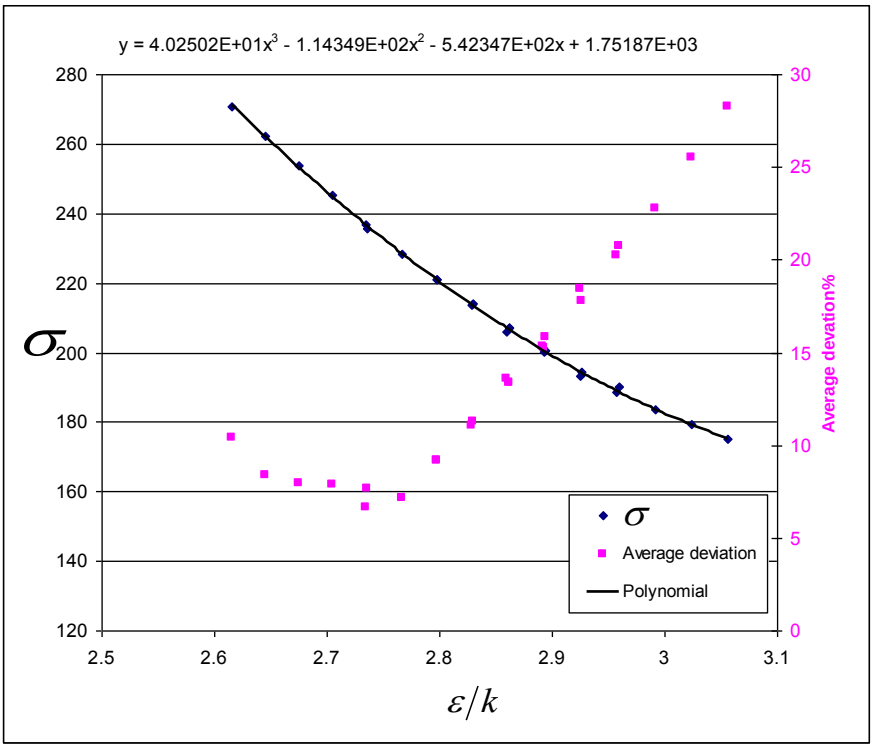

Figure 38 : ε/k versus σ at the minimum deviation with experimental data. Pressure and temperature equilibrium data for Kr hydrate are taken from de Forcrand (1923) and Barrer and Edge (1967) which cover a wide range of temperature from 90.2 to 283.2K and a pressure range from 14.5kPa to 27400kPa

The Kihara parameters have been retrieved for pure Kr clathrate hydrate The equilibrium data are few, (Figure 26, page 58) from de Forcrand (1923), Barrer and Edge (1967), Saito and Kobayashi (1965) compiled in Holder et al (1980) and Mohammadi and Richon (2011) which cover a wide range of temperature from 90.2 to 283.2K and a pressure range from 14.5kPa to 27400kPa.

8.2.6 Xe Kihara parameters

The Kihara parameters have been retrieved for pure Xe clathrate hydrate The equilibrium data are numerous, 47 experimental results (Figure 27, page 59). from Fray et al (2010), Barrer and Edge (1967), Makogon et al. (1996), Ewing and Ionescu (1974) and Dyadin et al. (1996) which cover a wide range of temperature from 165.47 to 310.55K and a pressure range from 0.099kPa to 9060kPa. OnFigure 39, the deviation presents a flat minimum in the range $\sigma = [3.2 - 3.3]$. We retain the value of $\sigma = 3.2$ (reported in Table 55).

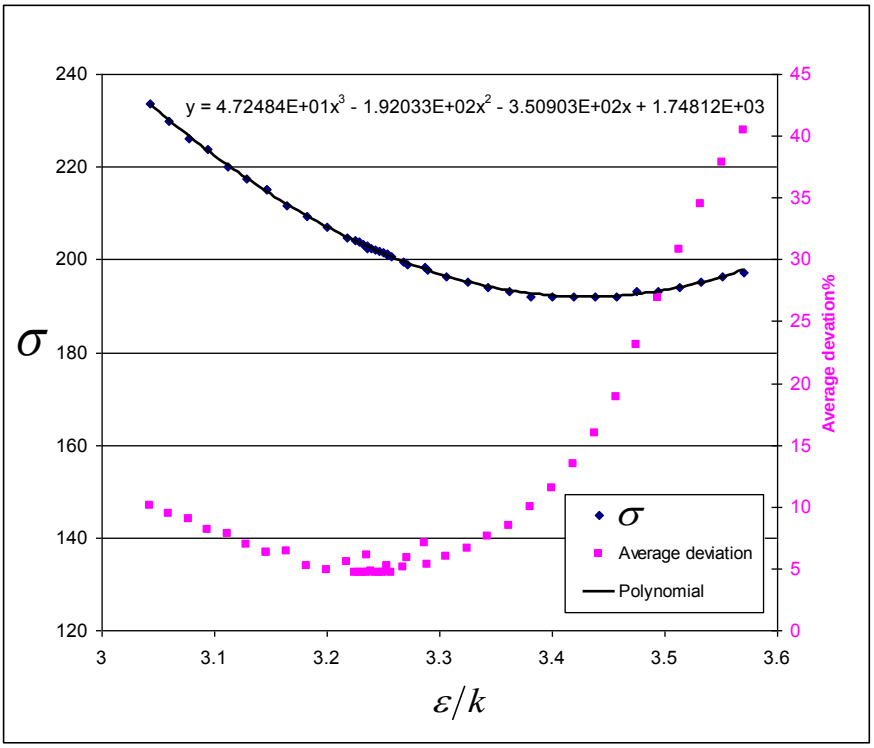

Figure 39 : $_{\varepsilon/k}$ versus σ at the minimum deviation with experimental data. Pressure and temperature equilibrium data for Xe hydrate are taken from Fray et al (2010), Barrer and Edge (1967), Makogon et al. (1996), Ewing and Ionescu (1974) and Dyadin et al. (1996) which cover a wide range of temperature from 165.47 to 310.55K and a pressure range from 0.099kPa to 9060kPa

Summary of the kihara parameters retrieved from the experiments from litterature

Table 55 Kihara parameters, after optimisation from experimental data with the GasHyDyn simulator, implemented with reference parameters from Table 52 (Dharmawardhana et al, 1980) and Table 53.

	$\frac{\varepsilon}{k}$	a	σ
CO_2	178.21(*)	0.6805(+)	2.873(*)
CH_4	166.36(*)	0.3834(+)	3.050(*)
C_2H_6	177.46(*)	0.5651(+)	3.205(*)
C_3H_8	209.20(*)	0.6502(+)	3.3901(*)
N_2	133.13($)	0.3526(+)	3.099($)
Ar	174.14(*)	0.184(=)	2.943(*)
Xe	207.00(*)	0.228(=)	3.200(*)

(*)-regressed from this work, (+)-from Sloan (1998,2005), (=)-Barrer and Edge (1967)) ($)-from Bouchemoua et al (2012)

9. DISCUSSION

The kihara parameters have been determined from the previous section from experimental data from the open literature. We propose here to check their validity on other results from the literature and our new results from this work.

9.1. ABOUT THE MODELLING OF KIHARA PARAMETERS OF CO_2, CH_4 AND C_2H_6

9.1.1 Modelling the equilibrium of single gas from CO_2, CH_4 and C_2H_6.

For modelling the pure gas equilibrium, we have seen that the prediction is very correct for the gases which kihara parameters have been optimised directly on pure gas equilibrium data. This optimisation has been easily possible for CO_2, CH_4 and C_2H_6.

- CO_2 pure gas H-Lw-V equilibria: at a given temperature in the range 151.52K to 298.9K, the calculated pressure deviates from the experimental pressure with a precision of about 5% (Figure 31, p111), whereas the pressure varies in a range of x10000, from 0.535kPa to 4370kPa.
- CH_4 pure gas H-Lw-V equilibria: at a given temperature in the range 145.75K to 286.4K, the calculated pressure deviates from the experimental pressure with a precision of about 3% (Figure 32, p112), whereas the pressure varies in a range of pressure of x4000 order of magnitude, from 2.4kPa to 10570kPa.
- C_2H_6 pure gas H-Lw-V equilibria: at a given temperature in the range 200.08K to 287.4K, the calculated pressure deviates from the experimental pressure with a precision of about 3% (Figure 33, p113), whereas the pressure varies in a range of pressure of x4000 order of magnitude, from 8.3kPa to 3298kPa.

9.1.2 Modelling the equilibrium of binary mixtures from CO2, CH4 and C2H6

Then, if we have a look to the hydrate equilibrium experimental data of binary gases from CO_2, CH_4 and C_2H_6, we can conclude that the simulation still continues to propose a correct evaluation of the equilibrium pressure at a given temperature, and a given gas composition.

- *CO_2 - CH_4 binary gas H-Lw-V equilibria:*

  The literature is well documented, and proposes equilibrium data given the Pressure, Temperature, Gas Composition, but also Hydrate Composition.

  - The data from Bouchemoua et al (2009), Table 27, p.68, is an important validation for us, because it is an experiment from our laboratory with the

same experimental procedure in this work. The model predicts both the equilibrium pressure (with a precision of 2.14%) but also the composition of gas in the hydrate phase, with a very precision of 2 % for CO_2, and a better precision of 1.4% for CH_4. Unfortunately, the data are few, 6 equilibrium points at the temperature of 4°C, in the range of pressure of [2.04-3.9 MPa] and range of molar fraction of [0-1].

- The validity of the model is maintained, with less precision, if applied to our experimental results (Table 28, p.68). During this work, we measured 30 equilibrium points, in the range of temperature of [2.2-7.9°C], range of pressure of [1.92-4.45 MPa] and range of CO_2 molar fraction of [0.147-0.77]. The model predicts both the equilibrium pressure (with a precision of 3.8%) but also the composition of gas in the hydrate phase, with a correct precision of 15.7 % for CO_2, and a correct precision of 11.7% for CH_4
- The comparison to the experimental results from Belandria et al (2011) is also a fruitful comparison, because it is an external source, but using an experimental protocol inherited from us. During their work, in collaboration with us in the framework of a national projet (ANR SECOHYA), they measured 40 equilibrium points (Table 29, p.70), in the range of temperature of [0.45-11.05°C], range of pressure of [1.51-7.19 MPa] and range of CO_2 molar fraction of [0.081-0.669]. The model predicts both the equilibrium pressure (with a precision of 7.8%) but also the composition of gas in the hydrate phase, with a acceptable precision of 18.8 % for CO_2, and a correct precision of 21.4% for CH_4.
- Ohgaki et al (1996) has given 31 equilibrium data , at temperature of 7.15°C, range of pressure of [3.04-5.46 MPa] and range of CO_2 molar fraction of [0-1] (Table 32, p.73). The prediction of the model to their equilibrium data is comparable to the prediction of the model to our experimental data. The equilibrium pressure is simulated with a precision of 5.9%), the composition of gas in the hydrate phase is simulated with a good precision, 15.4 % for CO_2, and 14.4% for CH_4.
- The experimental data from Seo et al (2000) can be regarded as a very good case study (Table 30, p.72, 14 equilibrium data in the range of temperature of

[-0.05-7.35°C], range of pressure of [2-3.5 MPa] and range of CO_2 molar fraction of [0.133-0.834]). The pressure is simulated with a very good precision of 3.3%, but the simulation of composition of the hydrate phase is totally un-correct, 34.8 % for CO_2, and 866.5% for CH_4. In fact, their hydrate phase seems to be considerably CO_2 enriched. For us, it gives an evidence that, for gas mixtures, the simulation of the correct equilibrium pressure is not enough to validate the exactness of the kihara parameters. Also, we can say that the experimental results of Seo et al (2000) are clearly no-coherent in regards to the others experimental results from our work and previous works from Bouchemoua et al (2011), Belandria et al (2011) and Oghaki et al (1996).

- Other experimental data are available in the literature, but they don't give the hydrate composition at the equilibrium, only the Temperature, Pressure and Gas Composition. Given the temperature, the model predicts the equilibrium pressure:
  - Adisasmito et al (1999), precision of 4.5% (Table 33, p.75)
  - Hachikuko et (2002), precision of 4.6 % (Table 34, p.76)
  - Unruh and Katz (1929), precision of 8.2 % (Table 35, p.77)

- *CO_2 - C_2H_6 binary gas H-Lw-V equilibria:*
  - Only one open source can be found in the literature, from Adisasmito and Sloan (1996) in Table 40, p.83, which gives 14 equilibrium data, at temperature of [0.55-14.65°C], range of pressure of [0.57-3.83 MPa] and range of CO_2 molar fraction of [0.189-0.417]. The composition of the hydrate phase is not given. The prediction of the model to their equilibrium data is 19.9%, a not correct value in our understanding.

- *CH_4 - C_2H_6 binary gas H-Lw-V equilibria:*

  There is no source giving the hydrate composition versus equilibrium, only Temperature, Pressure and Gas Composition.

  - Deaton and Frost (1946) has given 22 equilibrium data , at temperature range of [1.65-10.05], range of pressure of [1.289-6.088 MPa] and range of CH_4 molar fraction of [0.564-0.988] (Table 38, p.81). The prediction of the model to pressure is 11.0%. The composition of the hydrate phase is not given.

- Holder and Grigouriou (1980) has given 22 equilibrium data , at temperature range of [6.25-14.65], range of pressure of [0.99-3.08 MPa] and range of CH_4 molar fraction at very low value of [0.016-0.047] (Table 39, p.82). The prediction of the model to pressure is 6.3%. Due to the very low concentration of methane, the validation of the model via the simulation of the equilibrium pressure concerns more the validation of the kihara parameters of ethane rather than methane. But, because the composition of the hydrate phase is not given, this validation is partial.

9.1.3 Modelling the equilibrium from ternary gas mixture CO2, CH4 and C2H6

There is one source giving also the hydrate composition (our work) and another source (Kvenvolden et al, 1984) giving only Temperature, Pressure and Gas Composition.

- Kvenvolden et al (1984) have given 7 equilibrium data , at temperature of minus 4°C, range of pressure of [1.2-3.79 MPa] and range of CH_4 molar fraction at high value of [0.991-0.997] (Table 47, p.94). The prediction of the model to pressure is poor, giving an under estimation of 37.4% if the structure SI is assumed, and also an under estimation of 42.2% if the structure SII is assumed. The experimental composition of the hydrate phase is not given.
- In our work, we give 6 equilibrium data , at temperature range of [2.75-9.25°C], range of pressure of [3.54-5.99 MPa], range of CH_4 molar fraction at high values of [0.865-0.916], range of CO_2 molar fraction of [0.059-0.09] and range of C_2H_6 molar fraction of [0.026-0.045] (Table 46, p.93). The prediction of the model to pressure is poor, giving an under estimation of 21.7% if the structure SI is assumed, and also an under estimation of 26.5% if the structure SII is assumed. The experimental composition of the hydrate phase is given, and curiously, some facts would give evidence that the structure SII has been formed. In fact, the experimental methane fraction in the hydrate phase is modelled with a precision of 3.9% in the SII structure (precision of 11.4% in SI structure), the carbon dioxide fraction is modelled with a comparable precision in the SII structure (precision of 53.3%) and SII structure (precision of 48.2%), and the ethane is better modelled in the SII structure (precision of 32.1%) rather than in the SI structure (precision of 119.2%).

9.1.4 Conclusion

We consider that the kihara parameters of CO_2, CH_4 and C_2H_6 have been correctly estimated from pure gas equilibrium curves. In fact, the literature data are rich enough to cover a wide range of temperature and a wide range of pressure, and the optimisation of the kihara parameters clearly give a single solution.

If applied to gas mixture, we can say:

- In some cases, the model predicts very well the equilibrium data, especially for the CO_2-CH_4 gas mixture that is very well documented. This observation is very important because it allows to validating our experimental procedure. In fact, we get now an amount of experimental data on our side, from this work, or from previous works (Bouchemoua et al, 2011), or from literature, Belandria et al (2011) and Oghaki et al (1996), that can be simulated with the same model.
- But even in the case of CO_2-CH_4 gas mixture, we can observe one set of data (Seo et al, 2000) for which we can model the equilibrium pressure, but not the hydrate composition, whereas for all the other experimental data sources, the composition was pretty well modelled.
- For CO_2-C_2H_6 and CH_4-C_2H_6 gas mixtures, we don't have data to validate the model against the hydrate composition, but the modelling of the equilibrium pressure (given temperature and gas composition) is correct for CH_4-C_2H_6 (precision less than 11%) but could be not acceptable for CO_2-C_2H_6 (precision around 20%)
- For the ternary system CO_2-CH_4-C_2H_6 which has been experimented by us, the pressure is never well simulated, but the simulation of the hydrate composition could give evidence that the hydrate is Structure SII, whereas all the gas components forms a single hydrate of structure SI. From another data (Kvenvolden et al, 1984), we remains in the same confusing state because the pressure is also never well simulated both for SI and SII structure, and the author don't give hydrate composition.

But, in our understanding, these experimental facts confirm our original tuition that the hydrate could not form under equilibrium once the gas is a mixture (for example the ternary system CO_2- CH_4-C_2H_6). But also, they can form at equilibrium (for example in the major part of the CO_2-CH_4 experimental data).

So, it is a source of confusing, especially if we need to model a component which is not documented enough to try to optimise the kihara parameters from the single gas hydrate equilibrium curve. In that case, we need to extend the data base to gas mixture with the risk that hydrate is not form under equilibrium.

9.2. MODELLING THE EQUILIBRIUM OF C3H8

For C_3H_8, the optimisation of kihara parameters has not been possible directly from the pure gas equilibrium data. In fact, the range of temperature of experimental equilibrium data was too much tight, and the procedure of optimisation does not allow getting a clear minimum on the deviation curve between the experiments and the model (Figure 34, p.115). In the end, we obtain an infinite set of $\left(\varepsilon_{C_3H_8},\sigma_{C_3H_8}\right)_{C_3H_8}$ solutions. We needed to enrich the equilibrium data base by optimising the parameters from additional data where the component is in a mixture with another component which kihara parameters are well known.

- If we perform the optimisation with the CH_4-C_3H_8 mixture (Figure 35, p.116), we get a new infinite set of solution $\left(\varepsilon_{C_3H_8},\sigma_{C_3H_8}\right)_{CH_4-C_3H_8}$ that is identical to $\left(\varepsilon_{C_3H_8},\sigma_{C_3H_8}\right)_{C_3H_8}$ and does not allow determining a single solution.
- If we do this optimisation with the CO_2-C_3H_8 (Figure 37, 117), or Xe-C_3H_8 (Figure 36, p117), mixture, we get two infinite sets of solution $\left(\varepsilon_{C_3H_8},\sigma_{C_3H_8}\right)_{CO_2-C_3H_8}$ and $\left(\varepsilon_{C_3H_8},\sigma_{C_3H_8}\right)_{Xe-C_3H_8}$ but there is a common single solution at the intercept of the three curves.

At this level we can do a *reductio ad absurdum* method of reasoning, to conclude that the different experimental data sets from which have been performed the different optimisation are equilibrium data. In fact, if the different experimental sets are not equilibrium points, there are non equilibrium points, and their composition is controlled from kinetic considerations. If it is the case, Herri and Kwaterski (2012) showed that the kinetic contribution to the hydrate composition is a combination of mass transfer limitations at the different interfaces, with a contribution of the intrinsic growth properties rates at the crystal level. All that contributions result in a composition of the gas hydrates which depends on the geometry of the reactor. In

that case, if two experimental data sets are non equilibrium data set, the optimisation of the kihara parameters from each of them will logically give different sets of Kihara parameters:

- Firstly, we can affirm that the experimental data on CH_4-C_3H_8 gas mixture from which has been retrieved $\left(\varepsilon_{C_3H_8},\sigma_{C_3H_8}\right)_{CH_4-C_3H_8}$ are equilibrium data (Verma et al, 1971), because it is identical to $\left(\varepsilon_{C_3H_8},\sigma_{C_3H_8}\right)_{C_3H_8}$ that has been retrieved from equilibrium data on single gas. In both the simulation, the structure SII has been supposed to form.
- $\left(\varepsilon_{C_3H_8},\sigma_{C_3H_8}\right)_{CO_2-C_3H_8}$ and $\left(\varepsilon_{C_3H_8},\sigma_{C_3H_8}\right)_{Xe-C_3H_8}$ are also identical curves, and correspond logically to experimental equilibrium data. In both the optimization, the structure SI has been supposed to form, that explains the shape of the curve is different from $\left(\varepsilon_{C_3H_8},\sigma_{C_3H_8}\right)_{C_3H_8}$. The intercept in between the three curves is the single solution to describe all the equilibrium.

This part of the reasoning is important, because it gives of self-coherence of the kihara parameter that we retain to describe these experimental data sets. We will see now, that for other experimental data sets; the simulation does not predict correctly the equilibrium, and we consider it is due to a non equilibrium formation.

9.2.1 Modeling the equilibrium of binary mixtures from CO2, CH4, C2H6, C3H8

- *CH_4 – C_3H_8 binary gas H-Lw-V equilibria:*
  - Verma et al (1974) have given 12 equilibrium data , at temperature in the range [1.75-9.15°C], range of pressure of [0.263-0.945 MPa] and two CH_4 molar fraction of 0.2375 and 0.371 (Table 41, p.84). The prediction of the model to pressure is 12.6% if the structure SI is assumed, 36.3% if the structure SII is assumed. The experimental composition of the hydrate phase is not given.
  - Deaton and Frost (1946) have given 24 equilibrium data , at temperature in the range [1.75-9.15°C], range of pressure of [1.65-10.05 MPa] and five CH_4 molar fraction of [0.362, 0.712, 0.883, 0.952, 0.99] (Table 42, p.86). The prediction of the model to pressure is poor, 71.76% if the structure SI is assumed, 50.5% if the structure SII is assumed. The experimental composition of the hydrate phase is not given. The deviation seems anomalous, especially at

methane molar fraction of 0.990 and the experimental equilibrium pressure needs to converge to the equilibrium pressure of methane, and it is not experimentally observed.

- Mc Leod and Campbell (1961) have given 18 equilibrium data , at high temperature in the range [17.35-31.75°C], range of pressure of [6.93-62.23 MPa] and two high CH_4 molar fraction of [0.945,0.965](Table 43, p.88). The prediction of the model to pressure is poor, 85% if the structure SI is assumed, 68% if the structure SII is assumed. The experimental composition of the hydrate phase is not given. The deviation seems anomalous, especially because the methane molar fraction is high, and the experimental equilibrium pressure needs to converge to the equilibrium pressure of methane, and it is not experimentally observed.
- Thakhore and Holder (1987) have given 29 equilibrium data , at two temperatures [2,5°C], range of pressure of [0.25-1.31 MPa] and CH_4 molar fraction of [0-0.956](Table 44, p.89). The prediction of the model to pressure is poor, 41.4% if the structure SI is assumed, 27.4% if the structure SII is assumed. The experimental composition of the hydrate phase is not given.

- *C_2H_6 – C_3H_8 binary gas H-Lw-V equilibria:*
  - Mooijer-van den Heuvel (2004) have given 12 equilibrium data, in the range of temperatures [3.88-5.02°C], range of pressure of [0.54-0.96 MPa] and CH_4 molar fraction of [0.299,0.501](Table 45, p.92). The prediction of the model to pressure is low but better than previous cases, it under estimate the experimental pressure of 25.5% if the structure SI is assumed, and over estimate of 29.4% if the structure SII is assumed. The experimental composition of the hydrate phase is not given.

9.2.2 Modeling the equilibrium of a ternary mixtures from CO2, CH4, C2H6, C3H8

- *CH_4 – C_2H_6 – C_3H_8 binary gas H-Lw-V equilibria:*
  - In our work, we give 9 equilibrium data , at temperature range of [2.45-11.15°C], range of pressure of [3.31-4.50 MPa], range of CH_4 molar fraction at high values of [0.953-0.980], range of C_2H_6 molar fraction of [0.03-0.023] and range of C_3H_8 molar fraction of [0.017-0.024] (Table 48, p.95). The prediction of the model to pressure is good, giving a deviation of 15% if the structure SI

is assumed, and 73.3% if the structure SII is assumed. The experimental composition of the hydrate phase is given, and produces evidence that the structure SI has been formed. In fact, the experimental methane fraction in the hydrate phase is modelled with a precision of 7.3% in the SI structure (precision of 23.3% in SII structure), the ethane is modelled with a precision in the SI structure of 44.2% and 97.9% in the SII structure, and the propane ethane is also better modelled in the SI structure (precision of 113.8%) rather than in the SII structure (precision of 338.9%).

- *Conclusion*

The determination of the kihara parameters for the propane has not been trivial, because it has not been possible to retrieve them directly from a single gas equilibrium curve.

We needed to extend our data base to binary gas mixture, and optimise the Kihara parameters from the (Temperature, Pressure, Gas Composition) curve, without consideration to the Hydrate Composition which is not documented in the literature.

As we said before, the choice of equilibrium curves to feet the parameters is crucial. We had to exclude data from some authors because we suspect the data to be out of the equilibrium, and we retain other from a *reductio ad absurdum* method of reasoning.

The final test on $CH_4 - C_2H_6 - C_3H_8$ binary gas H-Lw-V equilibria from our results tends to validate our approach. The equilibrium is correctly described by the model, both to simulate the equilibrium pressure, and to determine the composition of the hydrate in the dominant methane gas. The other components, at low concentration in the gas, are also at low concentration in the hydrate. The deviation between the model and the results on these two last parameters can be due, firstly to the uncertainty of the experimental method at low gas concentration, but also to kinetic considerations.

9.3. MODELLING THE EQUILIBRIUM OF C4H10

The modelling of normal butane has not been possible, in respect to the lack of data in the literature. We produced equilibrium data, given in the Table 17, p.50 and Table 18, p.51, but the optimisation of the Kihara parameters has not been possible, especially because butane is at low concentration, and its benefice to the equilibrium pressure is second order.

10. CONCLUSIONS AND TWO PERPECTIVES

In this work, we have been studied the thermodynamics of gas mixtures from CO_2, CH_4, C_2H_6, C_3H_8 and n-C_4H_{10}.

1) We have presented new experimental data about the gas mixtures giving not only the Pressure, Temperature, Gas Composition, but also Hydrate Composition.

2) These experimental measurements, and all the literature data, have been systemically compiled in the data base of the GasHyDyn software package

3) We have extracted data that we consider to be equilibrium data. The other ones are considered as non equilibrium data

4) This extraction is based on the self-consistency of a thermodynamic model. We have optimized the kihara parameters for CO_2 CH_4, C_2H_6 and C_3H_8 components.

    a. The determination of kihara parameters for CO_2 CH_4, C_2H_6 has been trivial because the hydrate equilibrium curves of the respective single gases cover a wide range of temperature.

    b. The determination of kihara parameters of C_3H_8 has implied a *reductio ad absurdum* method of reasoning, to choice the experimental data and run the optimization, and to exclude the other equilibrium data.

5) The calculation of the kihara parameters for normal butane has not been possible because of the lack of experimental data, and because we measured equilibrium with it at low gas molar fraction.

6) New experimental data need to be measured to confirm the kihara parameters of propane, and to evaluate them for normal butane. To that aim, we propose to study only binary mixtures with a single gas, CO_2 CH_4, C_2H_6 because we are pretty sure of their kihara parameters.

7) Great amounts of experimental data have been excluded from our modeling, and are now considered by us as non equilibrium data. In our understanding, they correspond to a situation where the kinetic considerations control the hydrate composition. Following the model of Herri and kwaterski (2011), a Ph.D. is on-going to estimate the kinetic parameters controlling the hydrate composition.

11. LIST OF SYMBOLS

k_{A,CH_4} Slopes of calibration curve dimensionless

$V_m^{H-water}$ Hydrate Molar volume by molecule of Water $[V_m^{H-water}]$=m^3/molar

$V_m^{H-water}$ Hydrate Molar volume by molecule of gas $[V_m^{H-water}]$=m^3/molar

n_hyd Hydration number dimensionless

S_A Area of the peak in the chromatography $[S_A]$=

Hi Henry coefficient [Hi]= Pa

Δ Finite difference between two values of a quantity

Δ_α^β Finite difference between two values of a quantity for a process from a given initial state α to a final state β

eNRTL Electrolyte NRTL (Non-Random-Two-Liquid) model for the excess Gibbs energy

f Fugacity, $[f] = \mathrm{Pa}$

k_{H}^{∞} Henry's constant at saturation pressure of the pure solvent, i.e., at infinite dilution of the dissolved species, $[k_{\mathrm{H}}^{\infty}] = \mathrm{Pa}$

μ Chemical potential of a species or component, $[\mu] = \mathrm{J\ mol^{-1}}$

M Molar mass, $[M] = \mathrm{g\ mol^{-1}}$

n amount of substance, i.e. mole number, $[n] = \mathrm{mol}$

N_{a} Avogadro's number, $N_{\mathrm{Av}} = (6.02214129 \pm 0.000000027) \times 10^{23}\ \mathrm{mol^{-1}}$

ν Stoichiometric coefficient, or number of water molecules per number of guest molecules in a cage of of a given type I (hydration number), dimensionless

p Pressure, $[p] = \mathrm{bar}$

ρ (Mass) density, $[\rho] = \mathrm{kg\ m^{-3}}$

R Universal gas constant, $R = (8.314472 \pm 0.000015)\ \mathrm{J\ K^{-1}\ mol^{-1}}$, or radius of a cavity, assumed to be of spherical geometry, $[R] = \mathrm{nm}$

S Super saturation, dimensionless

T Absolute temperature, $[T]$=°K

θ Fraction of sites occupied (by a particular species and for a specific type of cavity as indicated by additional subscripts, dimensionless

V Volume, $[V] = \mathrm{m^3}$

x Mole fraction of a chemical species, dimensionless;

y Mole fraction of a chemical species, dimensionless

GC Gas chromatography dimensionless

Z Compressibility factor dimensionless

Subscripts

bulk	Referring to the bulk phase
eq	Referring to a state of equilibrium
exp	Referring to experiment
liq	Referring to liquid phase
LC	Local Composition model
w	Water
x	Indicating the reference to the mole fraction as reference frame for the composition variable
±	Mean ionic quantity

Superscripts

∘	Pure component state
∞	State of infinite dilution
β	Hypothetical reference phase for the hydrate phase corresponding to empty lattice
$\beta - \varphi$	Referring to the difference between any phase and the reference phase b
G	Gas/Vapour phase
H	Hydrate phase
I	Ice phase
L	Liquid phase
L_w	Liquid aqueous phase (depending on the context either an aqueous phase consisting of pure water or a liquid mixed aqueous phase composed of an aqueous solution of a single binary electrolyte
S	Solid phase in general
σ	Liquid-vapour saturation conditions
V	Vapour phase

References

Adamson, A.W., Jones, B.R., 1971, Physical absorption of Vapor on Ice. IV. Carbon dioxide, J. Colloid Interface Sci. 37, 831-835

Adisasmito, S., Frank, R.K., Sloan, E.D., 1991, Hydrate of carbon dioxide and methane mixtures, J. Chem. Eng. Data, 36,68-71

Assane,T., 2008, Etude des conditions thermodynamiques et cinetiques du procede de captage de CO_2 par formation d'hydrates de gaz : application au melange CO_2-CH_4, PhD Thesis, École des mines de Saint Etienne, France

Avlonitis, D., Danesh, A., Todd, A.C., 1988, Measurement and Prediction of Hydrate Dissociation Pressure of Oil-Gas Systems, Master of Science Thesis, Heriot-Watt University, Edinburgh, presented at NHRA Conference on Operationnel/ Consequences of Hydrate Formation and Inhibition Offshore, Cranfield, Uk, November 3, 1988

Barrer, R.M., Edge, A.V.J., 1967, Gas Hydrates Containing Argon, Krypton and Xenon: Kinetics and Energetics of Formation and Equilibria, Proc. R. Soc. London, Ser. A., A. 300, 1-24

Belandria, V., Eslamimanesh, A., Mohammadi, A.H., Theveneau, P., Legendre, H., Richon, D., 2011, Compositional Analysis and Hydrate Dissociation Conditions Measurements for Carbon Dioxide + Methane + Water System, Ind. Eng. Chem. Res., 50, 5783–579

Belandria, V., Eslamimanesh, A., Mohammadi, A.H., Richon, D., 2011, Gas Hydrate Formation in Carbon Dioxide + Nitrogen + Water System: Compositional Analysis of Equilibrium Phases, Ind. Eng. Chem. Res.

Bonnefoy, Olivier., 2004, ''Influence des cristaux d'hydrate ou de gaz sur la perméabilité d'un milieu poreux'', PhD Thesis, École des mines de Saint Etienne, France

Chen, C.C., Britt, H. I., Boston, J. F., Evans, L.B., 1982, Local Composition Model for Excess Gibbs Energy of Electrolyte Systems, AIChE J., 28, 588-596.

Chen, C.C., Evans, L. B., 1986, A Local Composition Model for the Excess Gibbs Energy of Aqueous Electrolyte Systems, AIChE J., 32, 444-454.

Child, W. C. Jr., 1964, Thermodynamic Functions for metastable Ice Structures I and II, J Phys Chem., 68(7) 1834-1838.

Danesh, A., 1998, "PVT and Phase Behaviour of Petroleum Reservoir Fluids", Elsevier

De Forcrand, M.R., 1923, Sur les hydrates de Krypton et d'Argon, Comptes rendus de l'Académie des Sciences, Vol. 176, pp. 355-358

Deaton, W.M., Frost, E.M., 1946, Gas Hydrates and Their Relation to operation of Natural-Gas Pipelines, U.S., Bur. Mines Monogr. Vol 8, 1-101

Delsemme A.H., Wenger A., 1970, Physical-Chemical penomena in comets -I. Experimental study of snows in a ccometary environment, Planet. Space Sci. 18, 709-715

Dharmawandhana,. P. B., 1980, The measurement of the thermodynamic parameters of the hydrate structure and application of them in the prediction of natural gas hydrates, PhD Thesis, Colorado School of Mines, Golden, CO

Dyadin, Yu.A. , Udachin, K.A., 1987, Clathrate polyhydrates of peralkylonium salts and their analogs, Translated from Zhurnal Strukturnoi Khimii, Vol. 28, No. 3, pp. 75-116, May-June, 1987

Dyadin, Y. A., Larionov, E. G., Mikina, T. V. and Starostina, L. I., 1996, Clathrate hydrate of xenon at high pressure, Mendeleev Commun. No. 2, 44-45

Dyadin. Y. A., Larionov. E. G., Mirinski. D. S., Mikina. T. V., Aladko. E. Y. and Starostina. L. I., 1997, Phase Diagram of the Xe-H_2O System up to 15 kbar, Journal of Inclusion Phenomena and Molecular Recognition in Chemistry 28. 271-285

Englezos, P., Kalogerakis, N., Dholabhai, P.D. and Bishnoi, P.R.,1987, Kinetics of Gas Hydrate Formation of Methane and Ethane Gas Hydrates, Chemical Engineering Science, 42, No.11, pp. 2647-2658.

Englezos, P., Dholabhai, P., Kalogerakis, N., Bishnoi, P.R., 1987b, “Kinetics of gas hydrate formation from mixtures of methane and ethane”, Chem. Eng. Sci., 42, (1987b) 2659-2666

Englezos, P., Bishnoi, P. R., 1988, Prediction of Gas Hydrate Formation Conditions in Aqueous Electrolyte Solutions”, AIChE J. 34, 1718-1721.

Englezos, P., Bishnoi, P. R., 1991, Experimental Study on the Equilibrium Ethane Hydrate Formation Conditions in Aqueous Electrolyte Solutions, Ind. Eng. Chem. 30, 1655-1659

Englezos, P. and Ngan, Y. T., 1993, incipient equilibrium data for propane hydrate formation in aqueous solutions of sodium chloride, potassium chloride and calcium chloride, J. Chem. Eng. Data 38, 250-253

Englezos, P., 1993, Chlathrate Hydrates, Ind. Eng. Chem. Res. 32, 1251-1274.

Eslamimanesh, A., Mohammadi , A.H., Richon, D., Naidoo, P., Ramjugernath, D., 2012, Application of gas hydrate formation in separation processes: A review of experimental studies, J. Chem. Thermodynamics 46, pp. 62–71

Ewing. G. J., Ionescu. L. G., 1974, Dissociation Pressure and Other Thermodynamic Properties of Xenon-Water Clathrate, J. Chem. Eng. Data 19(4). 367 - 369

Falabella, B.J., 1975, A Study of Natural Gas Hydrates, Ph.D. Chemical Engineering Dissertation, University of Massachusetts

Falabella, B.J., Vanpee, M., 1974, Experimental Determination of Gas Hydrate Equilibrium below the Ice Point, Ind. Eng. Chem. Fundam.13, 228-231

Fan, S.S., Guo, T.M., 1999, Hydrate formation of CO_2-rich binary and quaternary gas mixtures in aqueous sodium chloride solutions, Journal of chemical & engineering data 44(4) 829-832

Fray, N, Marboeuf, U., Brissaud, O., Schmidtt, B., 2010, Equilibrium Data of Methane, Carbon Dioxide, and Xenon Clathrate Hydrates below the Freezing Point of Water. Applications to Astrophysical Environments, J. Chem. Eng. Data 55(11), 5101-5108

Galfré, A., Cameirao, A., Chauvy, F., Lallemand, A., Herri, J.-M., 2012, Clathrate hydrates equilibrium points for carbon dioxide and nitrogen gas mixture in presence of cyclopentane in water emulsion, under preparation to Chem. Engineering. Science

Galloway, T. J., Ruska, W., Chappelear, P. S., Kobayashi, R., 1970, Experimental Measurement of Hydrate Numbers for Methane and Ethane and Comparison with Theoretical Values, Ind. Eng. Chem. Fundam. 9(2), 237-243

Goddard, J. D., 1981, Chem. Phys. Lett. 83, 312-316 (cited in Sloan, 1998)

Gutt, C.; Asmussen, B.; Press, W.; Johnson, M.; Handa, Y.; Tse, J. S., 2000, The structure of deuterated methane-hydrate, J. Chem. Phys., 113(11) 4713-4721

Handa, Y. P.; Tse, J. S.; 1986, Thermodynamic properties of empty lattices of structure I and structure II clathrate hydrates, J. Phys. Chem. 90, 5917-5921.

Handa, Y. P., 1986, Calometric determinations of the compositions, enthalpies of dissociation, and heat capacities in the range 85 to 270 k for clathrate hydrates of xenon and krypton, J. Chem. Thermodynamics,18 :915

Handa, Y. P., 1986, Composition Dependance of Thermodynamic Properties of Xenon Hydrate, J. Phys. Chem. 90, 5497-5498

Herri, J.M., 1996, Etude de la formation de l'hydrate de méthane par turbidimétrie in situ, Ph.D. Thesis, Université Paris VI. France

Herri, J.M., Chassefiere, E., 2011, Carbon dioxide, argon, nitrogen and methane clathrate hydrates: thermodynamic modeling, investigation of their stability in Martian atmospheric conditions and variability of methane trapping, submitted to Planetary and Space Sciences, December 2011

Herri, J.M., Cournil, M., Chassefière, E., 2011, Thermodynamic modeling of clathrate hydrates in the atmosphere of Mars, Proceedings of the 7th International Conference on Gas Hydrates (ICGH 2011), Edinburgh, Scotland, United Kingdom, July 17-21

Herri, J.M., Pic, J.S., Gruy, F. and Cournil, M., 1999a, Methane Hydrate Crystallization Mechanism from In-Situ Particle Sizing, AIChE Journal, Vol. 45, No. 3, pp. 590-602

Herri, J.M., Gruy, F., Pic, J.S., Cournil, M., Cingotti, B., Sinquin, A., 1999b, Interest of in situ particle size determination for the characterization of methane hydrate formation. Application to the study of kinetic inhibitors., Chemical Engineering Science, Vol. 54, No. 12, pp. 1849-1858

Herri, J.M. , Bouchemoua A., Kwaterski , M., Fezoua A., Ouabbas Y., Cameirao A., 2011, Gas Hydrate Equilibria from CO_2-N_2 and CO_2-CH_4 gas mixtures, - Experimental studies and Thermodynamic Modeling, Fluid Phase Equilibria, Vol. 301, pages 171-190

Herri, J.M., Kwaterski, M., 2012, Derivation of a Langmuir type of model to describe the intrinsic growth rate of gas hydrates during crystallization from gas mixtures, Chemical Engineering Science (81) 28-37

Herri, J.M., Chassefière, E., 2012, Carbon dioxide, argon, nitrogen and methane clathrate hydrates: thermodynamic modeling, investigation of their stability in Martian atmospheric conditions and variability of methane trapping, accepted for publication in Planetary and Space Sciences

Herri, J.M., Chassefiere E., 2012, Carbon dioxide, argon, nitrogen and methane clathrate hydrates: thermodynamic modeling, investigation of their stability in Martian atmospheric conditions and variability of methane trapping, Planetary and Space Science 73 (2012), pp. 376-386

Hester, K.C., Huo, Z., Ballard, A.L., Koh, C.A., Miller, K.T., Sloan, E.D., 2007, Thermal Expansivity for sI and sII Clthrate Hydrates, J. Phys. Chem. B, 111, 8830-8835

Holder, G. D., Corbin, G., Papadopoulos, K. D., 1980, Thermodynamic and Molecular Properties of Gas Hydrates from Mixtures Containing Methane, Argon and Krypton"; Ind. Eng. Chem. Fundam. 19, 282-286.

Holder, G.D., and Grigoriou, G.C., 1980, Hydrate Dissociation Pressure of Methane + Ethane + Water) - Existence of a locus of minimum pressures, Journal of Chemical Thermodynamics 12(11) 1093-1104

Holder, G.D., Hand, J.H., 1982, Multi-phase equilibria in hydrate from methane, ethane, propane and water mixtures, AICHE Journal, 28(3) 440-447

Holder, G.D.; Zetts, S.P., Pradhan, N., 1988, Phase Behavior in Systems Containing Clathrate Hydrates: A Review, Reviews in Chemical Engineering, 5 (1-4), 1-70

Holder, G.D., Kamath, V. A., 1982, Experimental determination of dissociation pressures for hydrates of the cis- and trans-isomers of 2-butene below the ice temperature, J. Chem. Eng. Data 14, 1119-1128

Ikeda, T., Yamamuro, O., Matsuo, T., Mori, K., Torii, M. S. J., 1999, Neutron diffraction study of carbon dioxide clathrate hydrate, 7th Institute-for-Solid-State-Physics Symposium on Frontiers in Neutron Scattering Research (ISSP7), TOKYO, JAPAN 24-27, in Phys. Chem. Solids 60(8-9) 1527-1529

Ikeda, T., Mae, S., Yamamuro, O., Matsuo, T., Ikeda, S., Ibberson, R.M., 2000, Distortion of host lattice in clathrate hydrate as a function of guest molecule and temperature, J. Phys. Chem. A 104 (46) 10623-10630

Jeffrey, G. A., 1984, "Hydrate inclusion compounds"; in Atwood, J. L.; Davies, J. E. D.; MacNicol, D. D.; eds., "Inclusion compounds", I, 135-190; Academic Press, New York

John, V. T., Holder, G. D., 1982, Journal of Physical Chemistry 86(4), 55-459.

John, V. T., Papadopoulos, K. D., Holder, G.D., 1985, A generalized model for predicting equilibrium conditions for gas hydrates, AIChE J., 31, 252-259.

Jones, C. Y., Marshall, S. L., Chakoumakos, B.C., Rawn, C. J.,Ishii, Y., 2003, Structure and thermal expansivity of tetrahydrofuran deuterate determined by neutron powder diffraction, J. Phys. Chem. B 107(25) 6026-6031

Kang, S. P., Lee, H., Lee, C.S., Sung, W. M., 2001, Hydrate phase equilibria of the guest mixtures containing CO_2, N_2 and tetrahydrofuran, Fluid Phase Equilibria, 185, 101–109.

Kihara, T., 1951, The second virial coefficient of non-spherical molecules; J. Phys. Soc. Japan 6, 289–296.

Kubota, H., Shimizu, K., Tanaka, Y., Makita, T., 1984, Thermodynamic properties of R13 ($CClF_3$), R_{23}(CHF_3), R152a($C_2H_4F_2$) and propane hydrates for desalination of sea water, J. Chem. Eng. Jpn. 17(4), 423- 429

Kwaterski, M., Herri, J.M., 2012, Modeling Gas Hydrate Equilibria using the Electrolyte Non-Random Two-Liquid (eNTRL) Model, Submitted to Fluid Phase Equilibria

Larson, S.D., 1955, Phase Studies of the Two Component Carbon Dioxide-Water System Involving the carbon Dioxide Hydrate, Ph.D. Thesis, University of Illinois, Urbana, IL

Makogon, T., Sloan, E.D., 1995, Phase Equilibria for Methane Hydrate from 190 to 262K. J. Chem. Eng. Data 40, 344

Makogon. T.Y., Mehta. A.P., Sloan. E. D., 1996, Structure H and Structure I Hydrate Equilibrium Data for 2.2- Dimethylbutane with Methane and Xenon, J. Chem. Eng. Data 41. 315-318

McKoy, V., Sinanoğlu, O. J., 1963, Theory of dissociation pressures of some gas hydrates; J Chem. Phys 38, 2946-2956.

McLeod, H. O., Campbell, J. M., 1961, Natural Gas Hydrates at Pressures to 10,000 psia, J. Petl Tech 222, 590-594

Miller, B., Strong, E.R., 1946, Am. Gas Assn Monthly, 28(2) , 63 (cited in Sloan, 1998)

Miller, S.L., Smythe, W.D., 1970, Carbon Dioxide Clathrate In The Martian Ice Cap, Science 170, 531-533

Mohammadi, A.H., Richon, D., 2010, Ice-Clathrate Hydrate-Gas Phase Equilibria for Air, Oxygen, Nitrogen, Carbon Monoxide, Methane or Ethane plus water, Ind. Eng. Chem. Res., Vol.48, pp. 2976-3979, 2010

Mohammadi, A.H., Richon, D., 2011, Phase equilibria of binary clathrate hydrates of nitrogen +c yclopentane/cyclohexane/methylcyclohexane and ethane + cyclopentane/cyclohexane/methyl cyclohexane. Chemical Engineering Science, 66(20), p.4936-4940

Mohammadi, A., Richon, D., 2011, Ice - Clathrate Hydrate - Gas Phase Equilibria for Argon + Water and Carbon Dioxide + Water Systems, Ind. Eng. Chem. Res. 2011, 50, 11452–11454

Mooijer-van den Heuvel, M. M.; 2004, Phase Behaviour and Structural Aspects of Ternary Clathrate Hydrate Systems; PhD thesis, Technical University of Delft, The Netherlands.

Nixdorf, J., Oellrich, L.R., 1997, Experimental determination of hydrate equilibrium conditions for pure gases, binary and ternary mixtures and natural gases, Fluid Phase Equilib. 139, 325-333

Ohgaki. K., Sugahara. T., Suzuki. M. and Jindai. H., 2000, Phase behavior of xenon hydrate system, Fluid Phase Equilib. 175. 1-6

Ogienko, A. G., Kurnosov, A. V., Manakov, A. Y., Larionov, E., G., Ancharov, A. I., Sheromov, M. A.; Nesterov, A. N., 2006, Gas hydrates of argon and methane synthesized at high pressures: Composition, thermal expansion, and self-preservation, J. Phys. Chem. B, 110(6) 2840-2846

Parrish, W.R., Prausnitz, J.M., 1972, Dissociation pressure of gas hydrates formed by gas mixtures. Ind. Eng. Chem. Process Develop. 11, 26-35.

Patil, S.L., 1987, Measurement of multiphase gas hydrate phase equilibria: effect of inhibitors and heavier hydrocarbon components, Master of Science Thesis, University of Alaska, Fairbanks, Alaska

Perry's Chemical Engineers' Handbook, McGRAW-HILL International Editions, Sixth Edition,1984

Pic, J.S., Herri, J.M., Cournil, M., 2000, Mechanisms of Methane Hydrate Crystallization in a Semibatch Reactor, Influence of a Kinetic Inhibitor: Polyvinylpyrrolidone, Annals of the New York Academy of Sciences, 912, pp. 564-575

Pic, J.S., Herri, J.M., Cournil, M., 2001, "Experimental influence of kinetic inhibitors on methane hydrate particle size distribution during batch crystallization in water", Canadian Journal of Chemical Engineering, 79, 374-383

Pitzer, K.S., 1973, Thermodynamics of Electrolytes. I. Theoretical Basis and General Equations, J. Phys. Chem. 77, 268-277.

Pitzer, K.S., 1980, Electrolytes: From Dilute Solutions to Fused Salts, J. Am. Chem. Soc. 102, 2902-2906.

Rawn, C.J., Rondinone, A. J., Chakoumakos, B. C., Marshall, S.L., Stern, L. A., Circone, S., Kirby, S., Jones, C.Y.; Toby, B.H., Ishii, Y., 2002, Neutron Powder Diffracion Studies as a Function of Temperature of sII Hydrate Formed from a Methane + Ethane Gas Mixture. Proceedings of the 4th International Conference on Gas Hydrates, Yokohama, Japan

Reamer, H.H., Selleck, F.T., Sage, B. H., 1952, Some properties of mixed paraffinic and other olefinic hydrate, Trans. Am. Inst. Min., Metall. Pet. Eng. 195, 197-202

Roberts, O.L., Brownscombe, E.R., Howe, L.S., 1940, Constitution diagrams and composition of methane and ethane hydrates, Oil & Gas J. 39(30), 37-43

Robinson, R.A., 1961, Activity coefficients of sodium chloride and potassium chloride in mixed aqueous solutions at 25°C, J. Phys. Chem. 65, 662–667.

Robinson, D.B., Mehta, B.R., 1971, Hydrates in the Propane-carbon Dioxide - Water System, J. Can. Petro. 10, 33-35

Robinson, R. A., Stokes, R. H., 2002, Electrolyte Solutions, 2nd rev. ed., Dover publications, Inc., Mineola, New York. Reprint of the rev. ed. 1970.

Rondinone, A.J., Chakoumakos, B.C., Rawn, C.J., Ishii, Y., 2002, Neutron Diffraction Study of sI and sII Trimethylene Oxide Clathrate Deuterate. Proceedings of the 4th International Conference on Gas Hydrates,Yokohama, Japan, 2002.

Saito S., Kobayashi, R., 1965, Hydrates and high pressures AIChE J., Vol. 11(1), pp 96

Scharlin, P., 1996, Carbon dioxide in water and aqueous electrolyte solutions (62), Oxford University Press

Schmitt, B., 1986, “La surface de la glace: structure, dynamique et interactions - implications astrophysique”, PhD Thesis, University of Grenoble, Grenoble, France

Seo, Y.T., Kang, S.P., Lee, C.H., Lee, H., Sung, W.M., 2000, Hydrate Phase Equilibria for Gas Mixtures Containing Carbon Dioxide: A Proof - of- Concept to Carbon Dioxide Recovery from Multicomponent Gas Stream, Korean Journal of Chemical Engineering 17(6), 659-667

Shpakov, V. P., Tse, J. S., Tulk, C.A., Kvamme, B., Belosludov V.R., 1998, Elastic module calculation and instability in structure I methane clathrate hydrate,

Sloan, E.D., 1990, “Clathrate Hydrates of Natural Gases”, 1st ed., Marcel Dekker, New York.

Sloan, E.D., 1998, “Clathrate Hydrates of Natural Gases”, 2nd ed., Marcel Dekker, New York.

Sloan, E.D., Koh, C.A., 2008, “Clathrate hydrates of natural gases”, 3rd ed., CRC Press, Boca Raton

Soave, G., 1972, Equilibrium constants from a modified Redlich-Kwong equation of state, Chem. Eng. Sci. 27, 1197-1203.

Sparks, K.A., Tester, J.W., 1992, Intermolecular potential-energy of water clathrates - The inadequacy of the nearest-neigbor approximation, Journal of Physical Chemistry, 96(22), 11022-11029

Takeya, S., Nagaya, H., Matsuyama, T., Hondoh, T., Lipenkov, V.Y., 2000, Lattice constants and thermal expansion coefficient of air clathrate hydrate in deep ice cores from Vostok, Antarctica , J. Phys. Chem. B 104(4) 668-670

Takeya, S., Kida, M., Minami, H., Sakagami, H., Hachikubo, A., Takahashi, N., Shoji, H., Soloviev, V., Wallmann, K., Biebow, N., Obzhirov, A., Saloatin, A., Poort., 2006, Structure and thermal expansion of natural gas clathrate hydrates, J. Chem. Eng. Sci. 61(8) 2670-2674

Thakore, J.L., Holder, G.D., 1987, Solid vapor azeotropes in hydrate-forming systems, Ind. Eng. Chem. Res., 26, 462-469

Tee, L.S., Gotoh, S., Stewart, W.E., 1996, Molecular parameters for Normal Fluids - The Kihara Potential with a spherical core, Ind. Eng. Chem. Fundam. 5, 363-367

Tohidi, B., Burgass, R. W., Danesh, A. and Todd, A. C., 1993, Measurement and Prediction of the Amount and Composition of Equilibrium Phases in Heterogeneous Systems containing Gas Hydrates, SPE Student Paper Contest, Aberdeen, Scotland, September 6, 1993

Tse, J.S., 1987, Thermal expansion of the Clathrate hydrates of Ethylene-Oxide and Tetrahydrofuran, J. Phys (Paris), C1, 48,

Uchadin, K.A., Ratcliffe. C.I., Ripmeester, J.A., 2002. Single Crystal Diffraction Studies of Structures I. II and H Hydrates: Structure. Cage Occupancy and Composition. Journal of Supra Molecular Chemistry, 2 (2002) 405-408

Van der Waals, J.H., Platteeuw, J.C., 1959 Clathrate solutions”, Adv. Chem. Phys. 2 (1959) 1-57

Verma, V.K., Hand, J.H., Katz, D.L., 1974, Gas Hydrates from Liquid Hydrocarbons (Methane-Propane-Water System), A.I.Ch.E.-VTG Joint Meeting, p. 10, Munich (Sept.1974)

Von Stackelberg, M., Müller, H.R., 1951, on the structure of gas hydrates, J. Chem. Phys. 19, 1319-1320

Vysniauskas, A., Bishnoi, P.R., 1985, Chemical Engineering Science, 40, pp. 299

Yasuda, K., Ohmura, R., 2008,. Phase Equlibrium of Clathrate Hydrates Formed with Methane, Ethane, Propane or Carbon Dioxyde at temperatures below the Freezing Point of Water, J. Chem. Eng. Data, 53, 2182-2188

École Nationale Supérieure des Mines
de Saint-Étienne

NNT : *2013 EMSE 0726*

Duyen LE QUANG

EQUILIBRIUM OF GAS HYDRATES IN PRESENCE OF A HYDROCARBON GAS PHASE

Speciality : Process Engineering

Keywords : Equilibrium of CO_2 CH_4, C_2H_6, C_3H_8, et C_4H_{10}, hydrate crystallization, Kihara parameters, thermodynamic, petroleum

Abstract :

Many studies have been conducted since 1778's to study the formation of clathrate hydrates of gas, especially under conditions of high pressure and low temperature to reproduce the conditions of oil production. My thesis mainly concerns the study of the thermodynamic of gas hydrates in presence of hydrocarbon: CO_2 CH_4, C_2H_6, C_3H_8, and C_4H_{10} pure or in gas mixtures. The experimental results of this work complete the literature experimental results, were used to optimize the internal parameters related to the thermodynamic model data base GasHyDyn software.

This model optimizes the parameters of Kihara and allows us to retain a second time , or to exclude a particular data set, considered as points of equilibrium , or balance points out . We finally discuss the reason for non-equilibrium of certain points, however, considered by their authors as equilibrium points. This seems kind of kinetic considerations related to a competition between gas hydrate structure to integrate during growth .

École Nationale Supérieure des Mines
de Saint-Étienne

NNT : *2013 EMSE 0726*

Duyen LE QUANG

ÉQUILIBRE DES HYDRATES DE GAZ EN PRESENCE D'UN MELANGE D'HYDROCARBURES GAZEUX

Spécialité: Génie des Procédés

Mots clefs : d'équilibres de CO_2 CH_4, C_2H_6, C_3H_8, et C_4H_{10}, cristallisation d'hydrates, paramètres de Kihara, thermodynamique, pétrolière

Résumé :

Différentes études ont été réalisées depuis les années 1778 pour étudier la formation des clathrates hydrates de gaz, notamment dans des conditions de haute pression et de basse température pour reproduire les conditions de production pétrolière.
Mon travail de thèse concerne principalement l'étude du comportement thermodynamique des hydrates d'hydrocarbures gazeux : CO_2 CH_4, C_2H_6, C_3H_8, et C_4H_{10}, pris purs ou bien en mélanges. Les résultats expérimentaux de ce travail, complétés des résultats expérimentaux de la littérature, ont été utilisé afin d'optimiser les paramètres interne du modèle thermodynamique lié à la base de données du logiciel GasHyDyn.
Ce modèle optimise les paramètres de Kihara, et nous permet dans un deuxième temps de conserver, ou bien d'écarter tel ou tel jeu de données, considéré comme des points d'équilibres, ou bien des points hors équilibre.
Nous discutons finalement de la raison de la nature hors équilibre de certains points, considérés pourtant par leurs auteurs comme des points d'équilibres. Cette nature nous semble liée à des considérations cinétiques d'une compétition entre les différents gaz pour intégrer la structure hydrate en cours de croissance.